Scalable Processing Strategies for Microencapsulation using Cellulose Nanocrystals

by

Marc Massicotte

B.Eng., McGill University, 2019

A THESIS SUBMITTED IN PARTIAL FULFILLMENT OF

THE REQUIREMENTS FOR THE DEGREE OF

MASTER OF APPLIED SCIENCE

in

THE FACULTY OF GRADUATE AND POSTDOCTORAL STUDIES

(Chemical and Biological Engineering)

THE UNIVERSITY OF BRITISH COLUMBIA

(Vancouver)

August 2022

The following individuals certify that they have read, and recommend to the Faculty of Graduate and Postdoctoral Studies for acceptance, the thesis entitled:

Scalable Processing Strategies for Microencapsulation using Cellulose Nanocrystals

submitted by Marc Massicotte in partial fulfilment of the requirements for

the degree of Master of Applied Science

in Chemical and Biological Engineering

Examining Committee:

Emily Cranston, Associate Professor, Wood Science, Chemical and Biological Engineering, UBC
Supervisor

Orlando Rojas, Professor, Chemical and Biological Engineering, Wood Science, Chemistry, UBC
Supervisory Committee Member

Feng Jiang, Assistant Professor, Wood Science, UBC
Supervisory Committee Member

Abstract

Bio-based materials are promising alternatives to less sustainable materials (i.e., petroleum-based chemicals), however, very few have been commercialized in advanced material roles. In addition to formulation development, new processing methods must be established to allow bio-based materials to make the leap from lab-scale to industrial-scale processing. In this work, we investigated the use of cellulose nanocrystals (CNCs) in the microencapsulation of oils. First, drying techniques including freeze drying, spray freeze drying, and spray drying were compared for producing corn oil-filled powders stabilized by CNCs, methyl cellulose (MC) and tannic acid. All three techniques produced dry oil powders with high encapsulated oil content (>90%). The oil powders could be redispersed in water to reform an emulsion and could be stored dry for weeks (in the fridge) without oil leakage. The three drying techniques imparted different surface morphologies that were linked to powder redispersibility and oil release properties. Spray freeze dried powders displayed the most tunable oil release when tested on a hydrophobic substrate. It was demonstrated that spray drying could be used to encapsulate a variety of oils that have different interfacial tensions and volatilities, including jojoba, lavender, and tea tree oil. Next, a dry jet wet spinning apparatus was designed and fabricated to use the same CNC and oil encapsulation system to produce oil-filled fibres. Coaxial extrusion provided a continuous spinning process whereby an external CNC-MC "shell" and internal oil "core" led to fibres with discrete oil-filled beads measuring ca. 2 mm in width along the fibre. The spun fibres were stable under ambient conditions, relatively flexible, and exhibited interesting optical properties. The encapsulated oil could be released by shearing or by re-wetting the fibres. Both the oil-filled powders and fibres were prepared using scalable processing techniques, employed plant-based and industrially-produced "building blocks", worked with commercially-relevant oils, and will hopefully contribute to the

development of environmentally sustainable emulsions, powders, and fibres for food, cosmetic, biomedical, pharmaceutical, agricultural and construction applications.

Lay summary

Many products in the food, cosmetic, agricultural, and pharmaceutical industries involve combining components that mix poorly, such as oil and water. To achieve a uniform mixture, additives that stabilize oil and water together can be used, however, these stabilizers are typically petroleum-based and are harmful to the environment. Natural plant-based materials, such as cellulose nanocrystals (tiny particles from trees), have shown promise as a sustainable alternative to produce new bioproducts at the lab scale. This research prepares oil-in-water mixtures, called emulsions, stabilized by cellulose nanocrystals. The emulsions are so stable that they can be dried using industrially-scalable techniques into powders that appear solid but contain 90% liquid oil. Furthermore, equipment was built to fabricate oil-filled fibres that release antibacterial oil “on demand” for wound dressing applications. Food-grade and essential oils were demonstrated, and other active ingredients could be dissolved in the oils, suggesting many potential uses for these new materials.

Preface

Chapter 3 has been submitted to a journal under the title “Comparison of techniques for drying cellulose nanocrystal Pickering emulsions into oil powders” and the findings have been presented at the TAPPI Nano 2022 conference as an oral presentation under the title “Processes for drying cellulose nanocrystal Pickering emulsions into oil powders”. I conducted all the research and wrote the manuscript under the supervision of Dr. Cranston.

The work discussed in Chapter 4 has been filed as a US provisional patent June 10th, 2022, under the title “Wet-spun cellulose fiber with encapsulated liquid oil." (tech ID23-027), application number 63/350,981. It has also been presented as a poster at the TAPPI Nano 2022 conference under the title “Encapsulation of liquid oil in cellulose nanocrystal-stabilized wet-spun fibres”. I conducted the design, research and wrote the manuscript under the supervision of Dr. Cranston.

Table of contents

List of tables

List of figures

List of abbreviations

AFM	Atomic force microscopy
BNC	Bacterial nanocellulose
CLSM	Confocal laser scanning microscopy
CNC	Cellulose nanocrystal
CNF	Cellulose nanofibril
CO	Corn oil
DP	Degree of polymerization
DTG	Derivative thermogravimetry
FD	Freeze drying
HEPES	2-[4-(2-hydroxyethyl)piperazin-1-yl]ethanesulfonic acid
IR	Infrared
JO	Jojoba oil
LO	Lavender oil
MC	Methyl cellulose
NEB	Nonenzymatic browning
PAH	Polyallylamine hydrochloride
PCL	Poly ε-caprolactone
PTFE	Polytetrafluoroethylene
SD	Spray drying
SEM	Scanning electron microscopy
SFD	Spray freeze drying

STDEV	Standard deviation
TA	Tannic acid
TEMPO	2,2,6,6-tetra-methylpiperidinyl-1-oxyl
TTO	Tea tree oil
UV	Ultraviolet

Acknowledgements

I would like to first acknowledge my supervisor, Dr. Emily Cranston for her continuous guidance and support, and who gave me the freedom to follow my curiosity. Her leadership, focus, and empathy have inspired me throughout this program to strive for excellence and care for others.

I would also like to thank the Cranston research group, who have been an integral part to my development as a researcher and who have made the long days in the lab much more enjoyable. I would like to especially thank our group's postdocs, Elina Niinivaara, Elisa Ferreira and Marcus Johns for their patience, guidance, and humour. A special thanks goes out to Julia Antoniw, who helped me navigate this strange world of academia, with whom I vented about the hardships, and celebrated the successes.

I would like to thank the faculty and staff of the Chemical and Biological Engineering department, as well as the BioProducts Institute. I would like to acknowledge the Natural Sciences and Engineering Research Council of Canada for granting me the opportunity to pursue this endeavor with financial support.

I am very grateful for all the people who have supported me through this journey. To my family in Montreal, thank you to the Petrellas who took me in as one of their own. I appreciate the great meals we shared and the board games we played to distract me from my menacing undergrad. Thank you to Jean, Juliette, and Bernard, for guiding me through a new chapter, a new city, and always making me laugh. Merci à vous tous, je vous aime beaucoup!

Thank you to my dear friends, the boys, who have taught me that no matter what, good times await us on Sunday.

I would like to thank all my family across B.C. too, for their support over the years. To my family in Kimberley, Cath, Cam and Megan, thank you for the love and support, the check ins, and the adventures. Thanks John and Barb, who have always asked the toughest research questions. I would especially like to thank my mom and dad, who have helped me through all the ups and downs, shaped me into the person I am, and still inspire me to continue to keep my foot on the gas, and reach for new challenges. I would like to thank my sister, Marie-Claire Massicotte, who has helped me get through the toughest of days by bringing me food, water, and music breaks, and who has always been there for me.

Finally, I want to thank my partner, and love, Cailyn Strachan, who has been the reason that any of this has been accomplished. She is my biggest motivation and my biggest supporter. I am so grateful to have her in my life. The laughter, joy, and positivity she brings has helped me out of the deepest of ruts. Thank you for reminding me to relax and not take it too seriously.

Je t'aime de tout mon coeur, mon tournesol.

Dedication

I would like to dedicate this work to all who have been negatively impacted by our society's dependence on petroleum.

It was not our decision to make this mess our reality, but it is us who bear the burden of fixing it.

Chapter 1: Introduction

1.1 Bio-based materials as an environmentally sustainable alternative for microencapsulation

The Intergovernmental Panel on Climate Change 2022 report offers a stark outlook on the current management of climate change, showing increasing greenhouse gas emissions and current operations and interventions falling short of curbing its devastating impact.[1] Thousands of governments of varying levels have declared a climate emergency, displaying the urgency of the situation, however many organizations continue to operate in a "business as usual" manner without dedicated efforts of decarbonizing.[2] With petrochemically-based plastic production and consumption contributing significantly to both greenhouse gas emissions and environmental pollution, the need for "greener" alternative platform materials is clear.[3] Showing the scalable processing of renewable biological feedstocks into more advanced materials, will help promote a new circular bioeconomy.[4]

A common material processing strategy known as microencapsulation currently relies heavily on petrochemically-derived materials. Microencapsulation is a technique that involves protecting a compound by encapsulating it with another material at the micro- or nano- scale, and is widely used in food processing, cosmetics, and pharmaceuticals. Reducing the use of petrochemically-based materials in the production of microcapsules, by offering bio-based alternatives, will help reduce the negative environmental impacts associated with production and end-of-life disposal of these materials.

Nanoscale bio-based materials, extracted or produced from biomass sources, have become a burgeoning topic for research. Bio-based nanomaterials can possess a wide variety of tunable

properties and have shown their potential to replace petroleum-based and inorganic chemicals in many advanced material applications.[5,6] Industrial scale production of bio-based nanomaterials has grown significantly in recent years; however, commercial applications are rather limited.[7] Cellulose nanocrystals (CNCs), a nanomaterial isolated from various natural cellulose resources, have exhibited impressive abilities to be used as bio-based encapsulating agents for microencapsulation.[8] In order for CNCs to have a noticeable positive environmental impact in the enormous world of microencapsulation, a scalable process with tunability is required. The development of such a process necessitates the evaluation of various processing techniques in order to find the best path forward for industrial scale bioproduct production and commercialization.

1.2 Research objectives

The goal of this research is to demonstrate that CNCs, a bio-based nanomaterials, can replace petrochemically-derived stabilizers currently used in encapsulation technologies for scalable applications in various sectors, notably the cosmetic and biomedical fields. This thesis explores the use of CNCs, along with other plant-derived materials (methyl cellulose and tannic acid), to encapsulate different liquid oils in both a dry powder and a filled fibre. More specifically the objectives of the work are:

- To explore the impact of three drying techniques, freeze drying, spray freeze drying and spray drying, for drying emulsions, and compare the resulting oil powders in terms of composition, oil release, and redispersibility in water. In this work we demonstrated that dry oil powders could be tailored for desired properties by tuning the emulsion concentration, stabilizer content, and drying technique. The presented CNC and methyl cellulose encapsulation strategy

was able to encapsulate a variety of oils, including corn oil, lavender oil, tea tree oil, and jojoba oil, offering a robust encapsulation strategy for a variety of commercial applications.

- To design and fabricate a fibre spinning apparatus capable of producing bio-based and biodegradable oil-filled fibres. Core/shell fibres were successfully produced with CNC and methylcellulose shells and a liquid tea tree oil core through coaxial dry jet wet spinning. The oil-filled fibres could be stored for weeks at ambient conditions and the encapsulated oil could be released by shearing or by wetting the fibres offering potential application as antibacterial fibres in biomedical wound dressings. Continuous fibre spinning was achieved showing commercial feasibility.

1.3 Thesis outline

This thesis has the following structure: Chapter 2 introduces the background of this research and literature the work builds on, Chapter 3 compares scalable drying techniques to successfully produce oil-filled powders encapsulated with CNCs, Chapter 4 presents a continuous method to produce oil-filled fibres encapsulated with CNCs employing a co-axial wet spinning apparatus built in-house, and Chapter 5 presents the main conclusions and suggestions for future work.

Chapter 2: Background and literature review

2.1 Encapsulation

Encapsulation means enveloping a substance for protection, by creating a material barrier between the internal component and the surrounding environment. Encapsulation can be used to protect substances from exposure to environmental factors such as oxygen, water, heat, light, or other surrounding materials. The effectiveness of an encapsulation method depends on the encapsulating material's properties as well as the conditions under which it is both prepared and utilized (for example: temperature, pH, humidity).[9]

Microencapsulation, which includes encapsulation at the micro- and nano- scales, is a rapidly advancing technology with many applications in biomedical, agricultural, material, and food science fields.[10] A microencapsulation is fundamentally composed of two components, one being the active ingredient in the internal phase or the core, the other being the structural matrix material in the external phase referred to as the shell or wall material. A single discrete domain between the core and shell materials creates a microcapsule and as the active ingredient becomes more and more divided into subdomains within the matrix, the particle is then considered a microsphere.

The internal material encapsulated can be in a solid, liquid, or gaseous state. The wall material used, as well as the placement of the active agent in relation to the matrix, influences the stability and release mechanism of the microcapsules. The release of a core material in a desired location at a specific rate triggered by certain conditions is referred to as controlled release.[11] A controlled release of active agents typically depends on mechanisms such as shear, diffusion, pH-based erosion, dissolution, or osmosis. The matrix materials can be tuned based on variable thickness, porosity, permeability, and inertness to achieve specific release kinetics. Techniques used to

prepare microencapsulations include emulsification, spray-drying, freeze-drying, coacervation, in situ polymerization, extrusion, fluidized-bed-coating, and supercritical fluid technology.[12]

2.1.1 Emulsions

Certain liquids are immiscible together, meaning that when combined the mixture is highly unstable, and the two liquids separate back into two distinct phases (i.e., oil and water). Emulsions allow a stable mixture of two or more immiscible liquids by using a stabilizer to encapsulate one liquid within droplets dispersed throughout the other liquid. In conventional emulsions, macroemulsions which have larger droplets (>1 μm) are kinetically stable, while smaller droplet microemulsions possess thermodynamic stability as well.[13] Encapsulation of liquid oils in microemulsions is used to encapsulate flavours, fragrances, and drugs for applications in the food, cosmetic, and pharmaceutical industries.[14,15,16]

The formation of emulsions is induced by inputting energy to deform larger droplets and absorb a stabilizer to the interface to form a dispersed phase.[17] Typical emulsification processes include high-pressure homogenization, ultra-sonication, microfluidization, and various forms of rotor/stator dispersing machines, i.e., toothed disc, colloid mill, among others (Figure 2.1).[18,19,20] A main component that impacts emulsion microstructure is the amount of energy input and the method by which the energy is delivered.[21] Lower energy systems, such as stirring vessels, form coarser emulsions (larger droplets) due to insufficient energy to break-up droplets into smaller sizes.[17] However, adding too much energy or "over-processing" the emulsion leads to re-coalescence and increases droplet size leading to emulsion instability.[22]

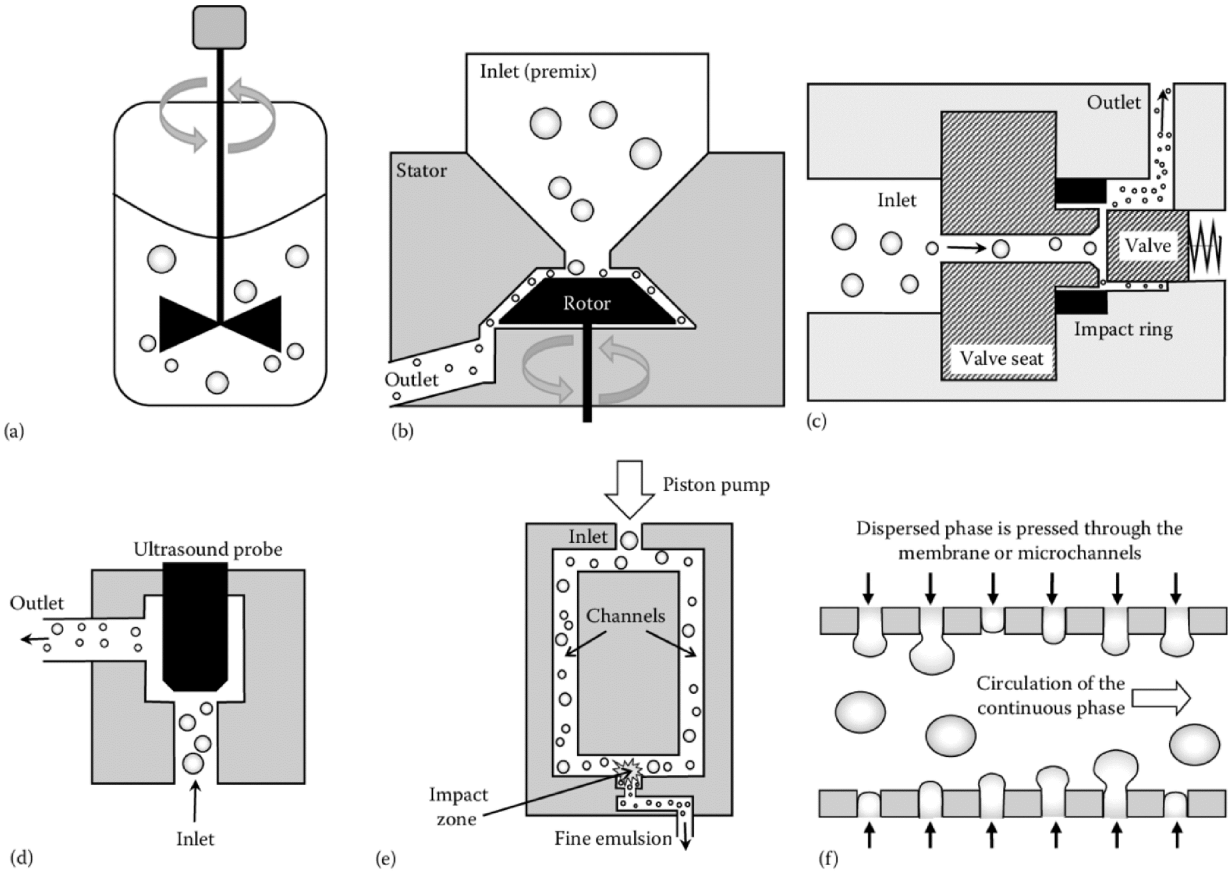

Figure 2.1. Schematic representation of emulsification processes including (a) stirrer vessel, (b) rotor-stator homogenizers (colloid mill), (c) high-pressure homogenizers, (d) ultrasonic probe, (e) microfluidizer, (f) membrane and microchannel emulsification. Figure adapted from Rayner.[23]

Common stabilizers or wall materials for preparing emulsions include synthetic molecules called surface active agents (surfactants), or bio-based polymers typically carbohydrates or proteins.[12] Synthetic surfactants are typically small amphiphilic molecules that orient themselves at the interface to have the hydrophilic "head" in the aqueous phase and the hydrophobic "tail" in the oil phase (Figure 2.2, left). Surfactants adsorb to the droplet surface of the dispersed phase and stabilize the emulsion by reducing the interfacial tension.[24] Synthetic surfactant molecules, such as anionic and non-ionic surfactants, are widely used in the microencapsulation of oil, however,

they show varying levels of ecotoxicity and can bioaccumulate posing long-term threats to natural ecosystems.[25] Additionally, synthetic surfactants are often petroleum-based chemicals and their production contributes to greenhouse gas emissions.[26]

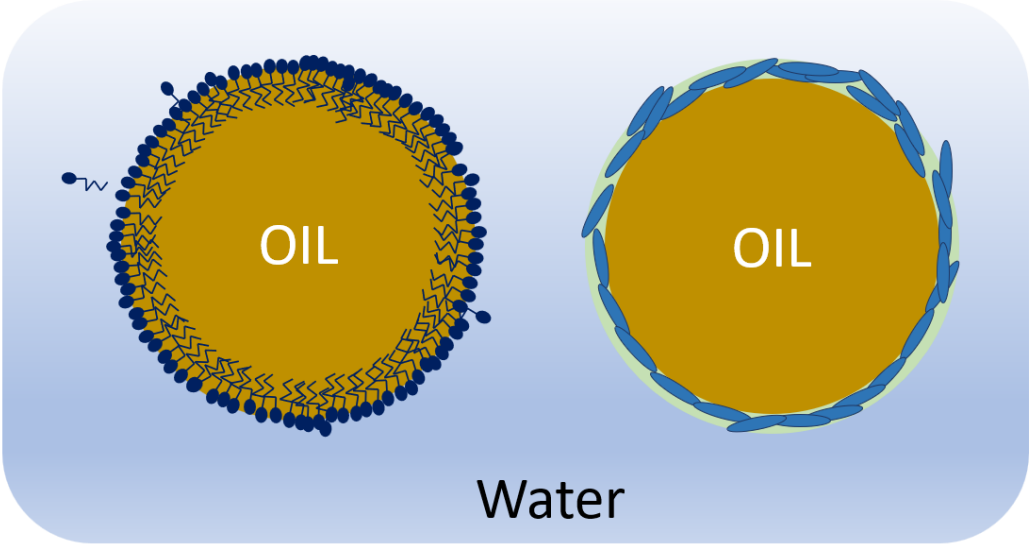

Figure 2.2. Schematic representation of oil-in-water emulsion droplets stabilized by (left) surfactants, and (right) solid particles (i.e., Pickering emulsions).

Stabilization of emulsions using solid particles, called Pickering emulsions, offers a surfactant-free alternative (Figure 2.2, right).[27] Pickering emulsions are formed by solid particles irreversibly adsorbing onto the surface of droplets of the dispersed phase producing emulsions with improved stability against coalescence and flocculation.[28]

Bio-based wall materials offer environmentally benign options for microencapsulation. There are many categories of bio-based wall materials including natural gums, carbohydrates, animal and plant proteins, lipids, fats, waxes, lecithins, and fibers.[9] Gum Arabic is one of the most commonly used natural emulsifiers, but being an extractive from the Acacia tree grown in drought-prone

regions, its quality and cost can fluctuate significantly.[29] Hydrolyzed starches, such as maltodextrin, are also widely used for emulsification, however their low emulsifying capacity requires them to either be chemically modified, or blended with better emulsifying agents further increasing their cost.[30] Proteins such as sodium caseinate, whey protein isolate (made from cow milk), and soybean protein, have shown good emulsifying and encapsulating properties. But when encapsulating oils containing carbonyl groups, common in flavour compounds, nonenzymatic browning (NEB) resulting from the Maillard reaction has been observed due to interactions of aldehydes with the amino groups in the proteins.[14] These conclusions have fueled the search for a bio-based wall material that possesses an adequate emulsifying capacity while having a variety of sources to ensure consistent price and supply.

2.2 Cellulose

Cellulose is the most abundant natural polymer in the world, making it an attractive feedstock for the development of sustainable bio-based materials.[31] Cellulose is a high molecular weight polysaccharide found in plants, marine invertebrate animals (e.g., Tunicates) and certain bacteria and fungi.[32,33] The chemical structure of cellulose consists of D-glucose units connected by β-1,4 glycosidic bonds. Cellulose chains are made of a repeating segment, a non-reducing and reducing end (Figure 2.3). The repeating segment, cellobiose, is a dimer of anhydroglucose made of glucose molecules rotated 180° with respect to each other. The degree of polymerization (DP) of the cellulose chain is determined by the number of glucose units and differs depending on the source of the cellulose.[32] In plants, the cellulose chains are generally stacked into elementary fibrils, which are then arranged into microfibrils that gather to form cellulose fibres, a key structural component of the plant cell wall. In the assembly of these microfibrils, twisting or tilting from internal strain

causes chain dislocations along elementary fibrils, giving rise to disordered, or amorphous, regions, while unaffected areas remain as highly-ordered, or crystalline, regions.[34] The ordered regions, stabilized by inter- and intramolecular hydrogen bonding and van der Waals forces, are more tightly packed than the disordered region, making them more resistant to degradation.[32] Chemical, enzymatic and mechanical degradation can be used to isolate different types of smaller particles from cellulose fibres. Nanocellulose refers to cellulosic materials that have at least one dimension in the nanoscale. "Top-down" extraction of nanocellulose produces cellulose nanofibrils (CNFs) and cellulose nanocrystals (CNCs), while "bottom-up" production of nanocellulose encompasses bacterial nanocellulose (BNC).[35]

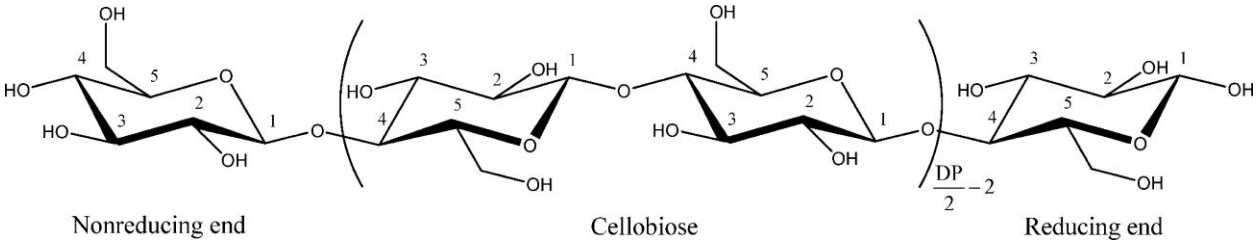

Figure 2.3. Chemical structure of cellulose. Figure reproduced from Habibi et al.[32]

2.2.1 Cellulose nanocrystals (CNCs)

The isolated nanoscale crystalline constituent of cellulose, the CNC, is becoming increasingly researched for its unique chemical, mechanical and optical properties.[36] The most common production method uses acid hydrolysis to selectively degrade the amorphous regions of the cellulose fibrils, isolating rod-shaped CNCs with lengths ranging from 50 to 350 nm and widths of 5 to 20 nm (Figure 2.4).[37,32] CNCs are often produced using sulfuric acid hydrolysis, which grafts covalently bonded sulfate half ester ($-OSO_3^-$) groups on the surface of the CNCs that impart high colloidal stability.[7] CNCs show intrinsically high aspect ratios, have relatively high thermal

stability, and are able to assemble at oil–water interfaces making them interesting candidates for an array of applications as sustainable nanomaterials.[38,39,35] Additionally, CNCs have been produced from a wide variety of biomass sources following different production routes, and are currently industrially produced at large scales around the world.[7]

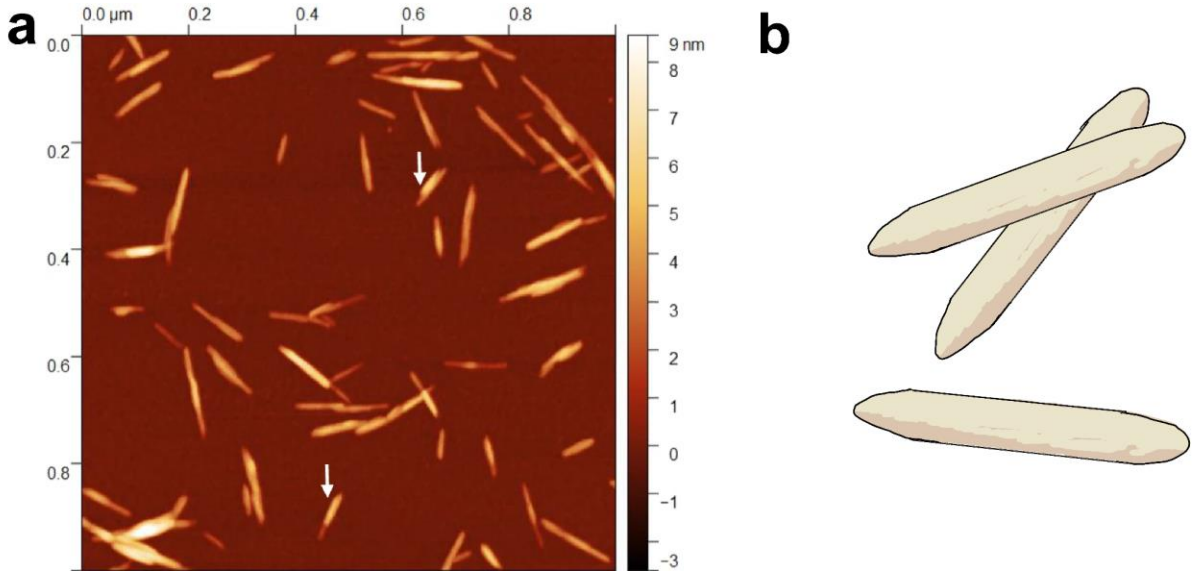

Figure 2.4. (a) Sulfated CNCs imaged by atomic force microscopy (AFM), and (b) schematic of rod-shaped CNCs. Figure adapted from Bushell et al.[40]

CNCs have been used as the wall material to form particle-stabilized (Pickering) emulsions.[8] Nanocellulose in general, including CNCs, CNFs and BNC, may offer an advantage compared to spherical solid particles (i.e., silica, metal oxide or iron nanoparticles) by stabilizing emulsions at lower concentrations with theoretically higher energies of attachment due to their abilities to form networks instead of requiring dense packing of nanoparticles into a monolayer around the droplet.[35] Additionally, CNCs offer the widest range of surface modification possibilities which have been used to improve their role as emulsion stabilizers.[41] At the same concentration, CNF stabilized emulsions have been shown to form gels while the CNC stabilized emulsions can still

flow, showing the impact of the difference in aspect ratio on the rheological properties.[42] When combined with a co-stabilizing polymer, CNCs can form highly stable and tunable Pickering emulsions.[43]

2.3 Emulsion drying techniques

Water removal from materials is a pivotal aspect of industrial processing due to the benefits drying offers in terms of preservation and weight reduction as well as the significant cost it can incur in processing time and energy consumption. Powdered forms of substances are often produced to prolong storability, "shelf-life", and reduce mass and, thus transportation costs, but can also allow for novel methods of encapsulation.[44,45] However, preserving delicate structures, such as microcapsules, during drying can be challenging. The removal of water can be achieved by various techniques that involve adjusting pressures and temperatures of the system, and include conventional oven drying, microwave oven drying,[46] heat pump drying,[47] drum drying,[48] spray drying,[49] freeze drying,[50] and spray freeze drying.[51] The three drying techniques that are investigated in this thesis work are described in more detail below.

2.3.1 Freeze drying

Lyophilization is the sublimation of water from a material that is first frozen and then placed in a high vacuum. This process is also known as freeze drying, and is commonly used in food, pharmaceutical and cosmetic industries.[52,53,50] Freeze drying is preferred for many applications, specifically in the field of food processing, because of its ability to preserve structures in the material through the drying process. The water in the solid state helps preserve the shape of the material, limiting shrinkage and collapse.[52] During the freezing step of the freeze drying process, ice-templating occurs, where ice crystals nucleate and grow, excluding solute around them. When

the material is sublimated, these ice crystals are removed and become voids, which form a porous structure.[54]

Freeze drying can be used to produce flaky porous monolithic materials or to dry larger structures. Nanocellulose has been freeze dried to make a variety of morphologies including absorbent aerogels[55] and foams,[56] conductive aerogels,[57] and insulating aerogels[58] and foams,[59] and further ground to make powders.[60] More specifically, the size, shape and orientation of the ice crystals that grow as a material is frozen (and template the microstructure) depend on the rate of freezing as well as the sample thickness and vessel in which it is frozen. Freezing rapidly, or "flash" freezing, by subjecting the sample to a very cold environment ($T < -80$ °C), produces more smaller ice crystals compared to slow freezing ($T < 0$ °C).[61] The freezing rate of a sample can be increased by decreasing the freezing temperature, but also by decreasing the sample thickness, effectively reducing the heat transfer resistance.[62] The freezing rate can significantly influence the morphology of the dried materials. For nanocellulose, it has been shown that a uniaxial temperature gradient while freezing can lead to anisotropic ice crystal growth which aligns the nanoparticles with the temperature gradient (Figure 2.5a & 2.5b), while a uniform temperature gradient produces a homogeneous distribution of ice crystals throughout the material creating non-connected pores (Figure 2.5c & 2.5d).[63]

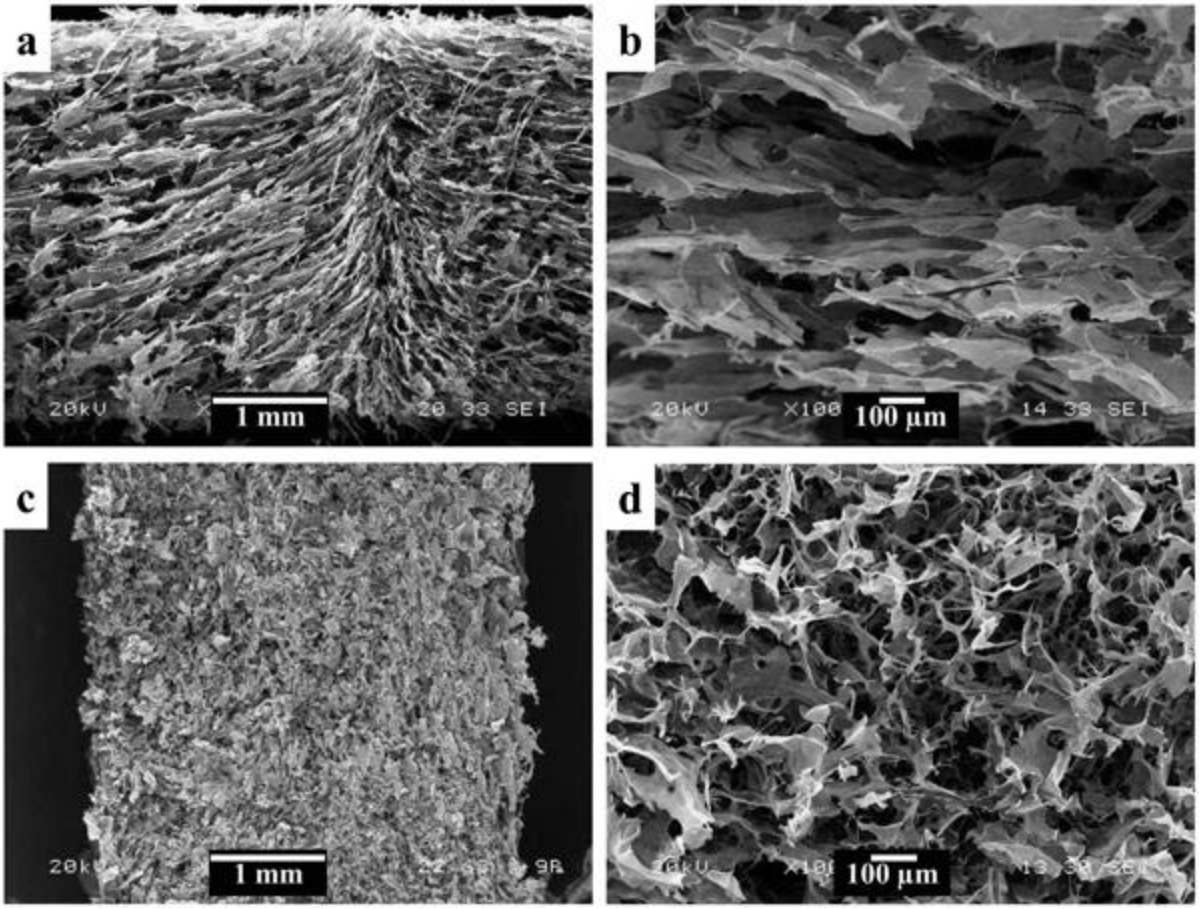

Figure 2.5. Scanning electron microscopy (SEM) images of CNF aerogels, showing the effect of freezing geometries on the microstructures of freeze dried aerogels with (a,b) having aligned layers of CNF and (c,d) having homogenously distributed pores. Figure reproduced from Jiménez-Saelices et al.[63]

The preservation of structure during freeze drying stems predominantly from the avoidance of capillary forces that arise from the evaporation of a solvent during heated drying.[64] As a liquid is heated and changes into a gas phase, surface tension of the remaining liquid pulls at the solid it is adhered to and can cause collapse. Another benefit from drying materials at low temperatures, is that it avoids deteriorating thermally sensitive compounds. Nevertheless, freeze drying is not

industrially feasible for all drying applications mainly because it is a batch process and requires a large energy input and long drying times.[44]

2.3.2 Spray drying

Spray drying is the process of atomizing a liquid sample and subjecting it to a hot gas, typically air, for a short period of time to quickly evaporate out water. The process requires significantly less energy than freeze drying, and can operate at a larger scale in a continuous system.[45,65,66] In general, using heat to remove water through evaporation can be a less expensive and faster route for drying large amounts of materials. Conversely, slower heating processes like oven drying subject materials to significant capillary forces over time which can collapse structures.[67] The effects of capillary forces can be reduced by rapidly heating samples and increasing the surface area to reduce exposure time required for drying.[67] Spray drying is also used extensively in industrial drying processes almost exclusively for creating dry powders.[65,66] However, spray drying can degrade thermally sensitive materials by exposing them to high heat if they are not suitably protected by a material barrier.

The temperature of the heated air (inlet temperature) and the temperature at the exit of the drying chamber (outlet temperature) influence the drying rates and surface morphology by creating pressure gradients around the sprayed samples. Additionally, the process of atomization, the formation of small droplets, shears the liquid feed sample which can damage sensitive structures such as microcapsules.[68] In similar spraying processes such as paint spraying, the pumping process of bringing the liquid feed to the nozzle, subjects the liquid to shear rate values ranging from 1-100 s^{-1}, while atomization has values as high as 10^6 s^{-1}.[69] The atomization step controls droplet size of the liquid feed and significantly influences drying rates, particle morphology and size

distribution.[70] Other spray drying parameters including feed pump rate, aspiration, and feed formulation/concentration, should all be considered to select optimal drying settings.

Spray drying has been used for drying nanocellulose at both the lab and industrial scale.[71,7] Spray drying CNFs produces fibrous agglomerates, while spray drying CNCs typically forms "mushroom cap" shaped aggregates (Figure 2.6).[72] Spray dried CNC aggregates typically measure from 5–30 μm and form a fine granular powder, but require additional energy (sonication) to break up the aggregates into a nano-dispersed colloidal suspension in water.[73] While drying, CNCs in acid form are able to orient themselves into the lowest energy position due to electrostatic repulsion between the charged surfaces, resulting in dense packing of CNCs into aggregates.[74] Spray drying CNCs in the neutralized form (exchanging the H^+ counterion with Na^+) allows for improved redispersibility.[73] The formation of CNC-CNC aggregates can be limited through additives that impart steric hindrance; adding a non-ionic surfactant to the liquid feed produces hollow dried particles that have improved wettability and thus redispersed better in water,[75] and uncharged non-adsorbing polymers like polyethylene glycol can also improve redispersibilty. When spray drying CNCs or CNFs, the liquid feed must have a relatively low concentration of nanocellulose of around 1.5–3 wt.% due to the increased viscosity above this threshold which can cause blockage in the spray dryer nozzle.[76]

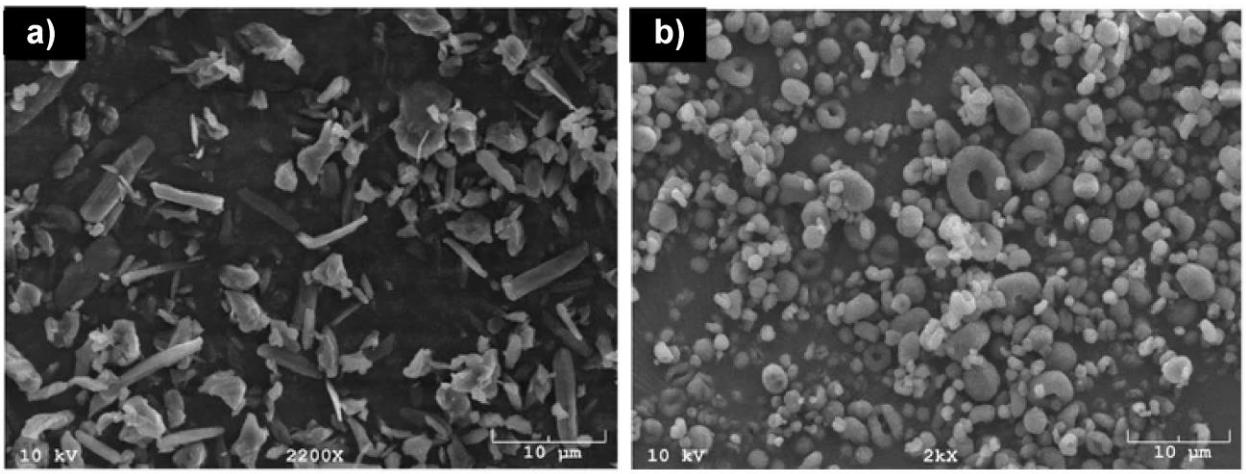

Figure 2.6. Scanning electron microscopy (SEM) images of spray dried (a) CNFs, forming fibrous aggregates, and (b) CNCs forming "mushroom cap" shaped aggregates. Figure adapted from Peng et al.[72]

2.3.3 Spray freeze drying

Spray freeze drying is a process that uses freeze drying but adds an initial atomization step to achieve smaller sized powders than conventional freeze drying.[77] Rather than using conventional freezing, spray freeze drying involves atomizing the liquid feed into liquid nitrogen (−196 °C) to rapidly form small frozen droplets and then sublimate the solvent. This step reduces the size of ice crystals that form from the freezing of water which reduces their impact on the structure of the final dried material and removes the need for mechanically grinding into a powder after drying.[78] The rapid freezing of the atomized droplets during spray freeze drying traps the internal phase throughout the wall material matrix to form microspheres which can help prevent phase separation.[79] Spray freeze drying (but not with nanocellulose) has been used to reduce oxidation of sensitive oils while drying microemulsions compared to freeze drying and spray freeze drying, and to achieve more porous morphologies.[51,80,81]

2.3.4 Drying CNC stabilized emulsions

Freeze drying emulsions stabilized by CNCs has typically been used for templating foams and aerogels where the oil is removed from the material rather than encapsulated and stored. To do so, low triple point oils, such as toluene or cyclohexane, are used in the Pickering emulsions whereby sublimation removes both the water and encapsulated oil to produce a porous CNC foam[82,83] or aerogel.[84] Previously in our group, oil-in-water Pickering emulsions have been stabilized with CNCs in combination with methylcellulose (MC) to create a completely bio-based copolymer encapsulation system that could be freeze dried into oil powders at relatively low concentrations of stabilizer.[85,86] The addition of tannic acid (TA), a plant-extracted polyphenol, to the surface of these CNC-MC microcapsules allows for the freeze dried powders to be redispersed in water to reform emulsions with little energy input requirements.[86]

Recently, spray drying has been used to prepare oil emulsion powders with CNCs used alone[49] and with co-stabilizers[87] as the wall material. Both studies report very high amounts of stabilizer used to encapsulate the oils such that the final dried material is primarily stabilizer and not oil.[49,87] This work aims to use small amounts of stabilizer to successfully encapsulate and redisperse various types of oils.

Lastly, while spray freeze drying has been explored for the production of nanocellulose aerogels and microspheres, to the best of our knowledge, has not been used to dry CNC-stabilized emulsion powders.[88,74,78] Spray freeze drying Pickering emulsions stabilized by polysorbates,[51] maltodextrin,[80] and silicate[81] (and not nanocellulose) have recently been shown, mostly as proof of principle. This thesis work demonstrates the first spray freeze dried CNC-stabilized oil powder

but moreover, systematically compares the three drying techniques mentioned: freeze drying, spray drying, and spray freeze drying of CNC-MC-TA emulsions.

2.4 Fibre spinning

Nanocellulose can be used to form continuous cellulosic fibres (also called filaments) without the requirement to first dissolve the cellulose. Nanocellulose fibres have been produced using various conventional fibre spinning techniques including dry spinning,[89] wet spinning,[90] and dry jet wet spinning (Figure 2.7).[91] These techniques involve the preparation of a nanocellulose dispersion dope, typically a solvent-gel or hydrogel, which is extruded through a narrow orifice (spinneret) and the solvent is removed. In dry spinning, the dope is extruded into air and evaporation removes the solvent whereas in wet spinning, coagulation is used to remove the solvent in a liquid bath. Dry jet wet spinning is a combination of the two techniques where the extruded dope is exposed to a small air gap prior to entering the coagulation bath. Coagulation is the simultaneous removal of solvent, often water, from the nanocellulose dispersion and the counter diffusion of the coagulant liquid. Coagulants used in wet spinning of nanocellulosic fibres need to have some polarity, be miscible in water, and possess hydrogen-bonding ability.[92] Coagulants used in wet spinning of nanocellulose include ethanol, isopropyl alcohol and acetone.[93] Non-woven matrices of ultrafine nanocellulose fibres have been prepared using a technique known as electrospinning, where an electric field is established between the needle tip and a fibre collector, whereby the solvent is evaporated as the fibre is ejected across the high-voltage field.[94,95]

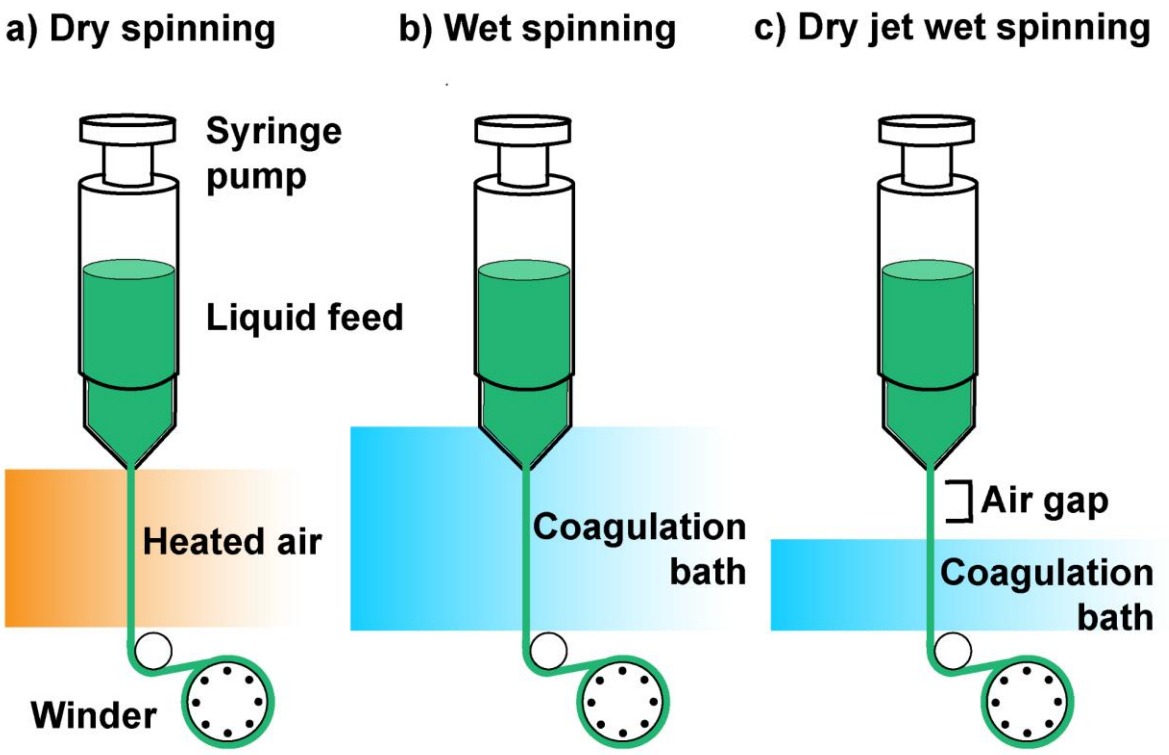

Figure 2.7. Schematic representation of common fibre spinning processes used for the preparation of nanocellulose fibres including (a) dry spinning, (b) wet spinning and (c) dry jet wet spinning.

Pure CNF fibres were first produced by wet spinning 2,2,6,6-tetra-methylpiperidinyl-1-oxyl (TEMPO) oxidized CNFs from tunicate and wood pulp by wet spinning from a 1 wt.% CNF liquid feed.[90] By better aligning the CNFs during extrusion, fibres with improved mechanical properties have been demonstrated.[96,97,98] CNCs have been used as additives to nanocomposite fibres to improve tensile strength and toughness.[99] Furthermore, CNCs have been combined with MC to produce a highly ductile bio-based fibre through wet spinning.[100]

A fibre can be used as an encapsulation system by surrounding an interior core component with an external sheath analogous to a tube with a filled centre. This can be achieved using a coaxial extrusion system, where the spinneret is composed of two (or more) needles aligned coaxially, one

inside the other (Figure 2.8). This allows for the simultaneous extrusion of an exterior shell component and an internal core component. Coaxial extrusion has been used to produce hollow CNF fibres, where the core is filled with air, as well as cellulose acetate and guar gum fibres with CNF-filled cores.[91,101] CNCs have been added as reinforcement agents in core-shell fibres prepared by electrospinning.[102,103] Herein we demonstrate coaxial fibres with oil cores and outer CNC-MC sheaths and discuss the advantages of emulsions/oil powders vs. filled fibres as encapsulation methods.

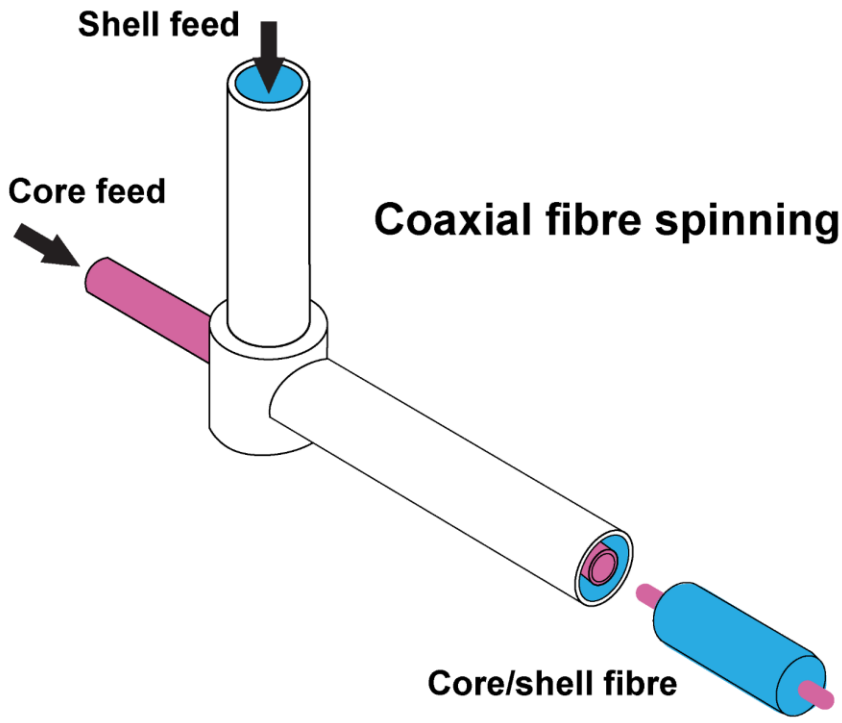

Figure 2.8. Schematic representation of coaxial fibre spinning needle (or spinneret) used to produce core (pink) and shell (blue) encapsulated fibres.

Chapter 3: Comparison of techniques for drying cellulose nanocrystal Pickering emulsions into oil powders

3.1 Abstract

A recent push for surfactant-free products driven by environmental awareness has propelled the use of bio-based materials in place of petroleum-derived components. However, both the formulation and processing need to be considered for scale-up feasibility and environmental sustainability. This work investigated the drying of corn oil-in-water emulsions stabilized by cellulose nanocrystals (CNCs), methyl cellulose (MC), and tannic acid via freeze drying, spray freeze drying, and spray drying. All three techniques produced oil powders with low moisture content and high encapsulated oil content (>90%). The oil powders could be redispersed in water by hand shaking to reform the original emulsion, and could be stored dry for weeks without oil leakage (in the fridge). The release of oil from the powders on hydrophobic substrates (at room temperature) was controlled by changing the CNC and MC stabilizer content; the spray freeze dried samples were the most tunable. The three drying techniques imparted different surface morphologies that were linked to powder redispersibility and oil release properties. The lack of freezing (and associated ice crystal growth) in spray drying minimized oil droplet agglomeration and it was the fastest, most scalable, and least energy intensive drying technique of the three, but it was also the most sensitive to emulsion concentration and susceptible to instabilities associated with high temperature and shear stress. It was demonstrated that essential oils with a range of interfacial tensions and volatilities (e.g., jojoba, lavender, tea tree oil) could also be encapsulated in spray dried oil powders. This general encapsulation strategy can be tailored based on the drying technique selected, uses plant-based industrially-produced feedstocks, works with commercially-

relevant oils, and will hopefully contribute to the development of sustainable emulsions and oil powders for food, pharmaceutical, agricultural, and cosmetic applications.

3.2 Introduction

The microencapsulation of oils to form oil-filled powders by spray or freeze drying is a commonly used approach for food processing and is a new area of interest for the pharmaceutical, agricultural, and cosmetic industries.[12] Oil powders offer opportunities to either be redispersed to reform liquid emulsions, or to be used in their dry form to reduce weight for transportation, or to incorporate "protected" oil into new systems.[12] These powders made from dried emulsions allow the preservation of sensitive oils (or oil-soluble compounds) by creating a material barrier around them that can, for example, prevent oxidation.[104] Applications of oil powders include drink powders, targeted and controlled drug delivery, livestock feed additives, and cosmetic powders.[105,12,106,107,108] Increasing concern regarding the environmental sustainability of products has led to growing interest in the development of bio-based materials for the encapsulation of oils, rather than using petroleum-derived surfactants.[109] Numerous bio-based encapsulating agents including natural gums, carbohydrates, animal and plant proteins, lipids, fats, waxes, lecithins, and lignocellulosic fibers have been used to stabilize oil-in-water (o/w) emulsions.[9]

An emulsion consists of small droplets of a liquid dispersed throughout a separate immiscible liquid, whereby the droplets are stabilized by molecular or particulate "shells" at the interface. Conventional emulsions use small molecule surfactants as the interfacial stabilizing layer, while Pickering emulsions use solid particles. The key difference between the two emulsion types is that Pickering emulsions have solid particles irreversibly adsorbed at the oil-water interface, whereas in conventional emulsions, surfactant molecules are continuously adsorbed and desorbed at the

oil-water interface.[27,110] The more permanent shell formed around each droplet in a Pickering emulsion improves emulsion stability against coalescence and flocculation, and makes the encapsulation robust enough to withstand various stresses, such as those that occur during drying.[111]

Cellulose nanocrystals (CNCs), are rod-shaped crystalline nanoparticles isolated from cellulose, with the potential to be used as encapsulating agents in Pickering emulsions due to their morphological, mechanical, and chemical properties.[8,35,112] CNCs can be produced from cellulosic sources such as cotton or wood following various routes, but are commonly isolated by sulfuric acid hydrolysis which imparts anionic sulfate half-ester groups on the surface of the nanoparticles.[7] Though colloidally stable, sulfated CNCs are not ideal for stabilizing oil-water interfaces due to their strong interparticle repulsion; however, screening the electrostatic repulsion with salt (NaCl) or desulfating the CNCs facilitates closer packing of the nanoparticles at the interface and leads to more stable emulsions.[8,113]

Our previous work has shown that adsorbing a non-ionic water-soluble polymer, such as methyl cellulose (MC), onto the surface of the CNCs also allows for the formation of highly stable emulsions that can be dried into powders by freeze drying (FD).[85,86] Further addition of tannic acid (TA), a plant-derived polyphenol, acts as a crosslinker and condenses the emulsion shell, which allows the oil powders to be redispersible in water with simple hand shaking (i.e., there is no need for high energy mixing like ultrasonication or homogenization to reform the emulsion).[86] Due to the stable emulsions demonstrated previously and the surface active nature of MC, the combination of CNCs with MC is herein used to produce Pickering emulsions destined to be dried, and where redispersibilty is required, TA is added to "set" the emulsion shell and prevent MC entanglement

as droplets come together. We also note that emulsions with nanocellulose and MC have recently been demonstrated as an emulsion-based dope for additive manufacturing due to their extreme stability, further showing the promise of this system in a range of applications.[114]

Essential oils are commonly used around the world for their scents or medicinal properties, and their increasing use in commercial applications is powered by growing demand for natural products.[115] Essential oils are plant-derived oils composed of mixtures of volatile aromatic compounds, namely terpenoids, phenylpropanoids, and aliphatic compounds.[116] Their abilities to be incorporated into products is limited by a combination of sensitivity to light and oxygen, high volatility, and interfacial tension.[117,118] In this work, we demonstrate an encapsulation system that work for oils with a variety of properties, including essential oils, where the encapsulation can either be in liquid form (the emulsion) or a solid-like oil powder, dried following various drying techniques.

Lyophilization or FD, is a widely used water removal process common in food and pharmaceutical processing, renowned for its preservation of sensitive compounds. However, its industrial acceptance is not guaranteed as the process is slow, non-continuous, and energy intensive.[44] FD involves the initial freezing of a material, during which ice crystals nucleate and grow in the solvent, excluding solute around them, followed by sublimation whereby the solvent is removed. FD with water-based systems normally produces a flaky monolithic material that may be powder-like but with large non-uniform particles, and can be mechanically ground to achieve a fine powder.[119] Some examples where FD gives a flowable powder have been reported, where using a solvent, such as *tert*-butanol, to replace a portion of the water in the dispersion reduces the ability of the particles to aggregate by providing steric hindrance between neighbouring particles.[120] This

approach has been shown to work for freeze dried CNC dispersions to improve redispersibility.[121,122] For nanocelluloses in water, the microstructure of the freeze dried material is predominantly determined by the freezing rate, concentration, and particle properties.[55,123] Milling or grinding would not be feasible to process more sensitive freeze dried materials such as microemulsions, and the use of petrochemical solvents would no longer make the system water-based.

Spray drying (SD), also commonly used in many industries, atomizes a liquid feed and exposes it to a hot gas, typically heated air, to evaporate the solvent from the mixture creating a powder. Spray drying can be much faster and is a semi-continuous process using significantly less energy than freeze drying; however, the liquid feed is exposed to many more stresses (Table 3.1). The fixed and manufacturing costs of industrial SD are around 8 and 5 times less than FD, respectively.[45]

There are a number of reported examples of using SD to dry o/w Pickering emulsions, however, many use non bio-based encapsulation materials or stabilizers with low commercial viability.[124,30] Specifically, spray dried emulsions stabilized by silica nanoparticles[125] have been demonstrated and the few SD examples using bio-based and food grade stabilizers include cellulose nanocrystals,[49,87] cellulose nanofibrils, [126] chitosan, [127] and plant proteins[128].. SD allows materials to not be affected by ice crystal formation wherein solids are excluded from slow water freezing front and forced together, nevertheless, it subjects the material being dried to (a) high heat which can damage sensitive encapsulated compounds and break emulsions, (b) capillary forces which can collapse the microcapsule walls, and (c) high shear forces from fine atomization through the nozzle.[129,78,69]

To overcome some of the disadvantages of SD, spray freeze drying (SFD) has more recently been introduced. SFD is similar to conventional FD, however, instead of freezing the sample gradually in a freezer before lyophilizing, it is atomized into a cryogenic fluid to instantly freeze the fine droplets and the frozen sample is then placed in the freeze dryer, which impedes the growth of larger ice crystals. SFD has been investigated for drying nanocellulose suspensions into highly porous materials (aerogels), and the effect of SFD drying parameters on nanocellulose particle size, morphology, porosity, crystalline structure and dispersibility in polymer matrices have been compared to FD and SD.[88,78,74] To the best of our knowledge, only one example of Pickering emulsions dried by SFD exists in the literature, wherein halloysite mineral stabilizers led to porous microstructured fine powders without shrinkage or deformation.[81] However, SFD has not been tested as a drying technique for emulsions stabilized by nanocelluloses previously.

Table 3.1. Stresses incurred on the liquid feed (in this work, an o/w Pickering emulsion) for the three drying techniques investigated: freeze drying, spray freeze drying and spray drying.

	Stresses			
	Heat	Capillary forces	Shear	Large ice crystal formation
Freeze drying (FD)	No	No	No	Yes
Spray freeze drying (SFD)	No	No	Yes	No
Spray drying (SD)	Yes	Yes	Yes	No

Two studies by Esparza et al.[49] and Xie et al.[87] have looked at using SD to dry a similar CNC stabilized Pickering emulsions to produce dry oil powders. The first study produced SD hempseed oil powders stabilized by CNCs alone at concentrations of ca. 1.1 to 1.4 g of CNCs per g of oil; the powders produced were stable against oil leakage.[49] To produce stable powders, multiple layers of CNCs (theoretically 10-14 layers) were required to sufficiently encapsulate the hempseed oil

suggesting that CNCs alone would not be a suitable wall material for higher oil fraction formulations.[49] The second study produced redispersible SD camellia oil powders stabilized by ca. 0.03 g of modified CNCs (complexed with carboxymethyl cellulose sodium) per g of oil, along with hydroxypropyl methylcellulose as a co-stabilizer at 0.5 g per g of oil.[87] Xie et al. concluded that cellulose derivatives were the best performing co-stabilizers in the modified CNC Pickering emulsions; they reduced the coalescence of droplets during SD, and increased the redispersibility of the powders.[87] This work showed that co-stabilizers, specifically cellulose derivatives, can be used as matrix formers allowing for spray dried emulsion powders to be produced with relatively low amounts of CNCs.[87] Overall, however, both examples used a large amount of total stabilizers and only investigated SD as a drying technique.[49,87]

Herein, we explore the impact of the three drying techniques, FD, SFD, SD, on drying emulsions and compare the resulting oil powders in terms of composition, oil release and redispersibility in water. To the best of our knowledge, no comparison studies of the drying methods exist and SFD has not been used to produce nanocellulose-stabilized oil powders previously. We demonstrate that dry oil powders with targeted performance can be tailored by adjusting the emulsion concentration, stabilizer content, and drying technique. Another important aim of this work is to reduce the amount of stabilizer required for producing oil powders and to use a simple emulsification process compared to the past work with a lengthy multistep protocol[87] to improve the overall industrial feasibility. Lastly, we show the ability of our CNC-MC Pickering emulsion system to encapsulate a variety of oils, including corn oil, lavender oil, tea tree oil, and jojoba oil, offering a one-size-fits-all encapsulation strategy for a variety of commercial applications.

3.3 Materials and methods

3.3.1 Materials

Methyl cellulose (MC, 400 cP), tannic acid (TA), Nile red, 2-[4-(2-hydroxyethyl)piperazin-1-yl]ethanesulfonic acid (HEPES buffer) were all purchased from Sigma-Aldrich. NaCl was purchased from Fisher Chemical. Corn oil was produced by Mazola, and jojoba oil, lavender oil and tea tree oil were purchased from Gaia Garden (Vancouver, BC). All water used was Milli-Q grade with a resistivity of 18.2 MΩ cm (Barnstead GenPure Pro, Thermo Fisher Scientific, Waltham). CNCs were prepared from cotton Whatman ashless filter aid by sulfuric acid hydrolysis as described in previous work.[130] The average dimensions of the CNCs were 128 × 8 nm measured by atomic force microscopy (AFM) and the surface charge content was 203 ± 6 mmol/kg CNCs determined by conductometric titration.[7] CNCs used in this work were in the acid form.

3.3.2 Methods

3.3.2.1 Preparation of Pickering emulsions

Emulsions composed of 20/80 corn oil/water stabilized by 0.25 wt.% CNCs and 0.25 wt.% MC (in the aqueous phase) were prepared as described previously,[86] and sonicated using a probe sonicator (Sonifier 450, Branson Ultrasonics) in 6 mL batches for 80 s with 50% pulses at 60% output in an ice bath. All samples contained 20 mM HEPES buffer and 50 mM NaCl in the water phase. For the emulsions prepared with TA (i.e., those designed to be redispersible after drying), 0.5 wt.% TA was added (in the aqueous phase) to the prepared CNC-MC emulsions and stirred and sonicated again in 45 mL batches for 90 s with 50% pulses at 60% output. “High stabilizer content” CNC-MC-TA corn oil emulsions were prepared with double the stabilizers, i.e., 0.5 wt.% CNCs and 0.5 wt.% MC. Nile red was dissolved in corn oil at a concentration of 0.03 mg/mL and emulsified to produce CNC-MC corn oil emulsions with dyed oil phase for CLSM imaging.

The initial 20/80 o/w emulsion was diluted with water to study the effect of emulsion concentration on processing: 1.5, 2, 4, and 20× dilutions by volume correspond to approximately 13/87, 10/90, 5/95, and 1/99 o/w ratios, respectively. Emulsions containing lavender oil, tea tree oil, jojoba oil, and oil mixtures (lavender and corn oil), were prepared at 10/90 o/w with "high stabilizer" content and without TA and were diluted 4× before drying. Initial emulsion droplet size was measured for the 1.5× dilution by laser diffraction using a Malvern Mastersizer 3000 (Malvern Panalytical, UK). All emulsions were stored in the fridge at 4 °C.

3.3.2.2 Drying of the emulsions

Three techniques, FD, SFD and SD, were used to dry the Pickering emulsions into powders (base case: a 30 mL sample of 20/80 o/w with 1.5 wt.% total stabilizer and then dilutions of 1.5, 2, 4 and 20× by volume). For FD, the samples were first left in the freezer at -17 °C overnight and then transferred to the freeze dryer (Labconco, Missouri). The SFD samples were initially atomized using a gravity feed spray gun (DeWalt, Maryland) at 1 bar of pressure into an insulated aluminum pan containing liquid nitrogen (−196 °C) then placed in the freeze dryer. Time in the freeze dryer was approximately 72 h for the most dilute FD and SFD samples. The SD samples were spray dried using a laboratory scale spray dryer (Buchi B-290, Switzerland) equipped with a two fluid nozzle. The inlet temperature was set at 90 °C with the outlet temperature between 50−55 °C. The spray gas flow of the compressed air was calculated to be 414 L/h, and the aspirator was at 75%. The feeding rate was approximately 2.1 mL/min whereby spray drying a batch took 20-300 min depending on the emulsion dilution. The emulsion feed was stirred throughout feeding into the spray dryer. Dried oil powders were stored in the fridge at 4 °C.

3.3.2.3 Redispersed oil droplet size analysis

After drying, powders were added to water and vortex mixed for 10 s. FD, SFD and SD powders (produced from emulsions at four dilutions of 1.5, 2, 4 and 20× the initial emulsion volume) were characterized. The "agglomerated" particle size of the redispersed emulsion droplets was measured using a Malvern Mastersizer 3000 (Malvern Panalytical, UK). The primary droplet size was analyzed by optical microscopy using a Nikon Eclipse LV100N POL microscope equipped with a Nikon DS-Ri2 camera (Nikon Instruments, Tokyo, Japan) at 50× magnification and measured using ImageJ analysis software with 50 droplets measured per sample. The values reported are the mean droplet size with their standard deviation.

3.3.2.4 Atomic force microscopy (AFM)

CNC length and height were measured from AFM images generated using a Jupiter XR atomic force microscope (Asylum Research - Oxford Instruments, Santa Barbara, CA, USA) in blue drive air tapping mode using an FS-1500 lever (resonance frequency: 1500 kHz; spring constant: 6 N m-1; tip material: Si; Asylum Research – Oxford Instruments). To prepare samples for AFM imaging, silicon wafers were treated with UV and ozone (UV/Ozone ProCleanerTM, BioForce Nanosciences Inc., Ames, IA) for 15 min before being spin coated with a 0.1 wt.% aqueous polyallylamine hydrochloride (PAH) solution using a WS-650-23 Spin Coater (speed: 3000 rpm; acceleration: 2300 rpm s-1; hold time: 30 s; Laurell Technologies, North Wales, PA), and rinsed with purified water. A 0.001-0.0025 wt.% CNC suspension was spin coated onto the PAH-coated Si wafer for the individual particle analysis. AFM height images were post treated in Gwyddion (polynomial background substitution and alignment of rows). Particle analysis was performed manually using ImageJ by selecting 50 non-touching particles, with a circularity less than 0.5, per image. Three images were acquired per sample. The distribution and quartile values of the heights,

lengths and aspect ratios of the CNC samples were determined and are reported with their standard error (Supporting Information (Appendix A), Figure A1).

3.3.2.5 Surface coverage calculation

CNC surface coverage on the CNC-MC-TA corn oil emulsion droplets was calculated using Equation 1, as previously described.[85,8]

$$C = \frac{mD}{6h\rho V} \qquad \text{Equation 1}$$

Where C is the ratio of the theoretical maximum surface area of one side of the CNCs to the total surface area of the emulsion droplet, m is the mass of CNCs, D is the volume mean diameter, D[4,3] of the emulsion droplets, h is the CNC height, 8 nm (determined by AFM measurements, Supporting Information (Appendix A), Figure A1), V is the volume of oil in the emulsion, and ρ is the density of CNC (1.59 g/cm^3).[100]

3.3.2.6 Thermogravimetric analysis (TGA)

A thermogravimetric analyzer instrument (model Q500, TA instruments-Water LLC, New Castle, DE) was used to measure the water content of the oil powders after drying (sample mass: 10-15 mg). Control samples of individual oils (corn oil, lavender oil, tea tree oil and jojoba oil) and FD stabilizers (CNC, MC, TA, HEPES buffer and NaCl) were measured separately. The samples were first equilibrated to 30 °C and then measured from 30–600 °C at ramp rate of 10°C/min under N_2 (40 mL/min). Measuring the area under the derivative thermogravimetric (DTG) curves, which are the rate of weight change plotted against temperature, of specific temperature intervals was used for quantifying approximate composition of materials.[131,132] Water content was measured between 30 and 120°C, stabilizer content between 150 and 325°C, and corn and jojoba oil content between

325 and 600°C, based on the controls. The dry oil powders encapsulating essential oils (jojoba oil, tea tree oil and lavender oil) were analyzed by TGA starting at 25°C. The temperature range used to determine lavender and tea tree oil content in the SD powders was 30–150°C.

3.3.2.7 Confocal laser scanning microscopy (CLSM)

The CNC-MC-TA corn oil emulsions and redispersed dry powders were prepared whereby the corn oil was stained with Nile red and then visualized on glass slides with sealed cover glass using a confocal laser scanning microscope (Olympus FV1000) at 60× magnification.

3.3.2.8 Cryogenic scanning electron microscopy (cryo-SEM)

Cryogenic scanning electron microscopy was performed using an FEI (now Thermo Fisher Scientific) Helios NanoLab 650 SEM/FIB system equipped with the Quorum PP3010T cryo system at 4D LABS (Simon Fraser University). Dry oil powders (individual and clusters of particles) were dropped onto a sticky carbon tape covered SEM stub and then frozen in liquid nitrogen. The frozen samples were then transferred to an SEM stage maintained at -140 °C for imaging as is (no coating), with a beam of 1 keV at 13 pA.

3.3.2.9 Oil release measurement

Emulsions with normal and double the stabilizer content were prepared and dried to test the oil release properties of the powders. The “high stabilizer content” CNC-MC-TA corn oil emulsion (with 0.5 wt.% CNCs and 0.5 wt.% MC) was dried by FD, SFD and SD and its oil release on waxed weighing paper (VWR brand, VWR International) was compared to the regular CNC-MC-TA corn oil emulsion (with 0.25 wt.% CNCs and 0.25 wt.% MC) designated as “low stabilizer content”. Each oil powder (ca. 200 mg) was placed on a sheet of waxed weighing paper at room

temperature (21°C) for 10 min then removed carefully by compressed air leaving only the oil residue. The change in mass of the waxed paper was measured gravimetrically.

3.3.2.10 Rheological behavior of Pickering emulsions

The viscosity of the emulsions at varying dilutions (1.5, 2, 4, and 20× the initial emulsion volume) was measured with a rheometer (MCR 302, Anton Paar, Germany), using cone plate geometry (CP50-1). The viscosity was tested over a shear rate range of 0.01 to 10 s^{-1} at 25°C and at 40°C.

3.3.2.11 Interfacial tension of oils

The interfacial tension of the oils was measured using a custom-built Pendant Drop Tensiometer equipped with a Flea3 FL3-U3-32S2M (Teledyne FLIR LLC, Wilsonville, OR) camera. Single drops of the aqueous phase were dispensed using a 14 gauge blunt needle into a standard quartz cuvette filled with 2-3 mL of oil. One frame was captured every 5 s by the camera for a total time of 15 min. The single frames were analyzed using OpenDrop (University of Melbourne and Monash University, Version 3.3.1), an open-source analysis tool for Pendant Drop experiments. The interfacial tension value at t = 15 min was used to compare between treatments. All measurements were performed in triplicates. Reported values are mean interfacial tensions with standard deviation.

3.4 Results and discussion

3.4.1 Pickering emulsion stability

Prior to drying the CNC-MC-TA corn oil-in-water emulsions into oil powders, their stability was assessed. As expected, the Pickering emulsions were highly stable against droplet coalescence over 25 days of storage (Figure 3.1). No significant change in oil droplet size distribution, or volume moment mean diameter (D[4,3], Figure 3.1 inset values) was observed over time. The D[4,3]

droplet diameter of ca. 7 μm falls within the range of other reported stable emulsions stabilized with CNCs, and with other particle stabilizers.[133,134] The primary droplet size of the initial emulsion was measured by optical microscopy to be 5 ± 2 μm (Supporting Information (Appendix A), Figure A2). The relatively small droplet size (for Pickering emulsions) and high stability to coalescence is attributed to the synergistic emulsifying ability of CNCs combined with surface active, water-soluble polymers, such as MC.[85,87,135]

TA is added after the emulsions are produced to cross-link/condense the stabilizing shell through catechol binding, as described previously.[86] However, we note that TA addition led to a slightly larger average droplet size than for CNC-MC only stabilized emulsions, whereby some droplet agglomeration due to TA bridging was inferred. According to Equation 1, the CNC surface coverage at the oil droplet–water interface is 92%, which is above the reported minimum coverage of 84% required to prevent droplet coalescence of emulsions made from CNCs with a similar aspect ratio.[111] The surface coverage calculation also suggests minimal "free" CNCs in suspension as the stabilizer has not been added in excess. A highly-stable emulsion with good surface coverage is assumed essential for the oil droplet "microcapsules" to remain intact through the drying processes.

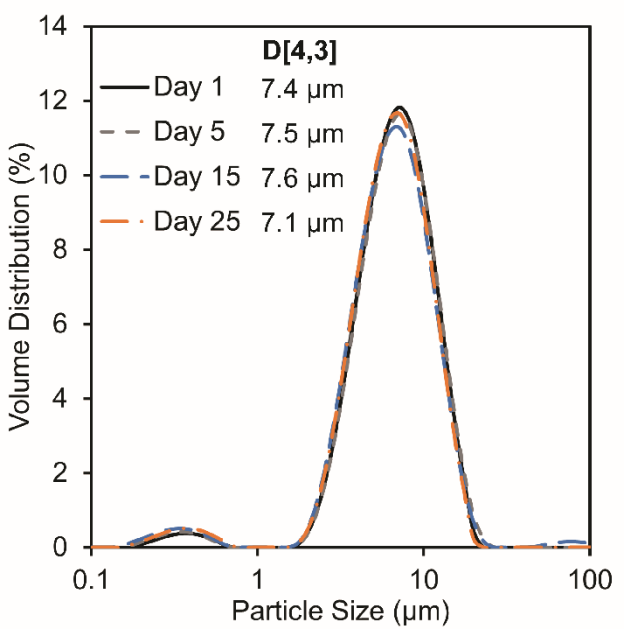

Figure 3.1. Oil droplet size distribution and (inset values) volume moment mean diameter (D[4,3]) determined by laser diffraction for the CNC-MC-TA corn oil-in-water emulsion over 25 days of storage in the fridge.

3.4.2 Composition of dried oil powders and encapsulation assessment

All three drying techniques, FD, SFD and SD, produced dry CNC-MC-TA powders encapsulating corn oil; the oil powders were white and slightly waxy in appearance (Figure 3.2a). Water was fully removed through all drying techniques (Figure 3.2b) and the dry powders preserved the encapsulated corn oil (Figure 3.2c), as measured by TGA. The three powders are indistinguishable by eye and have similar textures to the touch. Water contents calculated (from the mass loss between 30°C and 120°C in Figure 3.2b) were 0.22% for FD, 0.12% for SFD and 0.27% for SD. Despite the higher temperatures used in SD, the faster SD process (ca.1 hour) was not as effective at removing water as the slower low-pressure sublimation process (72 hours); however, the differences were minor, and all materials are considered fully "dried".

The encapsulated oil content was also determined by TGA. All spray dried powders had an initial peak at 287°C ("i" in Figure 3.2c) attributed to the stabilizers (CNC, MC, TA, HEPES buffer, NaCl), and a peak at 405°C ("ii' in Figure 3.2c) attributed to corn oil, indicating that a large proportion of oil remained after drying. The FD and SFD powders had similar TGA curves to SD powders (Supporting Information (Appendix A), Figure A3). Specifically, the SD powder contained 6.7% stabilizer and 90.7% oil, with the remaining mass being attributed to residual ash and moisture. The stabilizer and oil content of the FD powder was 5.9% and 93.3%, and for the SFD powder was 4.4 % and 92.5%. While all oil contents were high (perfect theoretical encapsulation would have been 92.3% oil) the drying technique with the least physical stresses, i.e., freeze drying, had the least oil loss, whereas spray drying with shear, heat and capillary force stresses, had the highest oil loss, as expected. This oil content compares to other studies that have reported "high" or "ultra high" oil content in spray dried powders stabilized with plant proteins (90% oil content),[128] whey protein (95% oil content),[136] and inorganics (nearly 90% oil content).[125]

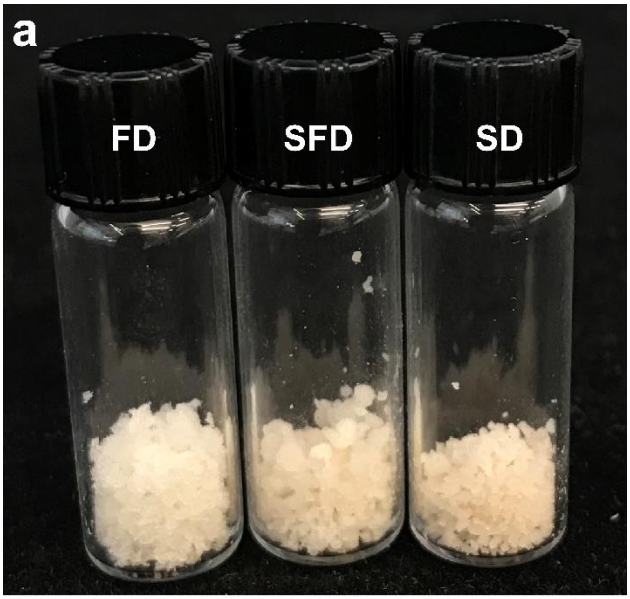
a
FD
SFD
SD

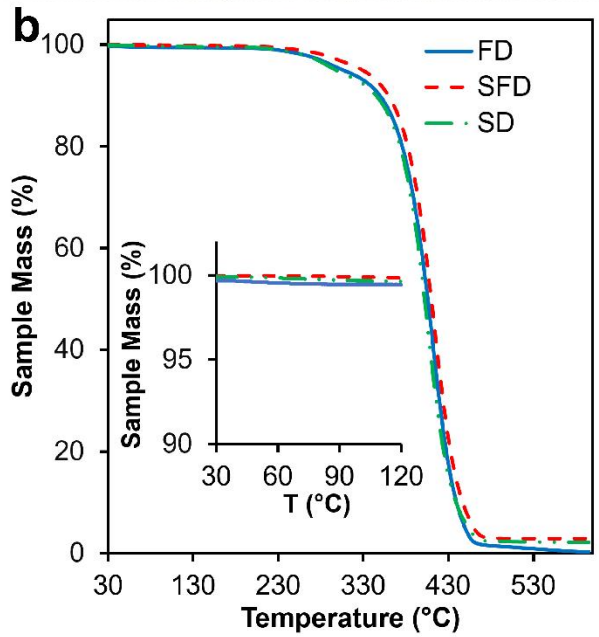
b
100
80
60
40
20
0
Sample Mass (%)
30
130
230
330
430
530
Temperature (°C)
FD
SFD
SD
100
95
90
Sample Mass (%)
30
60
90
120
T (°C)

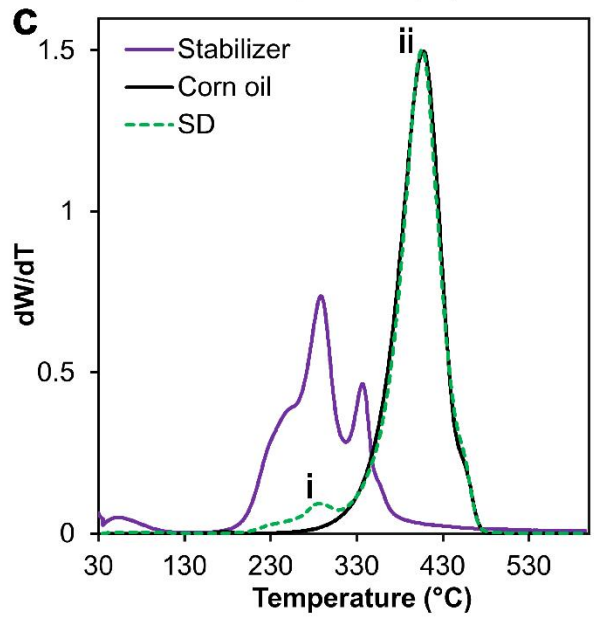
c
1.5
1
0.5
0
dW/dT
Stabilizer
Corn oil
SD
i
ii
30
130
230
330
430
530
Temperature (°C)

Figure 3.2. (a) Photograph of CNC-MC-TA corn oil-in-water emulsion samples after freeze drying (FD), spray freeze drying (SFD), and spray drying (SD). (b) TGA curves of FD, SFD, and SD powders with inset plot showing the 30-120°C range expanded where water content was calculated to be <0.3% for all powders, (c) DTG curves of the individual components (controls) and an SD oil powder (curves for FD and SFD powders are in Supporting Information (Appendix A), Figure A3a and A3b).

While the dried FD, SFD, and SD powders all contained >90% oil after drying, true encapsulation was assessed by redispersing the oil powders in water and imaging them using confocal microscopy. (That is, the TGA indicates the presence of oil but not the location in the dry oil powder, and the high shear in SD and SFD could have led to oil leakage and destruction of the droplet morphology). Figure 3.3 shows that individual microscale droplets of oil without coalescence persisted in the redispersed powders. Importantly, all three drying techniques were able to create redispersible emulsions, though powder redispersibility is discussed in more detail below. The redispersed powders contain small individual droplets similar in size to the original emulsion, but some droplet agglomeration (without coalescence) is observed after all three drying techniques.

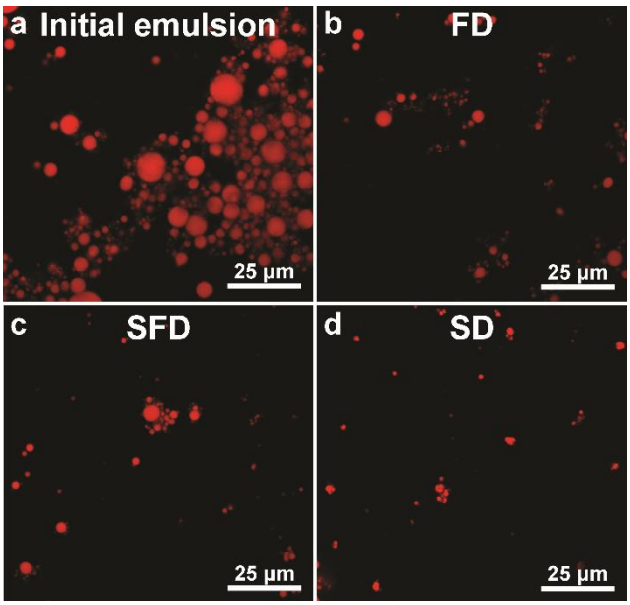

Figure 3.3. Confocal laser scanning microscopy images of (a) initial CNC-MC-TA corn oil-in-water emulsion where the oil is stained with Nile red, and images of the dried powder redispersed in water and vortexed (diluted 10-fold from original) after (b) freeze drying (FD), (c) spray freeze drying (SFD), and (d) spray drying (SD).

3.4.3 Oil powder morphology

Although SEM showed that the three dry oil powders form clumps of similar shape and size in the 1 mm range (Figure 3.4a-c), the FD, SFD and SD processes led to different surface morphologies visible at higher magnification (Figure 3.4d-f). The FD powder had a relatively smooth surface (Figure 3.4d & g), the SFD powder had a microporous structure (Figure 3.4e & 3.4h), and the SD powder had capsule-like structures (Figure 3.4f & 3.4i). The FD powder exhibited a sheet-like surface composed of stabilizer with low porosity similar to freeze dried CNC suspensions.[78] This morphology occurs due to the aggregation of CNCs during the initial slow freezing process where ice crystals grow and force particle-particle aggregation.[129] When the freezing time is reduced, in the case of SFD, larger ice crystal formation can be suppressed. Particle aggregation is not forced

to the same degree and the SFD powders maintain higher porosity morphologies. The capillary forces from the sudden temperature increase in SD also forces particle aggregation, producing densely packed surfaces on capsules.[78] It has been shown previously that the morphology of the wall of microcapsules influences the release of encapsulated components, more specifically, more amorphous surfaces with voids facilitate the diffusion of air into the microcapsules and allow more oil to escape to the surface.[137]

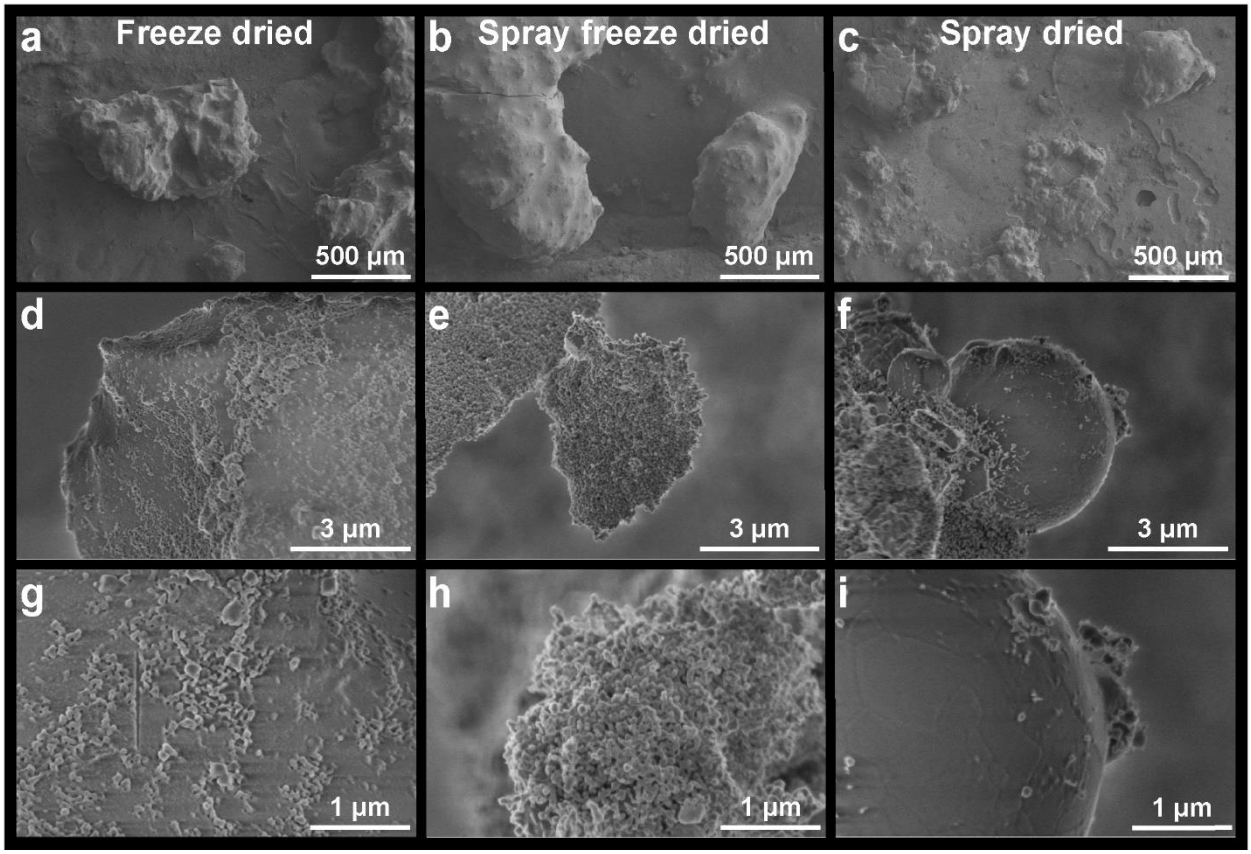

Figure 3.4. Cryo-scanning electron microscopy (cryo-SEM) images of the FD, SFD and SD corn oil powders stabilized by CNC, MC, and TA at low (top), medium (middle), and high (bottom) magnification.

3.4.4 Tailoring oil release from powders

The FD, SFD and SD oil powders can be stored for months in the fridge without observable oil leakage. Under certain conditions, however, the powders release oil slowly, and the rate is influenced by the concentration of stabilizer used in the initial emulsion, and the drying technique employed. In the regular stabilizer content FD, SFD and SD oil powders (denoted "low stabilizer content" in Table 3.2), oil release was observed when placed on waxed weighing paper at room temperature (21°C). The oil release is driven by capillary wicking from the hydrophobic porous substrate, i.e., the wax-coated weighing paper, drawing oil out of the microcapsules.[138,139] Doubling the amount of CNC and MC stabilizers in the emulsion, reduced the oil release of the powders for all three drying techniques (denoted "high stabilizer content" in Table 3.2) yet the total CNC content remains extremely low compared to other CNC-containing oil powders.[49] In fact, our "high stabilizer content" is still 4 and 10-fold less than previous works,[87,49] which is important for many envisioned applications where large amounts of excess stabilizer will change the texture and physical sensations (e.g., mouthfeel, tactile perception), reduce the "desired oil/oil soluble ingredient" to "filler" ratio, as well as increase the cost per unit of oil in the product.

The low stabilizer content powder produced by SFD released more oil than the FD and SD powders (Table 3.2). This difference is attributed to the unique microporous surface of the SFD powder (Figure 3.4). It has been shown previously that the rate of release of encapsulated material through a microcapsule wall is dependent on the ultrastructure of the shell, specifically, the quantity and size of surface micropores.[140] The SFD sample showed the largest decrease in oil release between the low and high stabilizer content powders, and the lowest oil release overall with high stabilizer content, implying that this system is most sensitive to the stabilizer content. It is challenging to compare released oil amounts directly to the literature as release is often tested in simulated liquid

environments and through accelerated studies, however we see similar trends in our release-in-air studies. For example, past work shows that microcapsules with a single core domain release encapsulated content quicker than microcapsules with multiple subdomains, and so at a higher stabilizer content, more smaller subdomains could form in the SFD powder matrices.[141] For this reason, SFD powders could be the most attractive for applications utilizing oil powders in their dry form with interest in tunable slow-release mechanisms. We emphasize that there is no visible oil leakage when the powders are placed overnight on more hydrophilic substrates such as glass at room temperature.

Table 3.2. Oil released from FD, SFD and SD powders containing the regular CNC-MC content (low stabilizer content) and doubled CNC-MC content (high stabilizer content) aged on waxed paper for 10 min at room temperature. The oil released is expressed as a percent of the total powder mass measured where encapsulated oil initially comprises ca. 90% of the powder mass. Photographs of the powder samples and resulting oil release are provided in the Supporting Information (Appendix A), Figure A4.

	Oil released from powder	
	Low stabilizer content	High stabilizer content
FD	0.92%	0.40%
SFD	2.75%	0.11%
SD	1.02%	0.44%

3.4.5 Influence of drying technique and emulsion concentration on oil powder redispersibility

To better understand if the emulsion concentration can help alleviate the physical stresses present during drying (Table 3.1), improve drying process efficiency, or change oil powder performance, a series of oil powders were produced from the same starting CNC-MC-TA 20/80 corn oil-in-water emulsion that was diluted with water 1.5, 2, 4 and 20-fold. All four dilution factors, with all three drying techniques, led to redispersible powders that gave micron-scale oil droplets when gently vortexed in water (Table 3.3). The D[4,3] of the redispersed powder droplets ranged from ca. 20-90 μm which is significantly larger than the initial emulsion (ca. 7 μm, Figure 3.1), which suggested that perhaps droplet coalescence had been induced during drying. However, optical microscopy (Table 3.3 and Supporting Information (Appendix A), Figure A5) showed that the mean primary droplet diameter remained almost the same as the initial emulsion (5 ± 2 μm) and was not statistically significantly different amongst the three techniques, therefore the larger sizes seen by laser diffraction were primarily due to droplet agglomeration but not coalescence.

The redispersed oil droplet D[4,3] values (Table 3.3), and size distribution plots (Supporting Information (Appendix A), Figure A6), display a general trend that the order of drying techniques from largest to smallest agglomerate size is FD > SFD > SD. This trend is rationalized based on stresses during drying techniques as follows. Ice crystal growth appears to dominate the agglomeration mechanism where all non-water components are excluded from the freezing front and are forced into close proximity. Thus, when ice growth is suppressed by fast freezing, less agglomeration occurs leading to the FD > SFD trend. As SD avoids this ice crystal growth mechanism entirely it has the least droplet agglomeration (at normal dilutions).[142] On the other

hand, SD subjects emulsion droplets to capillary forces which create some agglomeration, but seemingly less than the ice crystal templating occurring in FD and SFD. Oil powders were also stored for weeks in the fridge and then redispersed in water, and still no droplet coalescence was observed (Supporting Information (Appendix A), Figure A7).

For all drying techniques there is an observed agglomerate size jump between the three lower dilutions (1.5, 2 and 4×) and the highly diluted 20× samples (Table 3.3). As noted previously, the 20× sample is 99% water, and when left unagitated, a rapid formation of a creamed layer was observed. No overnight creaming was observed in the more concentrated (1.5, 2 and 4×) emulsions. This was expected as it has been shown that decreasing the droplet concentration of the dispersed phase increases the creaming velocity of o/w emulsions.[143] The large agglomerates in the 20× FD sample are likely due to the rapid creaming that occurs while the sample is frozen slowly, creating a close-packed layer of droplets frozen together prior to sublimation which appear to remain in the dried state. This close packing of droplets from creaming does not occur to the same extent during in the short freezing step of SFD hence the SFD < FD agglomerate result. In SD, the sample is agitated while being pumped and while creaming may still occur slightly, we believe the agglomeration is primarily attributed to the long run time which exposes the dried sample to high temperatures due to the heating of the equipment and collection glassware – more concentrated emulsion batches are spray dried significantly faster and exposed to less heat during SD and have the smallest agglomerates.

Table 3.3. Oil droplet size of redispersed CNC-MC-TA oil powders prepared from emulsions diluted with water by a factor of 1.5, 2, 4 and 20 and dried by FD, SFD and SD. Values displayed are from the Mastersizer particle size analyser (laser diffraction) as well as from digital analysis of optical microscopy images.[a]

		Agglomerated oil droplet size (Laser diffraction)		Primary oil droplet size (Optical microscopy)	
	Dilution	**D[4,3] (µm)**	Span	**Mean size (µm)**	STDEV
Freeze Dried	FD1.5	68.4	5.4	7	±4
	FD2	57.9	4.6	8	±6
	FD4	52.2	4.5	8	±4
	FD20	93.9	2.9	7	±3
Spray Freeze Dried	SFD1.5	56.6	2.6	5	±2
	SFD2	57.9	2.6	6	±4
	SFD4	52.9	2.3	6	±3
	SFD20	60.9	3.3	8	±7
Spray Dried	SD1.5	44.6	3.8	7	±5
	SD2	42.5	4.2	6	±3
	SD4	24.4	2.8	5	±2
	SD20	82.2	3.2	6	±4

[a] The initial emulsion before drying had a D[4,3] of 7.4 µm with span of 1.3 and primary droplet size from optical microscopy of 5 ± 2 µm.

In terms of processability, the emulsion concentration had the largest impact on the SD process. In the low dilution samples (1.5 and 2×), clogging was observed in the nozzle of the spray dryer, no clogging occurred for the 4× and 20× dilutions. During an SD run, the emulsion is fed into a nozzle that was found to be around 40°C (measured with IR thermal camera) – this heating increases the viscosity of the emulsion which can cause partial or complete nozzle blockage (Supporting Information (Appendix A), Figure A8). The increase in viscosity is due to thermogelation of the MC component in the emulsion (linked to the cloud point of MC), and has been previously reported to cause blockages during spray drying.[144] The thermal transition temperature for MC (as measured by an increase in the elastic modulus) is known to be approximately 39 °C,[145] although the presence of CNCs and background electrolyte are expected to shift this value slightly.

We measured the viscosity of the emulsions as a function of temperature and as expected, the more dilute the emulsion, the less effect the themogelation of MC had on the viscosity of the overall system (Figure 3.5). An impressive decrease in viscosity by ca. one order of magnitude was recorded between the 1.5× and 20× dilution measured at 40°C. All of the CNC-MC-TA emulsions displayed shear-thinning, and their viscosity values are similar to other reported CNC-stabilized o/w emulsions.[146,147]

While SD is the best option to achieve the smallest redispersed emulsion droplets, due to its limited agglomeration and small primary droplet size, the high temperature is problematic because it induces themogelation of MC. This themogelation was mitigated by dilution (or could perhaps be avoided by nozzle cooling) which would be critical to achieve a continuous drying process.

Another advantage is that SD dries emulsions quickly, taking hours rather than days by FD and SFD; however, high dilution of the emulsions (without increasing the sample feed rate) increases the overall run time proportionately. Longer processing times are obviously undesirable and furthermore, could allow for more emulsion creaming/phase separation in the feed and/or could potentially damage the collected dried oil powder by overheating.

The emulsion concentration also impacted the yield of powder collected, having the greatest effect on the SD technique. At high concentrations (1.5 and 2× dilutions), frequent nozzle blockages reduced the total amount of powder collected. The 4× dilution sample increased the total powder yield by a factor of 7 compared to the 1.5× sample, by overcoming the clogging of the nozzle with MC. However, further diluting the sample by 20× reduced the total yield due to the powder leaking oil and sticking to the walls from the overheating of the cyclone during the longer run. Low yields in SD are common and are generally remedied through optimization studies and furthermore, industrial scale SD equipment is known to be much more efficient than bench top spray dryers.[135,148] FD and SFD both had higher yields than SD (where powder loss is primarily attributed to human error), however the scalability of these processes is limited due to being batch rather than continuous processes. Spray drying a larger amount of emulsion led to a higher percentage yield showing that the SD yield is dependent on scale due to a fixed initial "sacrificial" layer that coats the cyclone prior to powder gathering in the collection vessel. Therefore, we suggest the optimization of the dilution factor and feed volume for each emulsion system to eliminate the risk of nozzle blockage without unnecessarily extending the run time or reducing yield.

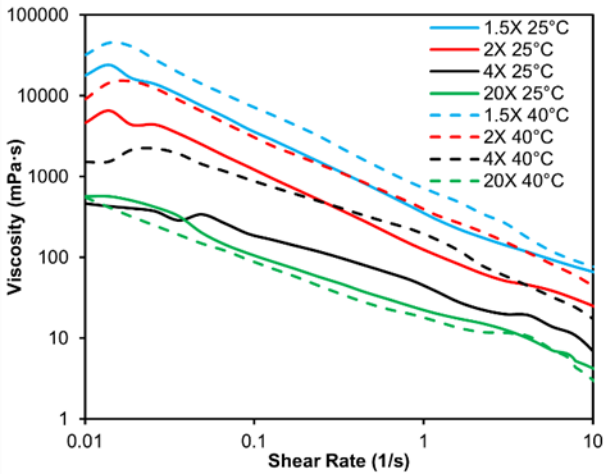

Figure 3.5. Viscosity of CNC-MC-TA 20/80 corn oil-in-water emulsions, diluted by 1.5× (blue), 2× (red), 4× (black) and 20× (green) the initial volume, measured at an increasing shear rate at 25°C (solid line), and 40°C (dashed line).

3.4.6 Example application: Encapsulation of higher value oils into dry powders

The oil encapsulation strategy demonstrated herein was also shown to be applicable to plant oils with varying volatilities and interfacial tensions. Similar emulsions stabilized by CNCs and MC were prepared using jojoba oil, lavender oil, and tea tree oil and were spray dried into dry oil powders. Plant and essential oils are complicated mixtures often containing some surface active compounds and different fatty acid compositions such that physical-chemical profiling is challenging and water-solubility, hydrophobicity and boiling point remain difficult to pin point. Essential oils are often classified by evaporation rates known in the fragrance industry as “notes” (i.e., top, middle, and base notes are oil classes ranked from fastest to slowest evaporation). We have used representative essential oils from different classes, with tea tree oil being a middle note and lavender oil being a top-middle note. Additionally, tea tree and lavender oil possess antibacterial properties.[149,150] Jojoba oil is a popular carrier oil, used to protect other essential oils from oxidation in cosmetic formulations and is growing in value in the pharmaceutical

industry.[151,152] These oils were selected to represent a variety of oil properties and potential applications.

The D[4,3] droplet size of the initial jojoba, lavender and tea tree oil emulsions were all in the micron range but were larger compared to the corn oil emulsions (Table 3.4). Optical microscopy images showed no droplet agglomeration or coalescence (Supporting Information (Appendix A), Figure A9); the increase in droplet size is attributed to the varying water solubility and interfacial tensions of the different oils (Table 3.4). The D[4,3] droplet size was found to increase with decreasing interfacial tension which has been shown previously in surfactant-stabilized essential o/w emulsions.[153] Furthermore, oils with higher polarity generally have decreased interfacial tension and increased susceptibility to Ostwald ripening and coalescence.[118] Tea tree and lavender oil each contain some water-soluble terpenoids that could explain their increased droplet size caused by Ostwald ripening.[154,155] Despite the large oil droplets in essential oil-containing emulsions, the Pickering emulsions were highly stable with minimal droplet size change over time. By eye, no changes were observed over a week except for a fine oil layer that was observed in the jojoba oil emulsion (Supporting Information (Appendix A), Figure A10).

Table 3.4. Interfacial tension of oils and resulting emulsion droplet size and span. The corn oil emulsion is the same as discussed previously (Figure 3.1) while the jojoba oil, lavender oil, and tea tree oil emulsions were made with double the stabilizer content and without TA.

	Oil only		**CNC-MC emulsion**		**SD powder**
	Interfacial tension (mN/m)	Oil classification[a]	D[4,3] (μm)	Span	Encapsulated oil (%)
Corn	17.6 ± 0.6	-	7.4[b]	1.3[b]	90.7[b]
Jojoba	16.4 ± 0.4	Carrier	33.8	7.1	55.4
Lavender	14.3 ± 0.1	Top/middle note	40.7	3.0	7.5
Tea tree	12.7 ±0.3	Middle note	128.2	2.0	7.8

[a] Based on role used in commercial fragrances
[b] Corn oil emulsion made with TA, the rest made without TA

The essential oil-containing emulsions can be spray dried which preserves the essential oils in oil powder form (Supporting Information (Appendix A), Figure A11). The use of CNC-MC as encapsulating wall materials shows promise for processing oils with a wide range of degradation temperatures (Supporting Information (Appendix A), Figure A12). However, comparing the area under the peaks of the DTG curves shows that the amount of oil in the dried essential oil powders is less than the SD corn oil powder. The percentage of essential oil that is preserved through drying can be increased by utilizing corn oil as a carrier oil and blending it with the more volatile/thermally sensitive oils prior to emulsification. Spray drying CNC-MC stabilized 100% lavender oil emulsions resulted in dried powders with only 7.5% of lavender oil. Conversely, combining lavender oil with 50% and 90% corn oil and then emulsifying and spray drying the mixture led to powders with 5.7% and 2.5% lavender oil, respectively (Supporting Information (Appendix A), Figure A13). This means that reducing the amount of lavender oil in the initial oil phase of the emulsion by 50% (replacing it with corn oil instead) only reduces the amount of

lavender oil in the dried powder by 24% compared to the 100% SD lavender oil powder. Similarly, when the amount of lavender oil is reduced by 90%, the amount of lavender oil in the SD powders is only reduced by 67% compared to the 100% SD lavender oil powder. Corn oil prevents the loss of lavender oil during spray drying, and less lavender oil in the oil phase means proportionately less lavender oil lost while drying.

Spray drying and coacervation are the most common techniques used for the microencapsulation of essential oils.[12] It has been shown that higher yields of essential oil powder can be achieved for the microencapsulation of lavender oil[156] and tea tree oil[157] by spray drying when large amounts of stabilizer are used. Jojoba oil has been encapsulated by phase separation but not spray dried previously.[158] The CNC-MC encapsulation technique was not optimized for each oil and adjusting emulsification energy, stabilizer content, and drying parameters could be used to tune for desired powder properties. The resulting powders could be used, for example, in biomedical textiles, cosmetics, and functional coatings/packaging.

3.5 Conclusion

Emulsions with a low concentration of bio-based stabilizers (namely CNC, MC and TA) were amenable to a range of drying techniques (with varying physical stresses) – i.e., FD, SFD, and SD. These processes led to fully dried oil powders that were also redispersible due to extreme emulsion stability to coalescence. Freezing (i.e., ice templating) as part of the drying process was found to be particularly detrimental because it promoted droplet agglomeration (albeit without coalescence), however faster freezing could partially mitigate this effect, making SFD preferred over FD. While shear and capillary forces present during SD were expected to be problematic, the remarkable stability of CNC-MC-TA emulsions allowed them to withstand these stresses with

only minor complications due to MC gelation at the higher temperatures required for SD. Overall, the SD process is recommended for drying CNC-stabilized emulsions because it produces redispersible powders with the same high oil content as FD and SFD, but generally offers faster processing speed with lower energy consumption.

The concentration of emulsion stabilizer can be used to tailor the oil release from dried oil powders for all three drying techniques. For specific applications where tunable slow-release of oil is desired, the SFD process would be ideal due to its microporous surface and range of tunability of oil release. For example, active agents such as fertilizers or fungicides could be encapsulated in the oil phase spray freeze dried into powders to be used as slow-release soil amendments for agricultural applications. This encapsulation strategy is also applicable to oils with varying volatilities, and interfacial tensions. The SD powders were able to encapsulate essential oils commonly used in cosmetics which could allow for the incorporation of sensitive scented oils in dry products.

3.6 Acknowledgements

We gratefully acknowledge support from the University of British Columbia Bio Imaging Facility (RRID: SCR_021304) and the Natural Sciences and Engineering Research Council of Canada (NSERC) including a Canada Graduate Scholarship to M.M. and Discovery Grant [RGPIN-2018-06818] to E.D.C. We thank Prof. Orlando Rojas, Prof. John Frostad and Prof. Scott Renneckar for access to equipment and expertise. E.D.C. is grateful for support and recognition through the University of British Columbia's President's Excellence Chair initiative, the NSERC E.W.R. Steacie Memorial Fellowship alongside the Canadian Foundation for Innovation (John R. Evans Leaders Fund) used to purchase the AFM, and for the spray dryer (project number 38623) used in

this work. We would also like to acknowledge the work of Jude Abu-Namous & Dr. Marcus A. Johns, who characterized the CNCs by AFM imaging and conductometric titration. We are grateful for the contribution from Dr. Roxanne Fournier who conducted the interfacial tension measurements.

Chapter 4: Encapsulation of liquid oil in cellulose nanocrystal-stabilized dry jet wet spun fibres

4.1 Abstract

This work presents a novel method to incorporate liquid oil into composite materials by encapsulating it inside a fibre. Using a coaxial wet-spinning extrusion system, an outer "sheath" of cellulose nanocrystals with adsorbed methyl cellulose was formed around droplets of trapped tea tree oil throughout the core of the fibre. The dried fibres had alternating thinner sections, with a diameter of ca. 500 μm, and wider sections, of ca. 2 mm, where the encapsulated oil was situated. Continuous spinning was demonstrated supporting the scalability of this dry jet wet-spun fibre processing technique. The new encapsulation system worked with oils with different physicochemical properties (i.e., tea tree oil and corn oil). The oil-filled fibres could be stored under ambient conditions and showed signs of oil release when wetted, potentially offering controlled release for an array of applications such as bioactive wound dressings or packaging materials.

4.2 Introduction

While we work across industries towards achieving a circular bioeconomy, in which we promote the reuse and recycling of products, there are certain materials that will remain as "single use" products for the near future. Biomedical products, such as wound dressings, are not easily reused due to biohazardous risks and therefore, to still participate in the circular bioeconomy, will need to be made entirely of materials that are bio-based and biodegradable.

To reduce the chance of infection, many modern wound dressings possess antimicrobial properties from the addition of inorganic components such as silver nanoparticles. Each year, around 120

tons of silver nanoparticles are produced and used for biomedical applications.[159] Through incineration or by leaching from solid waste, silver nanoparticles are released to terrestrial and aquatic ecosystems where they can have toxic effects on many organisms.[160] Many bio-based materials with excellent antimicrobial properties exist, such as certain essential oils, however, they can be difficult to process, incorporate, and protect within a useful material format. Essential oils that have antimicrobial properties such as eucalyptus, tea tree, and lavender oil are often quite volatile and evaporate rapidly in ambient conditions.[161,162] Storing these volatile plant oils within a material and controlling their release would offer a novel antibacterial composite that could be used for biomedical applications. The main objective of this work was to demonstrate a scalable method of encapsulating volatile essential oils in nanocellulose fibres to be used in composite materials such as antibacterial wound dressings.

Though uncommon to many, the encapsulation of liquid oil within fibres is quite common in the field of electronics, such as using fibre optic cables with oil filled cores for applications as temperature sensors.[163,164,165] Essential oils have been previously encapsulated in poly ε-caprolactone (PCL), a petroleum-based biodegradable polymer, via electrospinning.[166] Extract from the St. John's wort, *Hypericum perforatum*, plant was loaded into a non-woven mat and able to offer extended release when immersed in phosphate-buffered saline, a water-based buffer solution commonly used in biological research.[166] Bio-based materials, such as alginates, have been used as shell materials to encapsulate oils within the cores of fibres using microfluidics,[167,168,169] and have been tuned to control the geometry of the entrapped oil phase.[170] Similar to microfluidic devices, wet spinning apparatuses can be modified to allow for the production of core and shell fibres. Lundahl et al., prepared wet spun fibres with guar gum and

cellulose acetate shells and cellulose nanofibril (CNF) cores for absorbent filament applications using a coaxial needle.[101] The wet-spun fibres achieved high spinning speed, showing the potential for industrial application of nanocellulosic fibres.[101]

Our previous work on oil-filled powders has demonstrated the robustness of cellulose nanocrystals (CNCs) and methyl cellulose (MC) as encapsulating materials, therefore we have chosen to use the same shell material to produce oil-filled fibres.[171] Single (uniaxial) fibres made of CNC-MC, possessing high ductility and modulus of toughness, have been produced previously by wet spinning with ethanol as the coagulation medium.[100] In the current work, a coaxial fibre spinning apparatus was designed and built, and CNC-MC (shell) and plant-based oil (core) fibres were prepared by dry jet wet spinning. This work offers a continuous lab scale process for the preparation of bio-based oil-filled fibres.

4.3 Materials and methods

4.3.1 Materials

Methyl cellulose (MC, 400 cP), isopropyl alcohol, and Nile red were purchased from Sigma-Aldrich. Corn oil was produced by Mazola, and tea tree oil was purchased from Gaia Garden (Vancouver, BC). All water used was Milli-Q grade with a resistivity of 18.2 MΩ cm (Barnstead GenPure Pro, Thermo Fisher Scientific, Waltham). CNCs were prepared in-house from cotton Whatman ashless filter aid by sulfuric acid hydrolysis as described in previous work.[130] The average dimensions of the CNCs were 128 × 8 nm measured by atomic force microscopy (AFM) and the surface charge content was 203 ± 6 mmol/kg CNCs determined by conductometric titration.[7] CNCs used in this work were in the acid form.

4.3.2 Methods

4.3.2.1 Fabrication of fibre spinning apparatus

The assembled fibre spinning apparatus shown in Figure 4.1 is comprised of several components which include: two syringe pumps (Model Fusion 4000-X & Fusion 6000-X, Chemyx, Stafford, TX) a coaxial needle (Ramehart, New Jersey), coagulation bath (home-built), collection winder (home-built), infrared (IR) dryer (1500 W Ceramic Space Heater, Brightown, USA), and a submergible conveyor belt (home-built). The coagulation bath measures around 81 cm in length to allow for long dwell time for extruded fibres. The coagulation bath was made of stainless steel to have better resistance against certain coagulation media, such as acetone or concentrated sulphuric acid, compared to polycarbonate baths. The bath sits inside of a T-slot aluminum frame with height-adjustable levelling feet. Photographs of the actual apparatus are provided in Figure 4.2.

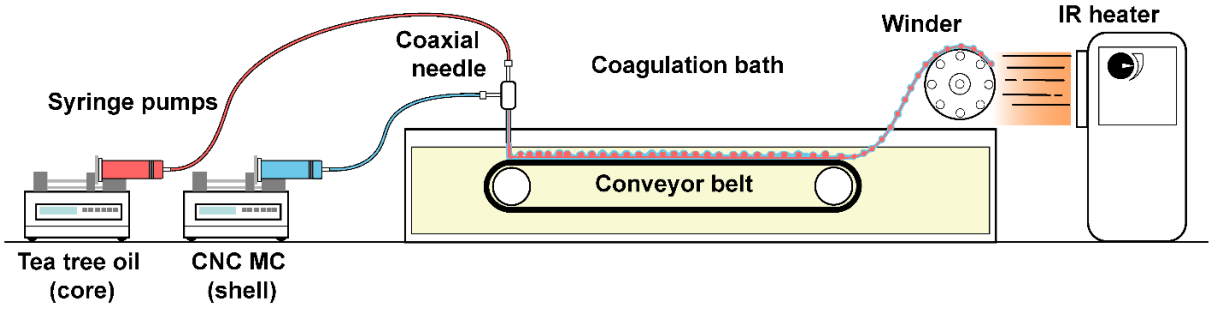

Figure 4.1. Schematic representation of wet spinning set up showing the main components as well as the two feeds, dyed tea tree oil (pink) and CNC-MC mixture (blue). Note that the placement of components in the schematic are in reverse order (process moves left to right) to the photo of the actual setup shown in Figure 4.2 (process moves right to left).

The T-slot frame acts as a rail around the bath to which the winder is attached (Figure 4.2). This allows for the adjustment of the position of the collection winder relative to the extrusion needle

to change dwell times by shortening or lengthening the distance the fibres travel immersed in the coagulation bath from the needle to the collection winder. This approach offers the ability to increase or decrease the dwell time without changing the extrusion and winding rates. The winder position along the length of the bath is adjusted by two knob fasteners set in the rail, and the winder height is adjusted by two additional knob fasteners on the "L" shaped flat-surface bracket (Figure 4.2a). Polytetrafluoroethylene (PTFE) was selected for the collection rods, that run across the winder, rather than stainless steel, to reduce the chance of fibres adhering to the surface while drying as well as reducing the weight of the winder allowing the winder to be rotated by a lower torque motor (Figure 4.2a).

A timing belt is used for the conveyor belt that is tensioned inside of an aluminum frame, all of which can be placed inside and easily removed from the coagulation bath. The conveyor belt is equipped with a variable speed motor that is elevated above the level of the coagulation liquid and transfers mechanical energy through a secondary timing belt to the main belt by a common shaft (Figure 4.2b). This motor placement eliminates the need for watertight motors in submergible conveyor belts, and allows the conveyor belt to have a slimmer and lower profile to be able to be placed inside the bath and sit below the maximum liquid level.

The fibre spinning apparatus can accommodate both wet spinning and dry jet wet spinning depending on the placement of the extrusion needle. Wet spinning can be achieved by affixing the needle to the end of the coagulation bath through the hole found 5 cm from the bottom (Supporting Information (Appendix B), Figure B1). This hole can be blocked, and the needle can be placed pointing downwards slightly above the coagulation liquid level, allowing an air gap for dry jet wet spinning, which is the geometry used in this work (Figure 4.2c).

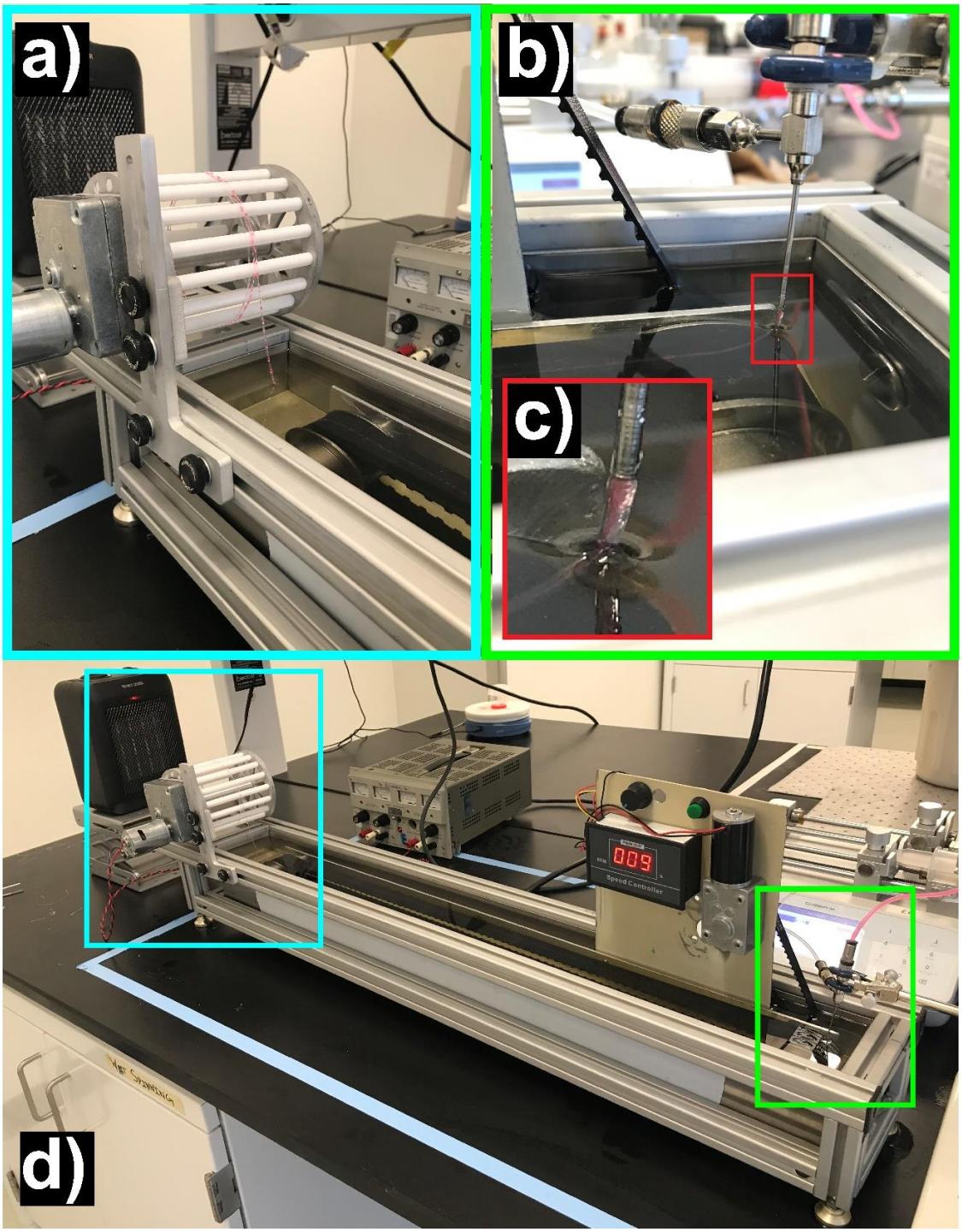

Figure 4.2. Photographs of fabricated fibre spinning apparatus in operation with insets of (a) winder collecting fibre from coagulation bath (blue inset) (b) coaxial needle extruding onto submerged conveyor belt (green inset) with (c) needle tip above liquid showing air gap (red inset) all from (d) the fibre spinning apparatus with conveyor belt placed inside coagulation bath.

4.3.2.2 Preparation of oil-filled fibres

Fibres containing encapsulated oil were prepared by dry jet wet spinning. MC was combined with ultrasonicated sulfated CNCs to form a 1 wt.% MC and 2 wt.% CNC hydrogel following the work by Hynninen et al.[100] Bubbles were removed from the hydrogel by transferring the prepared hydrogel into an open Pyrex crystallizing dish in a vacuum oven for 5 h (without heating) and then refrigerated at 4 °C overnight. This method showed significantly less bubbles than centrifugation and the removal of bubbles was crucial for successful fibre spinning. The hydrogel was then carefully transferred into a 20 mL stainless steel syringe (Chemyx, Stafford, TX). Nile red was dissolved in tea tree oil (0.1 mg/mL) and corn oil (0.1 mg/mL). A high-pressure syringe pump (Fusion 6000-X) was used to extrude the external shell material, due to its high viscosity, and a second syringe pump (Fusion 4000-X) was used to extrude the core material, oil.

The CNC-MC (shell) and dyed tea tree oil (core) feeds were extruded through a coaxial needle into the coagulation bath containing isopropyl alcohol (≥99.5%). The needle was positioned just above the surface of the isopropyl alcohol, allowing a small air gap to avoid premature coagulation at the tip that was observed during wet-spinning configuration attempts thus establishing a dry jet wet spinning configuration. The downward facing needle configuration was selected after fibre rupturing was observed in the wet spinning configuration, where segments of the newly extruded fibres would float to the surface, due to the buoyancy force exerted by the encapsulated oil, and break off, inhibiting continuous extrusion.[172] The CNC-MC and tea tree oil were extruded at rates of 0.5 mL/min and 0.1 mL/min, respectively, onto the submerged conveyor belt. The fibres were coagulated along the length of the entire bath and collected by the rotating winder and dried for 10 min using an infrared heater in a continuous process.

Optical microscopy

Fibres were analyzed by optical microscopy using a Nikon Eclipse LV100N POL microscope equipped with a Nikon DS-Ri2 camera (Nikon Instruments, Tokyo, Japan) at 5× magnification and fibres widths were measured using ImageJ analysis software.

4.4 Results and discussion

4.4.1 Fibre properties

The dry jet wet spun coaxial fibres showed alternating segments of wider oil-filled beads and narrower shell material filaments (Figure 4.3a). The collected fibres were brittle but flexible enough to be removed from the collection wheel without breaking. The fibres were stored for weeks under ambient conditions without showing signs of oil loss. The fibres possessed inherent curvature from drying on the collection wheel (Figure. 4.3b).

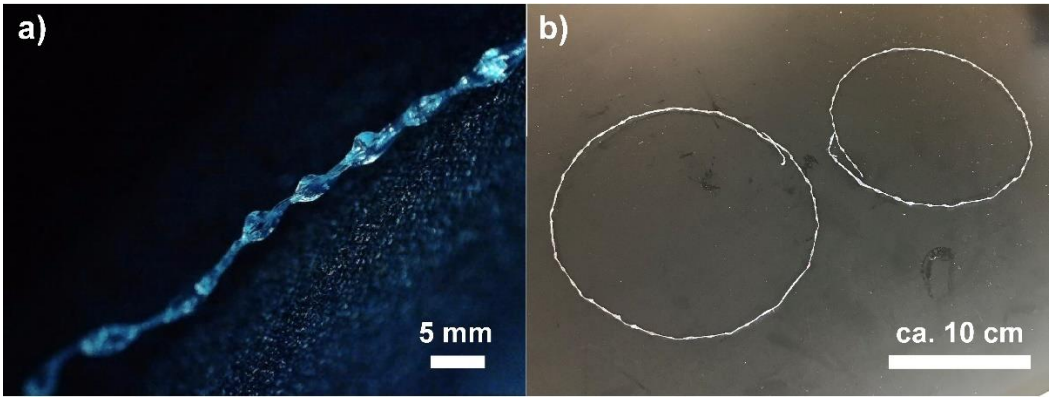

Figure 4.3. Dried tea tree oil filled CNC-MC fibre (a) showing oil-filled bead segments along the fibre and (b) long flexible fibre with curvature from drying on the winder.

The fibres exhibited iridescence which was capture by optical microscopy (Figure 4.4). The fibre had varying widths but in general the oil bead segments were ca. 2 mm and the connecting fibre segments were ca. 500 μm (Figure 4.4 inset values). The discrete encapsulated oil segments are

commonly found when encapsulating hydrophobic materials in aqueous shells due to high interfacial tension at the oil–water interface.[173] The oil bead size was slightly larger with corn oil compared to tea tree oil which agrees with the higher interfacial tension of corn oil.[171] However, continuous tubular internal phases of oil within fibres have been achieved in alginate fibres prepared by microfluidics.[170] By aligning the ends of the inner and outer glass capillaries, and increasing the flow rate of the extruded oil, continuous internal phases of oil are possible in fibres depending on the oil used.[170]

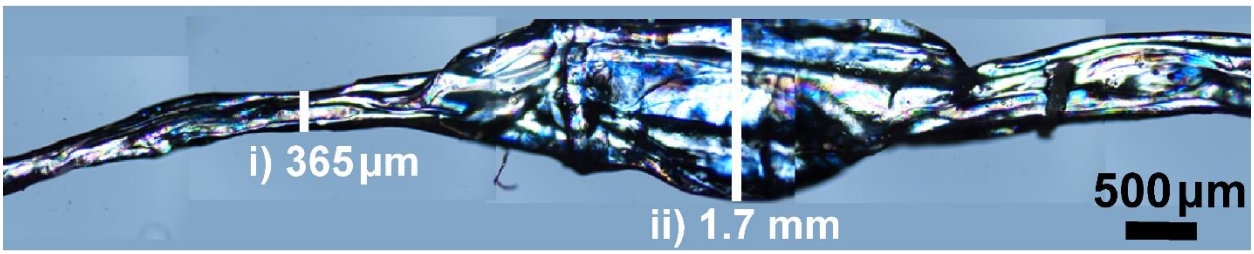

Figure 4.4. Optical microscope images stitched together to show full CNC-MC tea tree oil fibre under 5× magnification with inset measurements of (i) narrow fibre and (ii) oil-filled bead segments. Images taken with non-polarized light.

The tea tree oil was dyed pink prior to being encapsulated, and thus when extruded, is highly visible as pink beads along the fibre (Figure 4.5, left). After drying at ca. 35 °C with an infrared heater, the transition from pink beads to blue beads is observed (Figure 4.5, right). The reason for this change was not investigated as it was out of the scope of this work, however it was noted that when the two components are dried separately, without isopropyl alcohol, no blue colour occurs (Supporting Information (Appendix B), Figure B2). Additionally, the blue colour is most noticeable in the oil-filled beads and is not seen as vividly throughout the shell-material-only segments of the fibre.

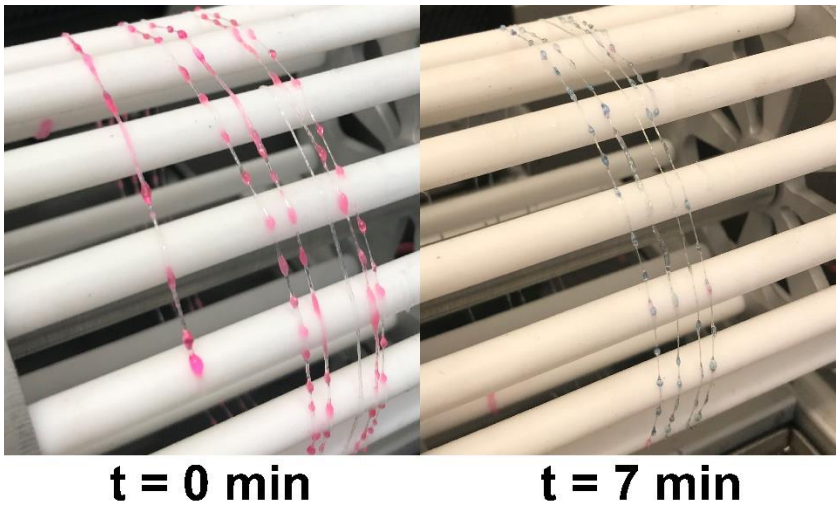

Figure 4.5. Photograph of fibre drying on the collection winder at time zero (left) when it has just been collected, and (right) after it has been dried for 7 minutes, demonstrating the change in colour of the oil-filled beads from pink to blue and the fibre from transparent to blue.

The fibres were able to release encapsulated oil when the beads were mechanically ruptured (Figure 4.6a and 4.6b). The compartmentalization of the oil along the fibre allowed for individual beads to be sheared without the neighboring beads being affected, potentially offering advantages over an oil-filled tube. The fibres also swelled when wetted with water and became softer and more malleable. When fully immersed in water, the fibres began to slowly disintegrate and the tea tree oil scent became much more discernable, demonstrating an alternative oil-release mechanism. The re-wetted fibres also showed the same colour change from blue, in the dry state to pink/purple, in the wet state (Figure 4.6c and 4.6d).

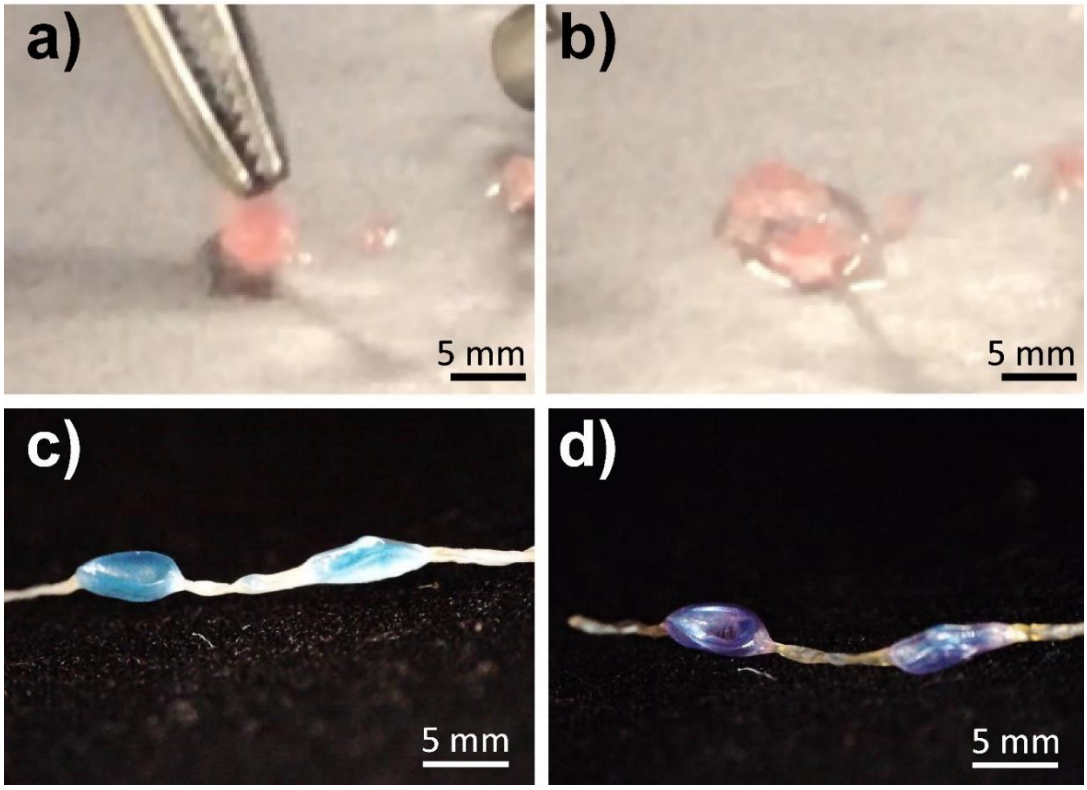

Figure 4.6. Photographs of oil-filled fibres releasing oil (a) before and (b) after shearing the oil filled bead, and (c) before and (d) after wetting with water, showing colour change.

4.4.2 Future work

Future work will explore methods to improve the mechanical properties of the fibres, perhaps by incorporating cellulose nanofibrils (CNFs) to improve their ability to be handled and potentially woven into composites textiles or coatings. Additionally, controlling the bead size of the encapsulated oil droplets in the fibre should be investigated with varying extrusion rates, coaxial needle end geometries, and inner and outer coaxial needle diameters. The resulting differences in fibre morphology should also be tested as a function of the various possible extrusion conditions. Efforts to produce continuous oil cores and not discrete beads will be attempted to demonstrate the tailorability and versatility of the fibre spinning method. Optical properties should be

investigated to better understand the observed colour changes and ways to control them. Antibacterial properties of tea tree oil, or other essential oil-filled fibres could be tested following standard testing such as that shown previously.[166,174,175] Adhesion of fibres onto different substrates could also be explored to help evaluate feasibility of their incorporation in different composite materials.

4.4.3 Potential applications

This oil-filled fibre will allow for new ways of processing, encapsulating, and releasing oils and oil-soluble materials. Being made from two cellulose components, this material offers a bio-based and biodegradable encapsulation strategy to industry where the properties of the encapsulated oil can be preserved and utilized in various applications. For example, by using tea tree oil we can make antimicrobial fibres that, when ruptured or wetted, can release liquid tea tree oil to create an inhibition zone to stop bacterial growth. This could be used as an environmentally sustainable alternative to silver nanoparticles used in commercial antibacterial materials, specifically in wound dressings. Utilizing tea tree oil in this manner was previously extremely challenging due to how quickly it evaporates, and so a simple means to encapsulate more volatile components and release them in a controlled manner can open the door for many new hybrid materials. The fibres could be used as low-tech moisture sensors or indicators by taking advantage of their colour change from dry (blue) to wetted (pink). A range of cosmetic/personal care applications could also be considered such as scented textiles. If we use a phase change material, such as coconut oil, in the oil phase of the fibre, we can create a thermally insulating material that, for example, could be added to construction composites. The collection winder could be replaced with a flat substrate to potentially produce a nonwoven mat instead of a continuous fibre. This material could even have

applications in new food product development to incorporate fats and new textures into edible products.

4.5 Conclusion

This work presents a novel method of encapsulating volatile essential oils into entirely bio-based and biodegradable fibres by dry jet wet spinning. The designed fibre spinning apparatus was able to produce continuous tea tree oil-filled fibres by utilizing a dry jet wet spinning configuration and a supporting submerged conveyor belt. The prepared fibres contain entrapped liquid tea tree oil that can be easily released by shear or by wetting. This work demonstrates the scalability of the oil-filled fibre technology, and shell/core components could be easily tailored to achieve desired fibre properties. The versatility of the presented systems offers numerous potential applications across many fields including biomedical, packaging, food/cosmetics, and construction.

4.6 Acknowledgements

We gratefully acknowledge support from the University of British Columbia Bio Imaging Facility (RRID: SCR_021304) and the Natural Sciences and Engineering Research Council of Canada (NSERC) including a Canada Graduate Scholarship to M.M. and Discovery Grant [RGPIN-2018-06818] to E.D.C. We thank Prof. Orlando Rojas for access to equipment and expertise. E.D.C. is grateful for support and recognition through the University of British Columbia's President's Excellence Chair initiative, the NSERC E.W.R. Steacie Memorial Fellowship alongside the Canadian Foundation for Innovation (John R. Evans Leaders Fund) used to purchase the AFM used in this work. We would also like to acknowledge the work of Jude Abu-Namous & Dr. Marcus A. Johns, who characterized the CNCs by AFM imaging and conductometric titration. We would like to thank Doug Yuen, who helped in the design and construction of the fibre spinning

apparatus. We are grateful for the guidance from Dr. Meri J. Lundahl & Dr. Guillermo Reyes Torres used in the development of the presented fibre spinning system.

Chapter 5: Conclusion and future work

Bioproducts, in their many forms, will play a decisive role in the implementation of a new circular bioeconomy. Displaying the ability of bio-based building blocks to be used in higher value products in the cosmetic, agricultural and biomedical industries, will help further spread the reach of the circular bioeconomy mission. In terms of material properties, some bio-based nanomaterials are poised to replace petroleum-based materials in many applications, or even enable the creation of new products, however, the steps to commercialize these technologies have been lagging. The aim of this work is to contribute to the path being built towards the development of bio-based nanomaterial products. Though the road remains long, the presented work will hopefully help in the overall circular bioeconomy movement.

In this thesis, microencapsulation of oil was achieved using bio-based nanomaterials called cellulose nanocrystals (CNCs) in combination with methyl cellulose (MC). Oil powders stabilized by CNC, MC, and tannic acid (TA) were prepared by freeze drying, spray freeze drying, and spray drying. The resulting powders contained large amounts of encapsulated oil (>90%), could be easily redispersed in water, and were able to be stored without oil leakage for weeks (in the fridge). The morphology and oil release of the powders could be tuned by adjusting the emulsion concentration, stabilizer content, and drying technique. Oils with different properties including corn oil, lavender oil, tea tree oil, and jojoba oil, were all able to be encapsulated and dried into powders offering a one-size-fits-all encapsulation strategy.

The same CNC-MC encapsulation system was used to produce oil-filled fibres. CNC-MC and tea tree oil were used to produce a coaxial shell and core fibre by dry jet wet spinning. The tea tree

oil-filled fibres could be produced continuously, and the encapsulated oil could be released by shear or wetting, offering potential applications in bio-based antibacterial wound dressings.

To add to this CNC microencapsulation work, additional steps could be taken to help these technologies along. First, higher throughput emulsification processes such as high-pressure homogenization for the preparation of CNC-MC emulsions should be explored. Additionally, investigating the changes in powder properties when conducting SFD at slightly higher temperatures (not using liquid nitrogen) could help improve industrial feasibility. Finally, optimization of parameters should be conducted for spray drying CNC-MC-TA emulsions to improve yields. For the fibres, the extrusion rates and needle diameters could be varied to see if oil-filled bead size could be tuned. The antibacterial performance of the fibres should be evaluated. For both the dried powders and coaxial fibres, the reinforcing shell materials could be further assessed, and the effect of other bio-based stabilizers, like CNF, could be tested to improve the mechanical and release properties.

References

1. Intergovernmental Panel on Climate Change. *Climate change 2022: impacts, adaptation and vulnerability*. *IPCC Sixth Assessment Report* (2022).

2. Davidson, K., Briggs, J., Nolan, E., Bush, J., Håkansson, I. & Moloney, S. The making of a climate emergency response: Examining the attributes of climate emergency plans. *Urban Clim.* **33**, 100666 (2020).

3. Shen, M., Huang, W., Chen, M., Song, B., Zeng, G. & Zhang, Y. (Micro)plastic crisis: Un-ignorable contribution to global greenhouse gas emissions and climate change. *J. Clean. Prod.* **254**, 120138 (2020).

4. De Jong, E., Higson, A., Walsh, P. & Wellisch, M. Product developments in the bio-based chemicals arena. *Biofuels, Bioprod. Biorefining* **6**, 606–624 (2012).

5. Isogai, A. Wood nanocelluloses: Fundamentals and applications as new bio-based nanomaterials. *J. Wood Sci.* **59**, 449–459 (2013).

6. Li, Y., Zheng, X. & Chu, Q. Bio-based nanomaterials for cancer therapy. *Nano Today* **38**, 101134 (2021).

7. Vanderfleet, O. M. & Cranston, E. D. Production routes to tailor the performance of cellulose nanocrystals. *Nat. Rev. Mater.* **6**, 124–144 (2020).

8. Kalashnikova, I., Bizot, H., Cathala, B. & Capron, I. New pickering emulsions stabilized by bacterial cellulose nanocrystals. *Langmuir* **27**, 7471–7479 (2011).

9. Fuchs, M., Turchiuli, C., Bohin, M., Cuvelier, M. E., Ordonnaud, C., Peyrat-Maillard, M. N. & Dumoulin, E. Encapsulation of oil in powder using spray drying and fluidised bed agglomeration. *J. Food Eng.* **75**, 27–35 (2006).

10. Singh, M. N., Hemant, K. S. Y., Ram, M. & Shivakumar, H. G. Microencapsulation: a promising technique for controlled drug delivery. *Res. Pharm. Sci.* **5**, 65 (2010).

11. Pothakamury, U. R. & Barbosa-Cánovas, G. V. Fundamental aspects of controlled release in foods. *Trends Food Sci. Technol.* **6**, 397–406 (1995).

12. Bakry, A. M., Abbas, S., Ali, B., Majeed, H., Abouelwafa, M. Y., Mousa, A. & Liang, L. Microencapsulation of oils: a comprehensive review of benefits, techniques, and applications. *Compr. Rev. Food Sci. Food Saf.* **15**, 143–182 (2016).

13. Ruckenstein, E. Microemulsions, macroemulsions, and the Bancroft rule. *Langmuir* **12**, 6351–6353 (1996).

14. Charve, J. & Reineccius, G. A. Encapsulation performance of proteins and traditional

materials for spray dried flavors. *J. Agric. Food Chem.* **57**, 2486–2492 (2009).

15. Martins, I. M., Barreiro, M. F., Coelho, M. & Rodrigues, A. E. Microencapsulation of essential oils with biodegradable polymeric carriers for cosmetic applications. *Chem. Eng. J.* **245**, 191–200 (2014).

16. Dima, Ş., Dima, C. & Iordăchescu, G. Encapsulation of functional lipophilic food and drug biocomponents. *Food Eng. Rev.* **7**, 417–438 (2015).

17. Walstra, P. Principles of emulsion formation. *Chem. Eng. Sci.* **48**, 333–349 (1993).

18. Karbstein, H. & Schubert, H. Developments in the continuous mechanical production of oil-in-water macro-emulsions. *Chem. Eng. Process. Process Intensif.* **34**, 205–211 (1995).

19. Charcosset, C., Limayem, I. & Fessi, H. The membrane emulsification process—a review. *J. Chem. Technol. Biotechnol.* **79**, 209–218 (2004).

20. Mahdi Jafari, S., He, Y. & Bhandari, B. Nano-emulsion production by sonication and microfluidization—a comparison. *Int. J. Food Prop.* **9**, 475–485 (2006).

21. Liu, E. H. & McGrath, K. M. Emulsion microstructure and energy input, roles in emulsion stability. *Colloids Surfaces A Physicochem. Eng. Asp.* **262**, 101–112 (2005).

22. Jafari, S. M., Assadpoor, E., He, Y. & Bhandari, B. Re-coalescence of emulsion droplets during high-energy emulsification. *Food Hydrocoll.* **22**, 1191–1202 (2008).

23. Rayner, M. Scales and forces in emulsification. in *Engineering Aspects of Food Emulsification and Homogenization* 3–32 (2015).

24. Baret, J. C. Surfactants in droplet-based microfluidics. *Lab Chip* **12**, 422–433 (2012).

25. Lechuga, M., Fernández-Serrano, M., Jurado, E., Núñez-Olea, J. & Ríos, F. Acute toxicity of anionic and non-ionic surfactants to aquatic organisms. *Ecotoxicol. Environ. Saf.* **125**, 1–8 (2016).

26. Patel, M. Surfactants Based on Renewable Raw Materials. *J. Ind. Ecol.* **7**, 47–62 (2003).

27. Pickering, S. U. CXCVI.—Emulsions. *J. Chem. Soc. Trans.* **91**, 2001–2021 (1907).

28. Wu, J. & Ma, G. H. Recent studies of Pickering emulsions: particles make the difference. *Small* **12**, 4633–4648 (2016).

29. Reineccius, G. Flavor production. in *Flavor Chemistry and Technology* 351–389 (CRC Press, 2005).

30. Gharsallaoui, A., Roudaut, G., Chambin, O., Voilley, A. & Saurel, R. Applications of spray-drying in microencapsulation of food ingredients: An overview. *Food Res. Int.* **40**,

1107–1121 (2007).

31. Kaplan, D. L. Introduction to biopolymers from renewable resources. *Biopolym. from Renew. Resour.* 5–6 (1998).

32. Habibi, Y., Lucia, L. A. & Rojas, O. J. Cellulose nanocrystals: chemistry, self-assembly, and applications. *Chem. Rev.* **110**, 3479–3500 (2010).

33. Iguchi, M., Yamanaka, S. & Budhiono, A. Bacterial cellulose—a masterpiece of nature's arts. *J. Mater. Sci. 2000 352* **35**, 261–270 (2000).

34. Rowland, S. P. & Roberts, E. J. The nature of accessible surfaces in the microstructure of cotton cellulose. *J. Polym. Sci. Part A-1 Polym. Chem.* **10**, 2447–2461 (1972).

35. Kedzior, S. A., Gabriel, V. A., Dubé, M. A. & Cranston, E. D. Nanocellulose in Emulsions and Heterogeneous Water-Based Polymer Systems: A Review. *Adv. Mater.* **33**, 2002404 (2021).

36. Lagerwall, J. P. F., Schütz, C., Salajkova, M., Noh, J., Park, J. H., Scalia, G. & Bergström, L. Cellulose nanocrystal-based materials: from liquid crystal self-assembly and glass formation to multifunctional thin films. *NPG Asia Mater. 2014 61* **6**, e80–e80 (2014).

37. Chen, L., Wang, Q., Kolby, •, Carlos Baez, H. •, Agarwal, U. P. & Zhu, • J Y. Tailoring the yield and characteristics of wood cellulose nanocrystals (CNC) using concentrated acid hydrolysis. *Cellulose*.

38. Moon, R. J., Martini, A., Nairn, J., Simonsen, J. & Youngblood, J. Cellulose nanomaterials review: structure, properties and nanocomposites. *Chem. Soc. Rev.* **40**, 3941–3994 (2011).

39. Tashiro, K. & Kobayashi, M. Theoretical evaluation of three-dimensional elastic constants of native and regenerated celluloses: role of hydrogen bonds. *Polymer (Guildf).* **32**, 1516–1526 (1991).

40. Bushell, M. *et al.* Particle size distributions for cellulose nanocrystals measured by atomic force microscopy: an interlaboratory comparison. *Cellulose* **28**, 1387–1403 (2021).

41. Habibi, Y. Key advances in the chemical modification of nanocelluloses. *Chem. Soc. Rev.* **43**, 1519–1542 (2014).

42. Jiménez Saelices, C. & Capron, I. Design of Pickering micro- and nanoemulsions based on the structural characteristics of nanocelluloses. *Biomacromolecules* **19**, 460–469 (2018).

43. Hu, Z., Ballinger, S., Pelton, R. & Cranston, E. D. Surfactant-enhanced cellulose nanocrystal Pickering emulsions. *J. Colloid Interface Sci.* **439**, 139–148 (2015).

44. Fang, Z. & Bhandari, B. Spray drying, freeze drying and related processes for food ingredient and nutraceutical encapsulation. *Encapsulation Technol. Deliv. Syst. Food Ingredients Nutraceuticals* 73–109 (2012).

45. Santivarangkna, C., Kulozik, U. & Foerst, P. Alternative drying processes for the industrial preservation of lactic acid starter cultures. *Biotechnol. Prog.* **23**, 302–315 (2007).

46. Bouraoui, M., Richard, P. & Fichtali, J. A review of moisture content determination in foods using microwave oven drying. *Food Res. Int.* **26**, 49–57 (1993).

47. Chua, K. J., Chou, S. K., Ho, J. C. & Hawlader, M. N. A. Heat pump drying: recent developments and future trends. *Dry. Technol.* **20**, 1579–1610 (2002).

48. Desobry, S. A., Netto, F. M. & Labuza, T. P. Comparison of Spray-drying, Drum-drying and Freeze-drying for β-Carotene Encapsulation and Preservation. *J. Food Sci.* **62**, 1158–1162 (1997).

49. Esparza, Y., Ngo, T. D. & Boluk, Y. Preparation of powdered oil particles by spray drying of cellulose nanocrystals stabilized Pickering hempseed oil emulsions. *Colloids Surfaces A Physicochem. Eng. Asp.* **598**, 124823 (2020).

50. Morais, A. R. D. V., Alencar, É. D. N., Xavier Júnior, F. H., Oliveira, C. M. De, Marcelino, H. R., Barratt, G., Fessi, H., Egito, E. S. T. Do & Elaissari, A. Freeze-drying of emulsified systems: A review. *Int. J. Pharm.* **503**, 102–114 (2016).

51. Karthik, P. & Anandharamakrishnan, C. Microencapsulation of Docosahexaenoic Acid by Spray-Freeze-Drying Method and Comparison of its Stability with Spray-Drying and Freeze-Drying Methods. *Food Bioprocess Technol.* **6**, 2780–2790 (2013).

52. Ratti, C. Hot air and freeze-drying of high-value foods: a review. *J. Food Eng.* **49**, 311–319 (2001).

53. Wang, W. Lyophilization and development of solid protein pharmaceuticals. *Int. J. Pharm.* **203**, 1–60 (2000).

54. Pawelec, K. M., Husmann, A., Best, S. M. & Cameron, R. E. Ice-templated structures for biomedical tissue repair: from physics to final scaffolds. *Appl. Phys. Rev.* **1**, 021301 (2014).

55. Jiang, F. & Hsieh, Y. Lo. Super water absorbing and shape memory nanocellulose aerogels from TEMPO-oxidized cellulose nanofibrils via cyclic freezing–thawing. *J. Mater. Chem. A* **2**, 350–359 (2013).

56. Mendoza, L., Hossain, L., Downey, E., Scales, C., Batchelor, W. & Garnier, G. Carboxylated nanocellulose foams as superabsorbents. *J. Colloid Interface Sci.* **538**, 433–439 (2019).

57. Wang, M. *et al.* Modifying native nanocellulose aerogels with carbon nanotubes for mechanoresponsive conductivity and pressure sensing. *Adv. Mater.* **25**, 2428–2432 (2013).

58. Jiang, S., Zhang, M., Li, M., Liu, L., Liu, L. & Yu, J. Cellulose nanofibril (CNF) based aerogels prepared by a facile process and the investigation of thermal insulation performance. *Cellulose* **27**, 6217–6233 (2020).

59. Yildirim, N., Shaler, S. M., Gardner, D. J., Rice, R. & Bousfield, D. W. Cellulose nanofibril (CNF) reinforced starch insulating foams. *MRS Online Proc. Libr.* **1621**, 177–189 (2014).

60. Arias, A., Heuzey, M. C., Huneault, M. A., Ausias, G. & Bendahou, A. Enhanced dispersion of cellulose nanocrystals in melt-processed polylactide-based nanocomposites. *Cellulose* **22**, 483–498 (2015).

61. Nakagawa, K., Hottot, B., Vessot, S. & Andrieu, J. Modeling of freezing step during freeze-drying of drugs in vials. *AIChE J.* **53**, 1362–1372 (2007).

62. Nowak, D. & Jakubczyk, E. The Freeze-Drying of Foods—The Characteristic of the Process Course and the Effect of Its Parameters on the Physical Properties of Food Materials. *Foods* **9**, 1488 (2020).

63. Jiménez-Saelices, C., Seantier, B., Cathala, B. & Grohens, Y. Effect of freeze-drying parameters on the microstructure and thermal insulating properties of nanofibrillated cellulose aerogels. *J. Sol-Gel Sci. Technol.* **84**, 475–485 (2017).

64. Koch, F. *et al.* Increasing the aperture of x-ray mosaic lenses by freeze drying. *J. Micromechanics Microengineering* **25**, 075015 (2015).

65. Sosnik, A. & Seremeta, K. P. Advantages and challenges of the spray-drying technology for the production of pure drug particles and drug-loaded polymeric carriers. *Adv. Colloid Interface Sci.* **223**, 40–54 (2015).

66. Anandharamakrishnan, C., Rielly, C. D. & Stapley, A. G. F. Effects of process variables on the denaturation of whey proteins during spray drying. *Dry. Technol.* **25**, 799–807 (2007).

67. Salem, K. S., Naithani, V., Jameel, H., Lucia, L. & Pal, L. A systematic examination of the dynamics of water-cellulose interactions on capillary force-induced fiber collapse. *Carbohydr. Polym.* 119856 (2022).

68. Singh, A. & Van den Mooter, G. Spray drying formulation of amorphous solid dispersions. *Adv. Drug Deliv. Rev.* **100**, 27–50 (2016).

69. Perše, L. S., Bizjak, A. & Orel, B. The role of rheological properties and spraying parameters on the spectral selectivity of Thickness Insensitive Spectrally Selective (TISS) paint coatings. *Sol. Energy Mater. Sol. Cells* **110**, 115–125 (2013).

70. Ziaee, A., Albadarin, A. B., Padrela, L., Femmer, T., O'Reilly, E. & Walker, G. Spray drying of pharmaceuticals and biopharmaceuticals: Critical parameters and experimental process optimization approaches. *Eur. J. Pharm. Sci.* **127**, 300–318 (2019).

71. Peng, Y., Gardner, D. J. & Han, Y. Drying cellulose nanofibrils: In search of a suitable method. *Cellulose* **19**, 91–102 (2012).

72. Peng, Y., Gardner, D. J. & Han, Y. Characterization of mechanical and morphological properties of cellulose reinforced polyamide 6 composites. *Cellulose* **22**, 3199–3215 (2015).

73. Beck, S., Bouchard, J. & Berry, R. Dispersibility in water of dried nanocrystalline cellulose. *Biomacromolecules* **13**, 1486–1494 (2012).

74. Khoshkava, V. & Kamal, M. R. Effect of drying conditions on cellulose nanocrystal (CNC) agglomerate porosity and dispersibility in polymer nanocomposites. *Powder Technol.* **261**, 288–298 (2014).

75. Esparza, Y., Ngo, T. D., Fraschini, C. & Boluk, Y. Aggregate morphology and aqueous dispersibility of spray-dried powders of cellulose nanocrystals. *Ind. Eng. Chem. Res.* **58**, 19926–19936 (2019).

76. Sinquefield, S., Ciesielski, P. N., Li, K., Gardner, D. J. & Ozcan, S. Nanocellulose dewatering and drying: current state and future perspectives. *ACS Sustain. Chem. Eng.* **8**, 9601–9615 (2020).

77. Werly, E. F. & Bauman, E. K. Production of submicronic powder by spray-freezing. *Arch. Environ. Heal. An Int. J.* **9**, 567–571 (1964).

78. Abdallah, W. & Kamal, M. R. Influence of process variables on physical characteristics of spray freeze dried cellulose nanocrystals. *Cellulose* **25**, 5711–5730 (2018).

79. Wanning, S., Süverkrüp, R. & Lamprecht, A. Pharmaceutical spray freeze drying. *Int. J. Pharm.* **488**, 136–153 (2015).

80. Elik, A., Koçak Yanık, D. & Göğüş, F. A comparative study of encapsulation of carotenoid enriched-flaxseed oil and flaxseed oil by spray freeze-drying and spray drying techniques. *LWT* **143**, 111153 (2021).

81. Ouadaker, M., Jiang, X., Bowen, P., Bienia, M., Pagnoux, C. & Aimable, A. Porous granules by freeze granulation of Pickering emulsions stabilized with halloysite particles. *Colloids Surfaces A Physicochem. Eng. Asp.* **585**, 124156 (2020).

82. Tasset, S., Cathala, B., Bizot, H. & Capron, I. Versatile cellular foams derived from CNC-stabilized Pickering emulsions. *RSC Adv.* **4**, 893–898 (2013).

83. Li, Y., Liu, X., Zhang, Z., Zhao, S., Tian, G., Zheng, J., Wang, D., Shi, S. & Russell, T. P.

Adaptive Structured Pickering Emulsions and Porous Materials Based on Cellulose Nanocrystal Surfactants. *Angew. Chemie Int. Ed.* **57**, 13560–13564 (2018).

84. Qiao, M., Yang, X., Zhu, Y., Guerin, G. & Zhang, S. Ultralight Aerogels with Hierarchical Porous Structures Prepared from Cellulose Nanocrystal Stabilized Pickering High Internal Phase Emulsions. *Langmuir* **36**, 6421–6428 (2020).

85. Hu, Z., Patten, T., Pelton, R. & Cranston, E. D. Synergistic stabilization of emulsions and emulsion gels with water-soluble polymers and cellulose nanocrystals. *ACS Sustain. Chem. Eng.* **3**, 1023–1031 (2015).

86. Hu, Z., Marway, H. S., Kasem, H., Pelton, R. & Cranston, E. D. Dried and redispersible cellulose nanocrystal Pickering emulsions. *ACS Macro Lett.* **5**, 185–189 (2016).

87. Xie, J., Luo, Y., Chen, Y., Liu, Y., Ma, Y., Zheng, Q., Yue, P. & Yang, M. Redispersible Pickering emulsion powder stabilized by nanocrystalline cellulose combining with cellulosic derivatives. *Carbohydr. Polym.* **213**, 128–137 (2019).

88. Jiménez-Saelices, C., Seantier, B., Cathala, B. & Grohens, Y. Spray freeze-dried nanofibrillated cellulose aerogels with thermal superinsulating properties. *Carbohydr. Polym.* **157**, 105–113 (2017).

89. Shen, Y., Orelma, H., Sneck, A., Kataja, K., Salmela, J., Qvintus, P., Suurnäkki, A. & Harlin, A. High velocity dry spinning of nanofibrillated cellulose (CNF) filaments on an adhesion controlled surface with low friction. *Cellulose* **23**, 3393–3398 (2016).

90. Iwamoto, S., Isogai, A. & Iwata, T. Structure and mechanical properties of wet-spun fibers made from natural cellulose nanofibers. *Biomacromolecules* **12**, 831–836 (2011).

91. Reyes, G., Ajdary, R., Yazdani, M. R. & Rojas, O. J. Hollow filaments synthesized by dry-jet wet spinning of cellulose nanofibrils: structural properties and thermoregulation with phase-change infills. *ACS Appl. Polym. Mater.* **4**, 2908–2916 (2022).

92. Zhang, L., Mao, Y., Zhou, J. & Cai, J. Effects of coagulation conditions on the properties of regenerated cellulose films prepared in NaOH/Urea aqueous solution. *Ind. Eng. Chem. Res.* **44**, 522–529 (2005).

93. Lundahl, M. J., Klar, V., Wang, L., Ago, M. & Rojas, O. J. Spinning of cellulose nanofibrils into filaments: A review. *Ind. Eng. Chem. Res.* **56**, 8–19 (2017).

94. Pasaoglu, M. E. & Koyuncu, I. Substitution of petroleum-based polymeric materials used in the electrospinning process with nanocellulose: A review and future outlook. *Chemosphere* **269**, 128710 (2021).

95. Wang, H., Kong, L. & Ziegler, G. R. Fabrication of starch - nanocellulose composite fibers by electrospinning. *Food Hydrocoll.* **90**, 90–98 (2019).

96. Lundahl, M. J., Cunha, A. G., Rojo, E., Papageorgiou, A. C., Rautkari, L., Arboleda, J. C. & Rojas, O. J. Strength and water interactions of cellulose I filaments wet-spun from cellulose nanofibril hydrogels. *Sci. Rep.* **6**, 1–13 (2016).

97. Mohammadi, P., Toivonen, M. S., Ikkala, O., Wagermaier, W. & Linder, M. B. Aligning cellulose nanofibril dispersions for tougher fibers. *Sci. Reports 2017 71* **7**, 1–10 (2017).

98. Håkansson, K. M. O. *et al.* Hydrodynamic alignment and assembly of nanofibrils resulting in strong cellulose filaments. *Nat. Commun. 2014 51* **5**, 1–10 (2014).

99. Son, S. M., Lee, J. E., Jeon, J., Lim, S. I., Kwon, H. T., Eom, Y. & Chae, H. G. Preparation of high-performance polyethersulfone/cellulose nanocrystal nanocomposite fibers via dry-jet wet spinning. *Macromol. Res. 2021 291* **29**, 33–39 (2021).

100. Hynninen, V., Mohammadi, P., Wagermaier, W., Hietala, S., Linder, M. B., Ikkala, O. & Nonappa. Methyl cellulose/cellulose nanocrystal nanocomposite fibers with high ductility. *Eur. Polym. J.* **112**, 334–345 (2019).

101. Lundahl, M. J., Klar, V., Ajdary, R., Norberg, N., Ago, M., Cunha, A. G. & Rojas, O. J. Absorbent filaments from cellulose nanofibril hydrogels through continuous coaxial wet spinning. *ACS Appl. Mater. Interfaces* **10**, 27287–27296 (2018).

102. Patiño Vidal, C., Velásquez, E., Galotto, M. J. & López de Dicastillo, C. Development of an antibacterial coaxial bionanocomposite based on electrospun core/shell fibers loaded with ethyl lauroyl arginate and cellulose nanocrystals for active food packaging. *Food Packag. Shelf Life* **31**, 100802 (2022).

103. Rojas, A., Velásquez, E., Garrido, L., Galotto, M. J. & López de Dicastillo, C. Design of active electrospun mats with single and core-shell structures to achieve different curcumin release kinetics. *J. Food Eng.* **273**, 109900 (2020).

104. Brückner, M., Bade, M. & Kunz, B. Investigations into the stabilization of a volatile aroma compound using a combined emulsification and spray drying process. *Eur. Food Res. Technol.* **226**, 137–146 (2007).

105. Vega, C. & Roos, Y. H. Invited review: spray-dried dairy and dairy-like emulsions—compositional considerations. *J. Dairy Sci.* **89**, 383–401 (2006).

106. Parris, N., Cooke, P. H. & Hicks, K. B. Encapsulation of essential oils in zein nanospherical particles. *J. Agric. Food Chem.* **53**, 4788–4792 (2005).

107. Singh, H., Kumar, Y. & Meghwal, M. Encapsulated oil powder: processing, properties, and applications. *J. Food Process Eng.* **45**, e14047 (2022).

108. Binks, B. P., Sekine, T. & Tyowua, A. T. Dry oil powders and oil foams stabilised by fluorinated clay platelet particles. *Soft Matter* **10**, 578–589 (2013).

109. McClements, D. J. & Gumus, C. E. Natural emulsifiers — Biosurfactants, phospholipids, biopolymers, and colloidal particles: Molecular and physicochemical basis of functional performance. *Adv. Colloid Interface Sci.* **234**, 3–26 (2016).

110. Binks, B. P. Particles as surfactants—similarities and differences. *Curr. Opin. Colloid Interface Sci.* **7**, 21–41 (2002).

111. Kalashnikova, I., Bizot, H., Bertoncini, P., Cathala, B. & Capron, I. Cellulosic nanorods of various aspect ratios for oil in water Pickering emulsions. *Soft Matter* **9**, 952–959 (2012).

112. Gauthier, G. & Capron, I. Pickering nanoemulsions: An overview of manufacturing processes, formulations, and applications. *JCIS Open* **4**, 100036 (2021).

113. Kalashnikova, I., Bizot, H., Cathala, B. & Capron, I. Modulation of cellulose nanocrystals amphiphilic properties to stabilize oil/water interface. *Biomacromolecules* **13**, 267–275 (2012).

114. Gestranius, M., Kontturi, K. S., Mikkelson, A., Virtanen, T., Schirp, C., Cranston, E. D., Kontturi, E. & Tammelin, T. Creaming Layers of Nanocellulose Stabilized Water-Based Polystyrene: High-Solids Emulsions for 3D Printing. *Front. Chem. Eng.* **0**, 51 (2021).

115. Raut, J. S. & Karuppayil, S. M. A status review on the medicinal properties of essential oils. *Ind. Crops Prod.* **62**, 250–264 (2014).

116. Turek, C. & Stintzing, F. C. Stability of Essential Oils: A Review. *Compr. Rev. Food Sci. Food Saf.* **12**, 40–53 (2013).

117. de Souza, H. J. B., Fernandes, R. V. de B., Borges, S. V., Felix, P. H. C., Viana, L. C., Lago, A. M. T. & Botrel, D. A. Utility of blended polymeric formulations containing cellulose nanofibrils for encapsulation and controlled release of sweet orange essential oil. *Food Bioprocess Technol.* **11**, 1188–1198 (2018).

118. Chanama, R., Horn, G. & McClements, D. J. Influence of Oil Polarity on Droplet Growth in Oil-in-Water Emulsions Stabilized by a Weakly Adsorbing Biopolymer or a Nonionic Surfactant. *J. Colloid Interface Sci.* **247**, 167–176 (2002).

119. Tang, Y. C. & Chen, B. H. Pigment change of freeze-dried carotenoid powder during storage. *Food Chem.* **69**, 11–17 (2000).

120. Wittaya-Areekul, S., Needham, G. F., Milton, N., Roy, M. L. & Nail, S. L. Freeze-drying of tert-butanol/water cosolvent systems: A case report on formation of a friable freeze-dried powder of tobramycin sulfate. *J. Pharm. Sci.* **91**, 1147–1155 (2002).

121. Jiang, F. & Hsieh, Y. Lo. Assembling and redispersibility of rice straw nanocellulose: Effect of tert-butanol. *ACS Appl. Mater. Interfaces* **6**, 20075–20084 (2014).

122. Jiang, F. & Hsieh, Y. Lo. Cellulose nanocrystal isolation from tomato peels and assembled

nanofibers. *Carbohydr. Polym.* **122**, 60–68 (2015).

123. Han, J., Zhou, C., Wu, Y., Liu, F. & Wu, Q. Self-assembling behavior of cellulose nanoparticles during freeze-drying: Effect of suspension concentration, particle size, crystal structure, and surface charge. *Biomacromolecules* **14**, 1529–1540 (2013).

124. Mohammed, N. K., Tan, C. P., Manap, Y. A., Muhialdin, B. J. & Hussin, A. S. M. Spray drying for the encapsulation of oils—a review. *Molecules* **25**, 3873 (2020).

125. Adelmann, H., Binks, B. P. & Mezzenga, R. Oil powders and gels from particle-stabilized emulsions. *Langmuir* **28**, 1694–1697 (2012).

126. Sungsinchai, S., Niamnuy, C., Wattanapan, P., Charoenchaitrakool, M. & Devahastin, S. Spray drying of non-chemically prepared nanofibrillated cellulose: Improving water redispersibility of the dried product. *Int. J. Biol. Macromol.* **207**, 434–442 (2022).

127. Tabatabaei, M., Ebrahimi, B., Rajaei, A., Movahednejad, M. H., Rastegari, H., Taghavi, E., Aghbashlo, M., Gupta, V. K. & Lam, S. S. Producing submicron chitosan-stabilized oil Pickering emulsion powder by an electrostatic collector-equipped spray dryer. *Carbohydr. Polym.* **294**, 119791 (2022).

128. Mezzenga, R. & Ulrich, S. Spray-dried oil powder with ultrahigh oil content. *Langmuir* **26**, 16658–16661 (2010).

129. Lee, J. & Cheng, Y. Critical freezing rate in freeze drying nanocrystal dispersions. *J. Control. Release* **111**, 185–192 (2006).

130. Vanderfleet, O. M., Reid, M. S., Bras, J., Heux, L., Godoy-Vargas, J., Panga, M. K. R. & Cranston, E. D. Insight into thermal stability of cellulose nanocrystals from new hydrolysis methods with acid blends. *Cellulose* **26**, 507–528 (2019).

131. Pereira, L. H., Catelani, T. A., Costa, É. D. '., Garcia, J. S. & Trevisan, M. G. Coffee adulterant quantification by derivative thermogravimetry and chemometrics analysis. *J. Therm. Anal. Calorim.* 1–10 (2021).

132. Renneckar, S., Zink-Sharp, A. G., Ward, T. C. & Glasser, W. G. Compositional analysis of thermoplastic wood composites by TGA. *J. Appl. Polym. Sci.* **93**, 1484–1492 (2004).

133. Dong, H., Ding, Q., Jiang, Y., Li, X. & Han, W. Pickering emulsions stabilized by spherical cellulose nanocrystals. *Carbohydr. Polym.* **265**, 118101 (2021).

134. Binks, B. P. & Lumsdon, S. O. Pickering emulsions stabilized by monodisperse latex particles: Effects of particle size. *Langmuir* **17**, 4540–4547 (2001).

135. Hu, Z., Cranston, E. D., Ng, R. & Pelton, R. Tuning cellulose nanocrystal gelation with polysaccharides and surfactants. *Langmuir* **30**, 2684–2692 (2014).

136. Sarkar, A., Arfsten, J., Golay, P. A., Acquistapace, S. & Heinrich, E. Microstructure and long-term stability of spray dried emulsions with ultra-high oil content. *Food Hydrocoll.* **52**, 857–867 (2016).

137. Anwar, S. H. & Kunz, B. The influence of drying methods on the stabilization of fish oil microcapsules: Comparison of spray granulation, spray drying, and freeze drying. *J. Food Eng.* **105**, 367–378 (2011).

138. Xu, Y., Shen, H., Cao, L. & Xu, G. Oil release behavior and kinetics of oil-impregnated kapok fiber powder. *Cellulose* **27**, 5845–5853 (2020).

139. Washburn, E. W. The Dynamics of Capillary Flow. *Phys. Rev.* **17**, 273 (1921).

140. Atkins, T. W. Fabrication of microcapsules using poly(ethylene adipate) and a blend of poly(ethylene adipate) with poly(hydroxybutyrate-hydroxyvalerate): Incorporation and release of bovine serum albumin. *Biomaterials* **18**, 173–180 (1997).

141. Yeo, Y., Bellas, E., Firestone, W., Langer, R. & Kohane, D. S. Complex coacervates for thermally sensitive controlled release of flavor compounds. *J. Agric. Food Chem.* **53**, 7518–7525 (2005).

142. Choi, M. J., Ruktanonchai, U., Min, S. G., Chun, J. Y. & Soottitantawat, A. Physical characteristics of fish oil encapsulated by β-cyclodextrin using an aggregation method or polycaprolactone using an emulsion–diffusion method. *Food Chem.* **119**, 1694–1703 (2010).

143. Chanamai, R. & McClements, D. J. Dependence of creaming and rheology of monodisperse oil-in-water emulsions on droplet size and concentration. *Colloids Surfaces A Physicochem. Eng. Asp.* **172**, 79–86 (2000).

144. Christensen, K. L., Pedersen, G. P. & Kristensen, H. G. Preparation of redispersible dry emulsions by spray drying. *Int. J. Pharm.* **212**, 187–194 (2001).

145. Desbrières, J., Hirrien, M. & Ross-Murphy, S. B. Thermogelation of methylcellulose: rheological considerations. *Polymer (Guildf).* **41**, 2451–2461 (2000).

146. Ma, T., Cui, R., Lu, S., Hu, X., Xu, B., Song, Y. & Hu, X. High internal phase Pickering emulsions stabilized by cellulose nanocrystals for 3D printing. *Food Hydrocoll.* **125**, 107418 (2022).

147. Qi, W., Li, T., Zhang, Z. & Wu, T. Preparation and characterization of oleogel-in-water pickering emulsions stabilized by cellulose nanocrystals. *Food Hydrocoll.* **110**, 106206 (2021).

148. Maa, Y.-F., Nguyen, P.-A., Sit, K. & Hsu, C. C. Spray-drying performance of a bench-top spray dryer for protein aerosol powder preparation. *Biotechnol. Bioeng.* **60**, 301–309 (1998).

149. Carson, C. F. & Riley, T. V. Antimicrobial activity of the major components of the essential oil of Melaleuca alternifolia. *J. Appl. Bacteriol.* **78**, 264–269 (1995).

150. Cavanagh, H. M. A. & Wilkinson, J. M. Lavender essential oil: a review. *Aust. Infect. Control* **10**, 35–37 (2005).

151. Blaak, J. & Staib, P. An updated review on efficacy and benefits of sweet almond, evening primrose and jojoba oils in skin care applications. *Int. J. Cosmet. Sci.* **44**, 1–9 (2022).

152. Sánchez, M., Avhad, M. R., Marchetti, J. M., Martínez, M. & Aracil, J. Jojoba oil: a state of the art review and future prospects. *Energy Convers. Manag.* **129**, 293–304 (2016).

153. Treesuwan, W., Neves, M. A., Uemura, K., Nakajima, M. & Kobayashi, I. Preparation characteristics of monodisperse oil-in-water emulsions by microchannel emulsification using different essential oils. *LWT* **84**, 617–625 (2017).

154. Hart, P. H., Brand, C., Carson, C. F., Riley, T. V., Prager, R. H. & Finlay-Jones, J. J. Terpinen-4-ol, the main component of the essential oil of Melaleuca alternifolia (tea tree oil), suppresses inflammatory mediator production by activated human monocytes. *Inflamm. Res. 2000 4911* **49**, 619–626 (2000).

155. Plotto, A. & Roberts, D. Aroma quality of lavender water: a comparative study. *Perfum. Flavorist* **26**, 44–64 (2001).

156. Burhan, A. M., Abdel-Hamid, S. M., Soliman, M. E. & Sammour, O. A. Optimisation of the microencapsulation of lavender oil by spray drying. *J. Microencapsul.* **36**, 250–266 (2019).

157. Zhang, S., Chen, J., Yin, X., Wang, X., Qiu, B., Zhu, L. & Lin, Q. Microencapsulation of tea tree oil by spray-drying with methyl cellulose as the emulsifier and wall material together with chitosan/alginate. *J. Appl. Polym. Sci.* **134**, 44662 (2017).

158. Jaâfar, F., Lassoued, M. A., Sahnoun, M., Sfar, S. & Cheikhrouhou, M. Impregnation of ethylcellulose microcapsules containing jojoba oil onto compressive knits developed for high burns. *Fibers Polym. 2012 133* **13**, 346–351 (2012).

159. Pourzahedi, L. & Eckelman, M. J. Environmental life cycle assessment of nanosilver-enabled bandages. *Environ. Sci. Technol.* **49**, 361–368 (2015).

160. Pandiarajan, J. & Krishnan, M. Properties, synthesis and toxicity of silver nanoparticles. *Environ. Chem. Lett.* **15**, 387–397 (2017).

161. Williams, L. R., Stockley, J. K., Yan, W. & Home, V. N. Essential oils with high antimicrobial activity for therapeutic use. *Int. J. Aromather.* **8**, 30–40 (1998).

162. Cross, S. E., Russell, M., Southwell, I. & Roberts, M. S. Human skin penetration of the major components of Australian tea tree oil applied in its pure form and as a 20% solution

in vitro. *Eur. J. Pharm. Biopharm.* **69**, 214–222 (2008).

163. Zhao, C., Qiu, H., Chen, H., Hu, X., Yu, Q., Lian, Z., Li, J. & Qu, H. In-fiber Mach-Zehnder temperature sensor using silicone-oil-filled dual core fiber. *Sensors Actuators A Phys.* **323**, 112644 (2021).

164. Kumar, A. G., Wang, L., Li, X., Tan, X., Geng, Y. & Xu, Y. Wavelength multiplexing of four-wave mixing based fiber temperature sensor with oil-filled photonic crystal fiber. *Opt. Express, Vol. 26, Issue 21, pp. 27907-27916* **26**, 27907–27916 (2018).

165. Chen, Y. *et al.* Temperature Monitoring for 500 kV Oil-Filled Submarine Cable Based on BOTDA Distributed Optical Fiber Sensing Technology: Method and Application. *IEEE Trans. Instrum. Meas.* **71**, (2022).

166. Pourhojat, F., Sohrabi, M., Shariati, S., Mahdavi, H. & Asadpour, L. Evaluation of poly ε-caprolactone electrospun nanofibers loaded with Hypericum perforatum extract as a wound dressing. *Res. Chem. Intermed.* **43**, 297–320 (2017).

167. Um, E., Nunes, J. K., Pico, T. & Stone, H. A. Multicompartment microfibers: fabrication and selective dissolution of composite droplet-in-fiber structures. *J. Mater. Chem. B* **2**, 7866–7871 (2014).

168. Sun, T., Hu, C., Nakajima, M., Takeuchi, M., Seki, M., Yue, T., Shi, Q., Fukuda, T. & Huang, Q. On-chip fabrication and magnetic force estimation of peapod-like hybrid microfibers using a microfluidic device. *Microfluid. Nanofluidics* **18**, 1177–1187 (2015).

169. Ji, X., Guo, S., Zeng, C., Wang, C. & Zhang, L. Continuous generation of alginate microfibers with spindle-knots by using a simple microfluidic device. *RSC Adv.* **5**, 2517–2522 (2014).

170. Chaurasia, A. S., Jahanzad, F. & Sajjadi, S. Flexible microfluidic fabrication of oil-encapsulated alginate microfibers. *Chem. Eng. J.* **308**, 1090–1097 (2017).

171. Massicotte, M. & Cranston, E. D. Comparison of techniques for drying cellulose nanocrystal Pickering emulsions into oil powders [Submitted]. *ACS Sustain. Chem. Eng.* (2022).

172. Chaurasia, A. S. & Sajjadi, S. Flexible asymmetric encapsulation for dehydration-responsive hybrid microfibers. *Small* **12**, 4146–4155 (2016).

173. Yu, Y., Wen, H., Ma, J., Lykkemark, S., Xu, H. & Qin, J. Flexible Fabrication of Biomimetic Bamboo-Like Hybrid Microfibers. *Adv. Mater.* **26**, 2494–2499 (2014).

174. Chowdhury, M. N. K., Beg, M. D. H., Khan, M. R. & Mina, M. F. Synthesis of copper nanoparticles and their antimicrobial performances in natural fibres. *Mater. Lett.* **98**, 26–29 (2013).

175. Lopez-Esparza, J., Francisco Espinosa-Cristobal, L., Donohue-Cornejo, A. & Reyes-Lopez, S. Y. Antimicrobial activity of silver nanoparticles in polycaprolactone nanofibers against gram-positive and gram-negative bacteria. *Ind. Eng. Chem. Res.* **55**, 12532–12538 (2016).

Appendices

Supporting information for Chapter 3, Figures A1-A13, are found in Appendix A.

Supporting information for Chapter 4, Figures B1 & B2, are found in Appendix B.

Appendix A (Chapter 3)

Supporting information for Chapter 4

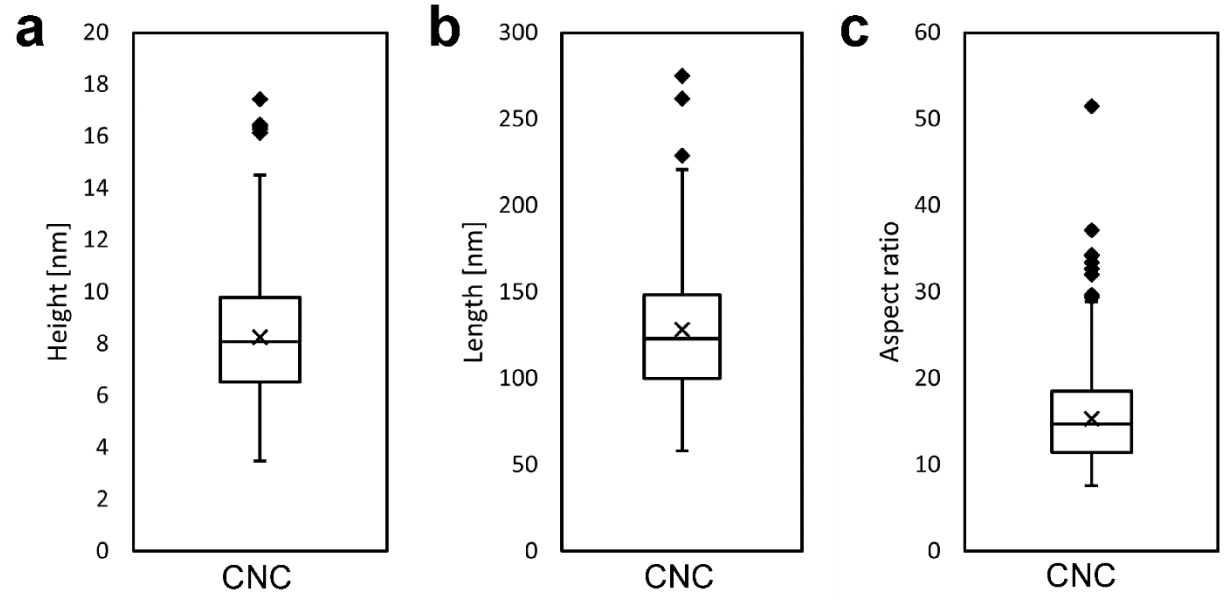

Figure A1. Mean value of measurements from AFM images for CNC (a) height, (b) length and (c) aspect ratio. Error bars represent standard error and outlier measurements (diamonds) were excluded from analysis.

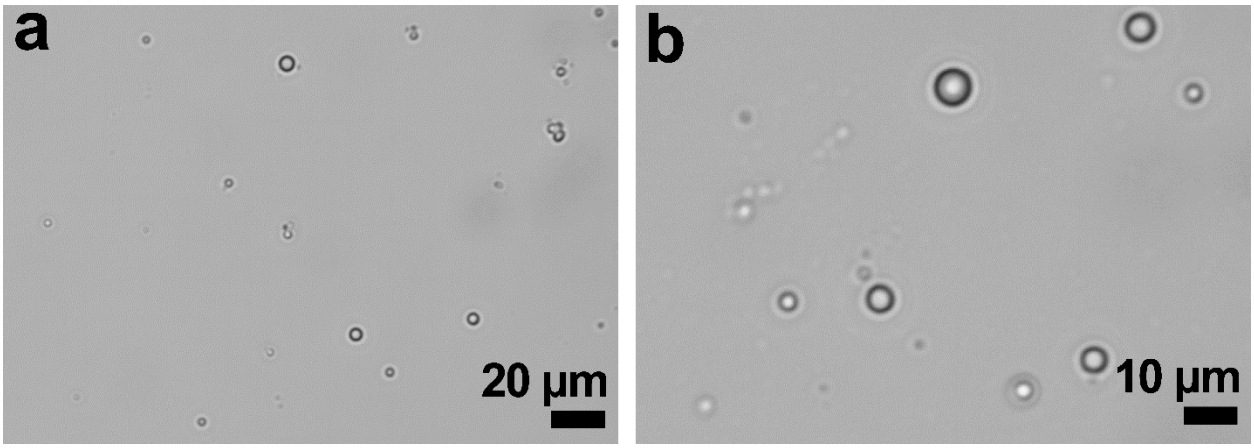

Figure A2. Optical microscope image of (a) initial CNC-MC-TA corn oil emulsion (b) zoomed in section showing individual primary droplets. Emulsion diluted 10× before imaging.

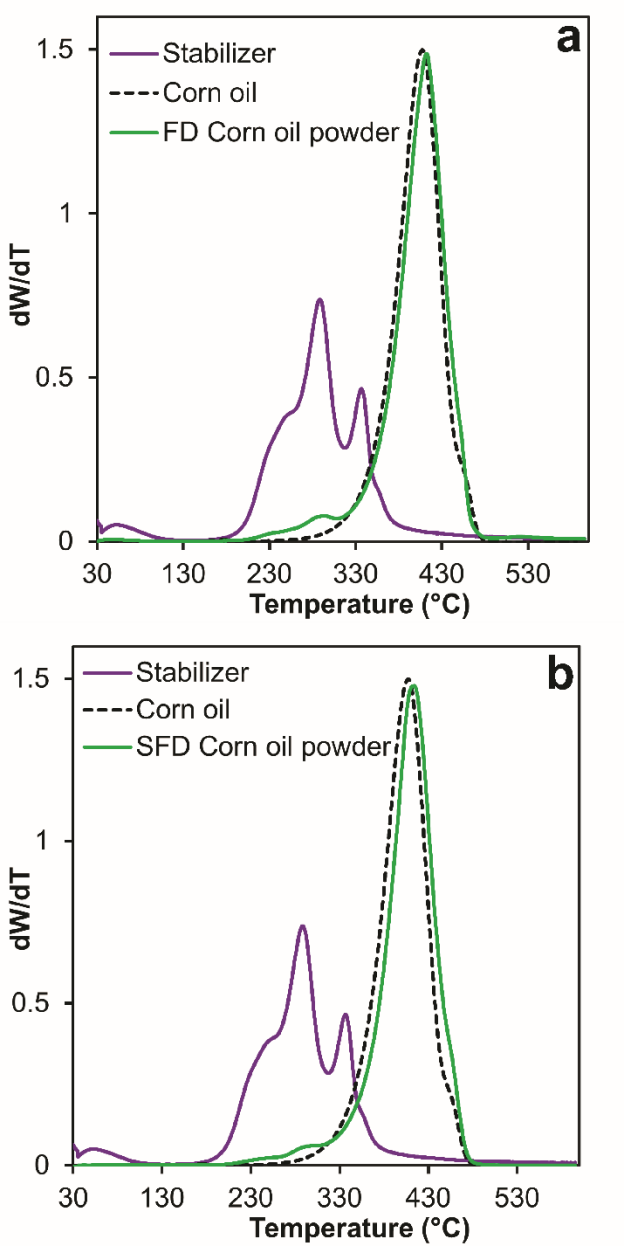

Figure A3. Representative sample mass loss rate (dW) with respect to temperature (dT), as a function of increasing temperature for the individual components for a (a) freeze dried and (b) spray freeze dried emulsion.

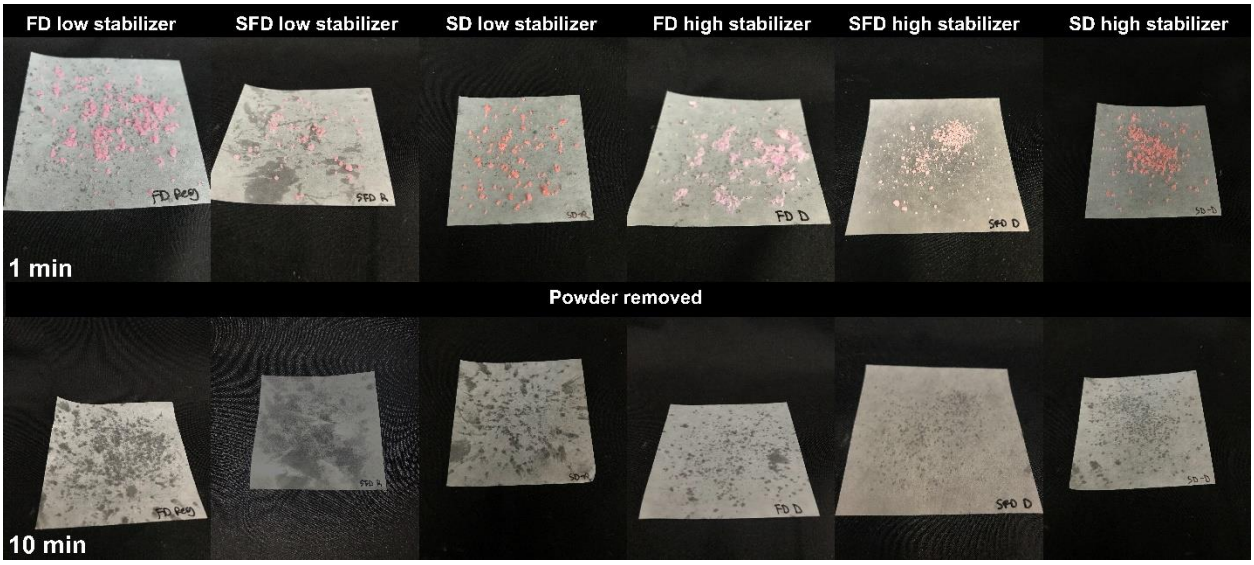

Figure A4. Photographs of oil powders (stained with Nile red) on waxed weighing paper after 1 minute (top) and then with the powder removed after 10 minutes (bottom). The change in mass of the weighing paper was measured and is reported in Table 3.2.

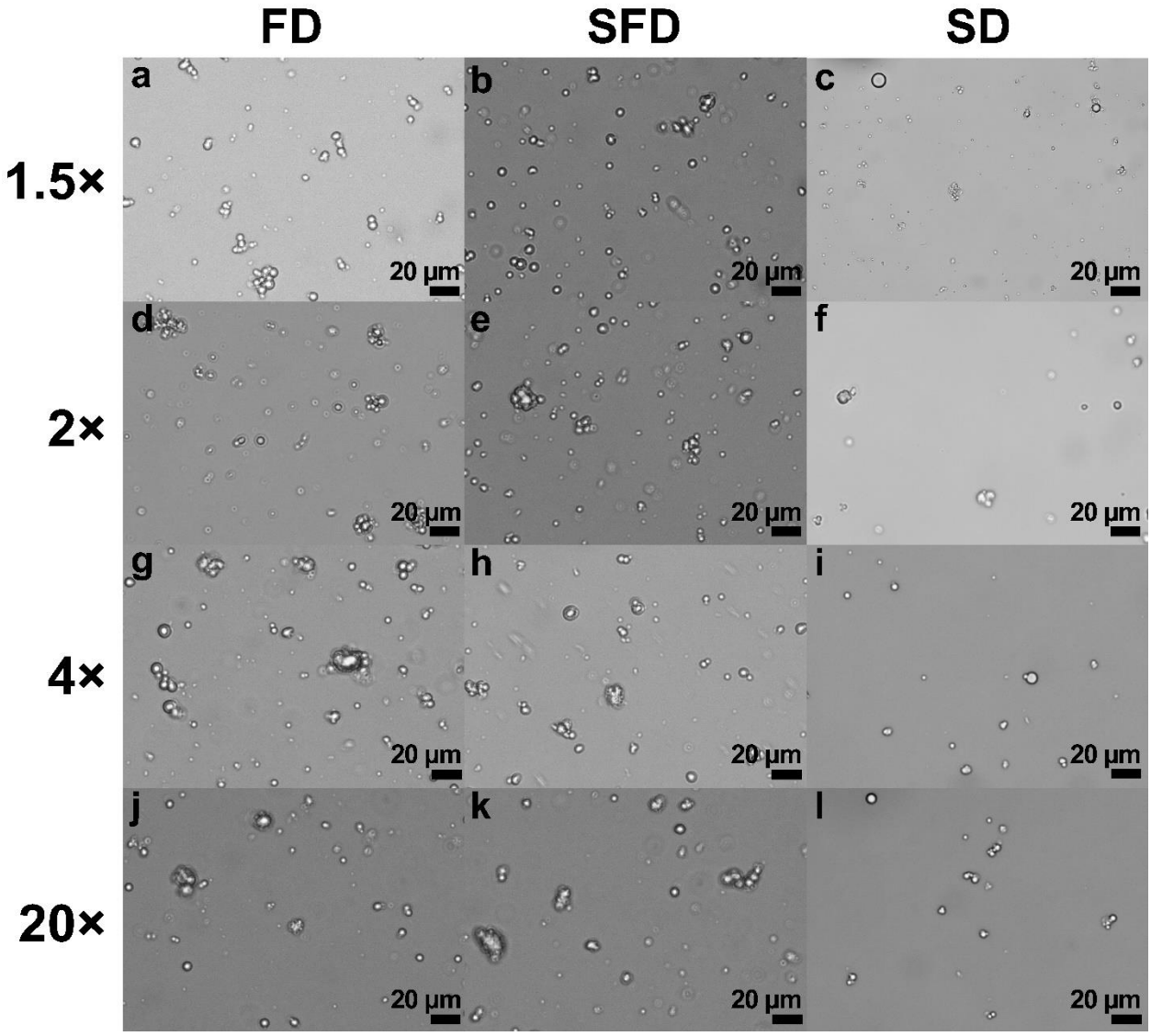

Figure A5. Optical microscope images at 50× magnification of redispersed dried powders produced from the different dilutions indicate along the left hand side. Optical microscope images of the initial emulsion droplets can be found in Figure A2 for comparison.

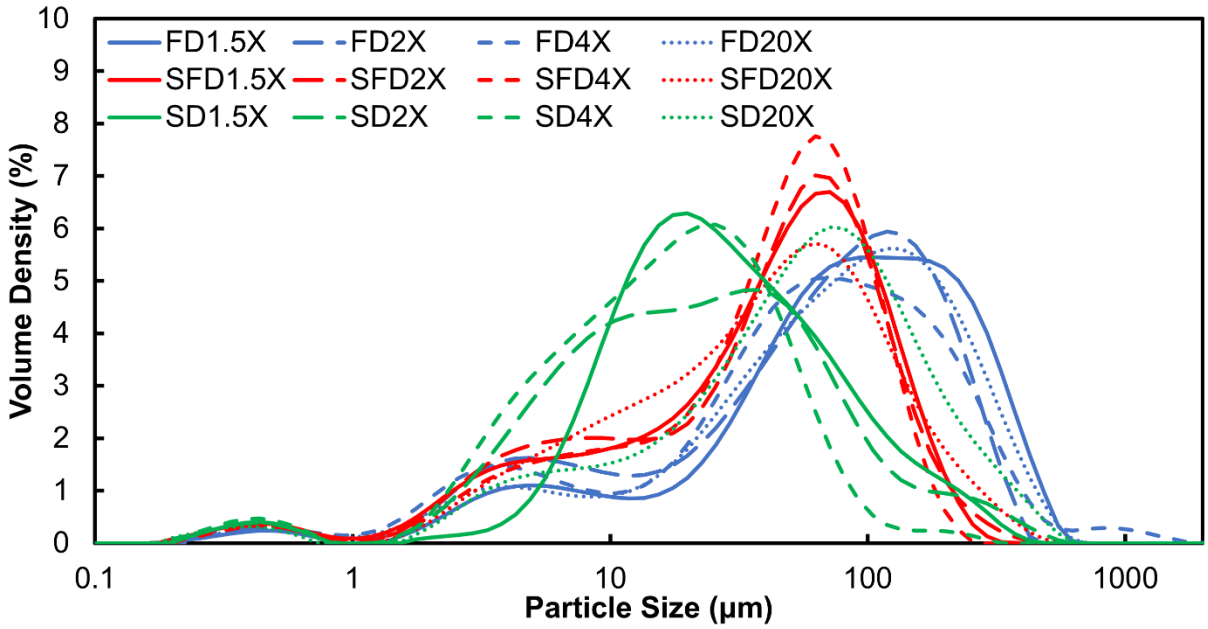

Figure A6. Particle size distribution of redispersed oil powders from freeze drying (blue), spray freeze drying (red) and spray drying (green) dried from emulsions diluted 1.5, 2, 4 and 20× their original volume.

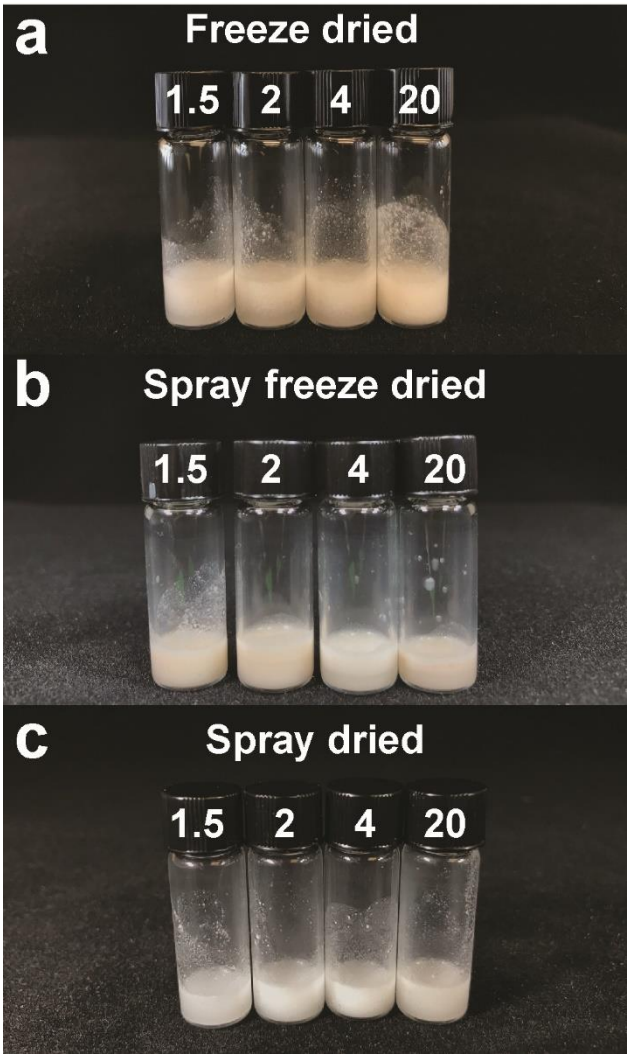

Figure A7. Redispersed emulsions prepared from oil powders that were (a) freeze dried, (b) spray freeze dried, and (c) spray dried from initial emulsions that were diluted with water by 1.5, 2, 4, and 20× their initial volume**.**

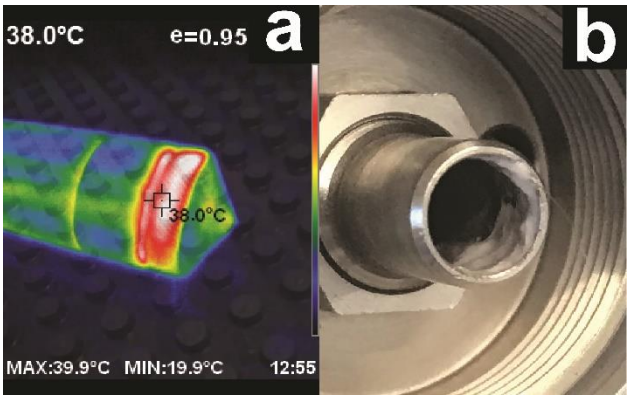

Figure A8. Heating of the spray drying nozzle in a typical run shown by (a) an infrared photo quantifying the temperature reached after a run, and (b) the white gelled material buildup on internal tubing of spray dryer nozzle (i.e., thermogelation of MC).

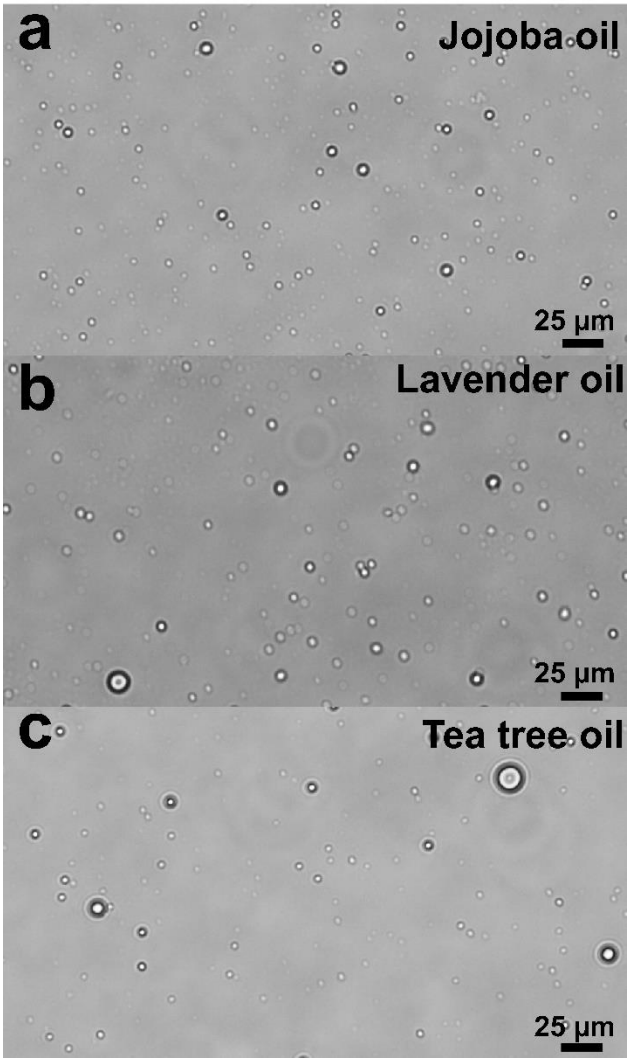

Figure A9. Optical microscopy images of emulsions made with (a) jojoba oil, (b) lavender oil, and (c) tea tree oil. Prepared as 10/90 o/w emulsions diluted to 4×.

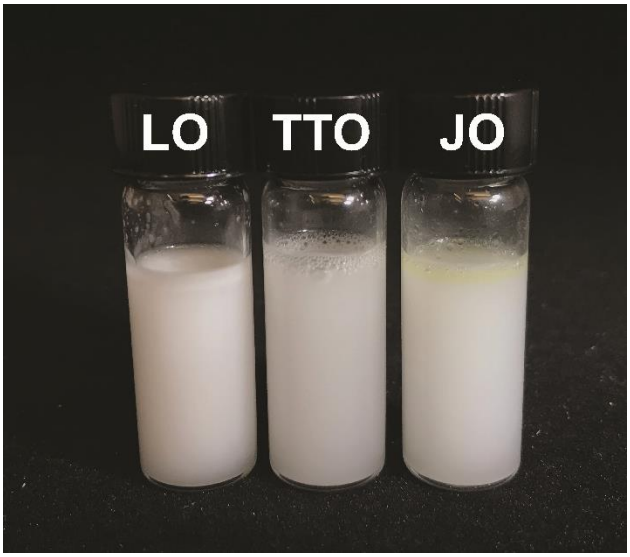

Figure A10. Photo of CNC-MC stabilized essential oil emulsions made with lavender oil (LO), tea tree oil (TTO) and jojoba oil (JO) after one week of storage in fridge showing no creaming and minimal oil leakage (except in the jojoba oil sample where the yellow top layer indicates slightly more phase separation of the oil).

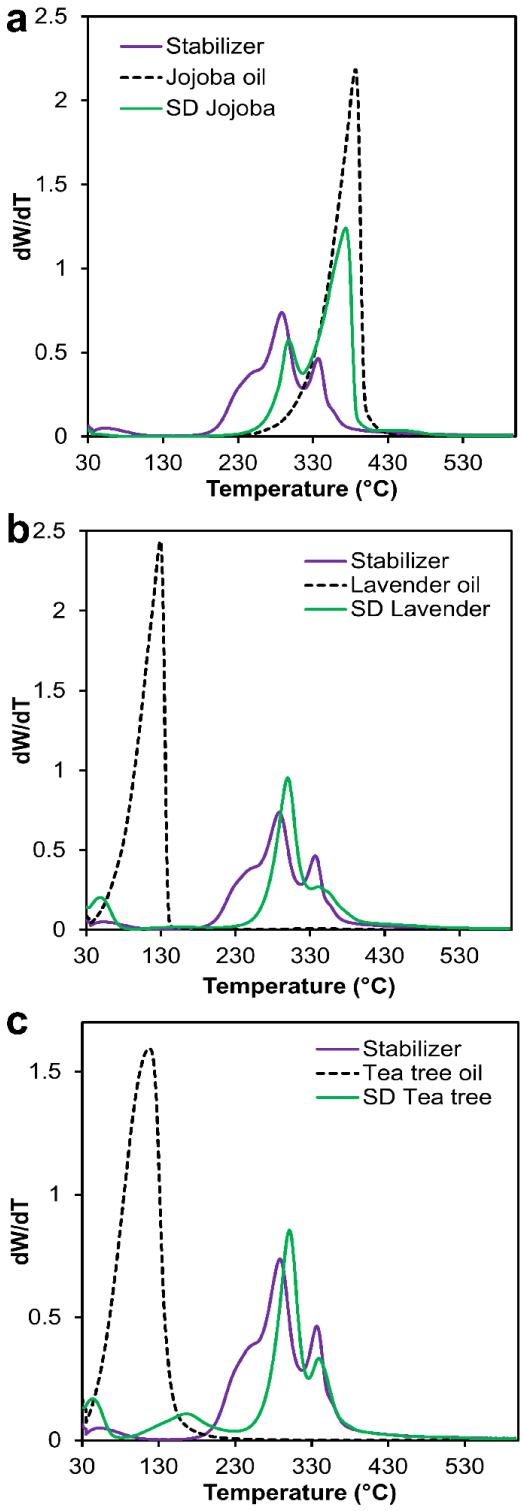

Figure A11. DTG curves of spray dried essential oil powders (green) plotted with the curves of the stabilizer (purple), and the encapsulated oil (black) for the three essential oils, (a) jojoba oil, (b) lavender oil, and (c) tea tree oil.

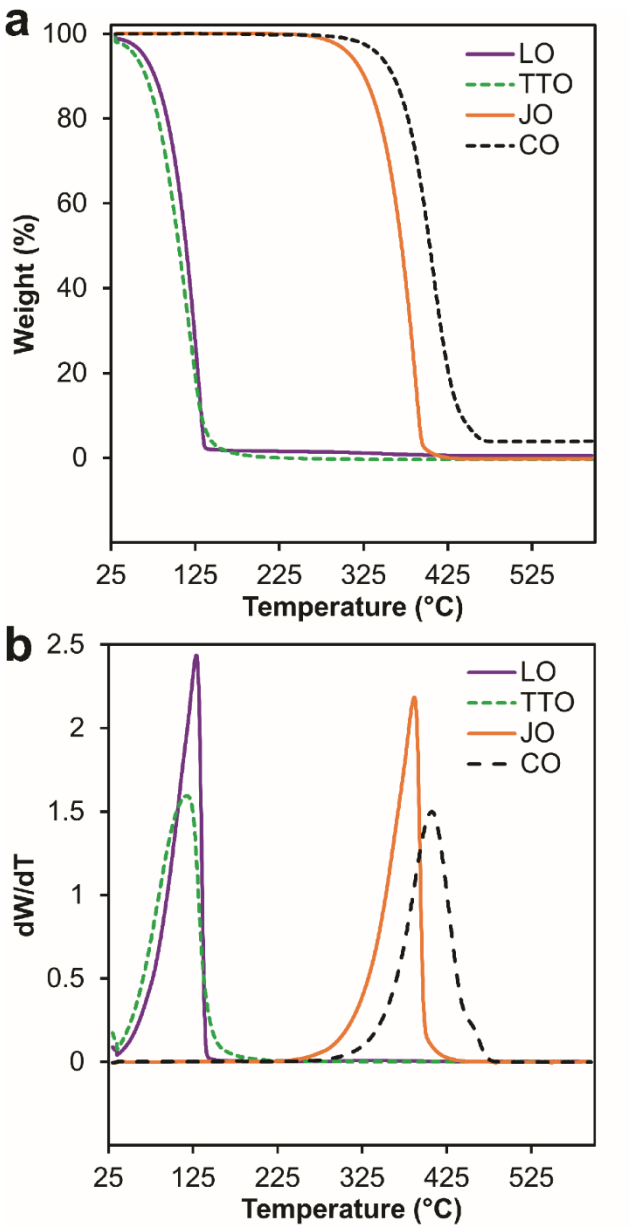

Figure A12. (a) TGA and (b) DTG curves of lavender oil (LO), tea tree oil (TTO), jojoba oil (JO) and corn oil (CO), oils only (control samples).

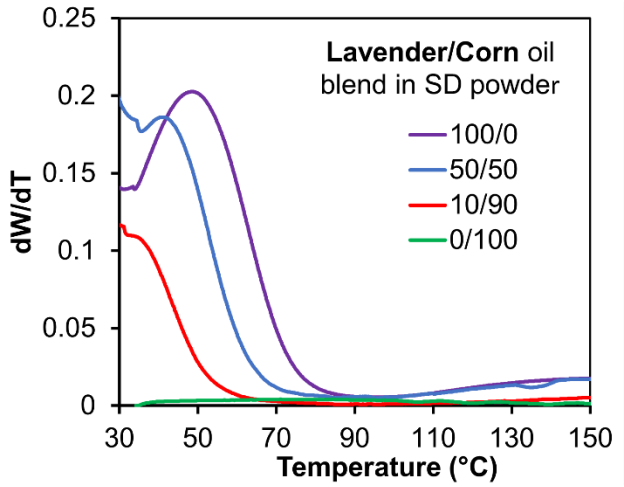

Figure A13. DTG curves of CNC-MC stabilized spray dried oil powders containing varying blends of lavender oil and corn oil. Oil blend composition noted as (% lavender//% corn oil). Oils were mixed by magnetic stirrer for an hour before emulsification.

Appendix B (Chapter 4)

Supporting information for Chapter 4

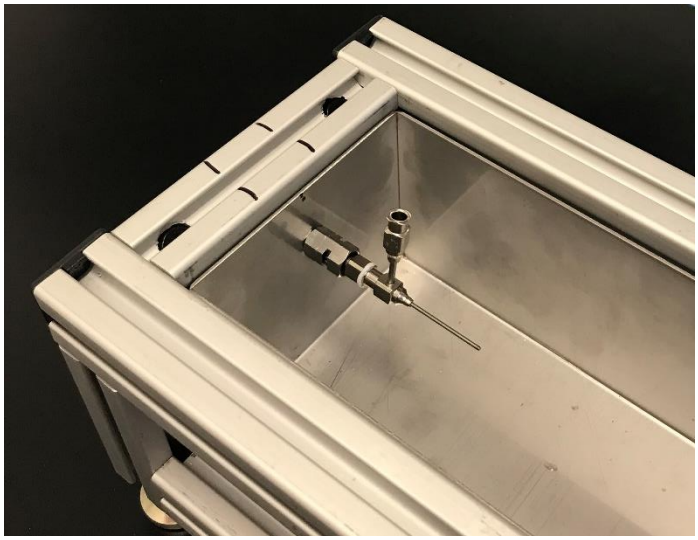

Figure B1. Photo of coaxial needle in wet spinning configuration where it is affixed to the wall of the coagulation bath to extrude parallel to the floor of the bath. The downward needle position used to produce the presented fibres in this work is shown in Figure 4.2b.

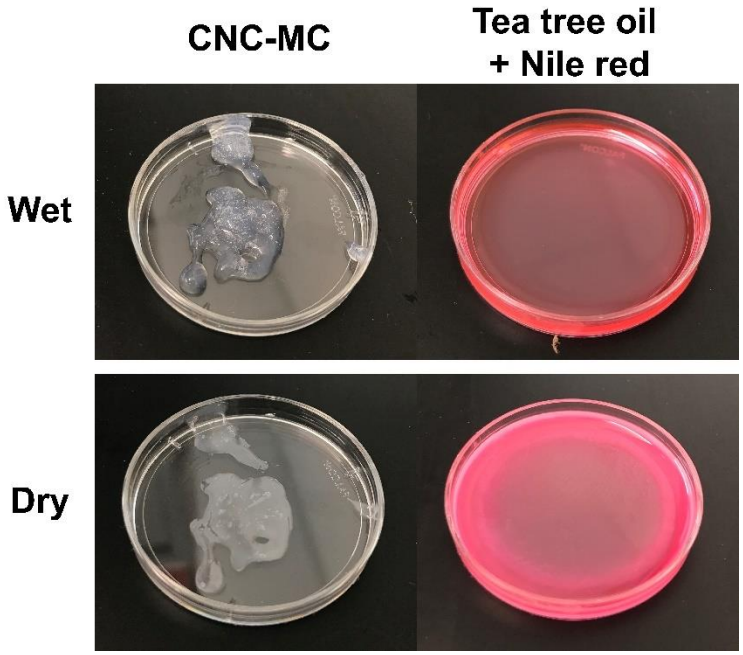

Figure B2. Shell (CNC-MC) and core (Tea tree oil and Nile red) materials left to dry with infrared heater overnight to observe changes in colour from drying. No blue colour was observed in either sample.